

Towards the Use of Piezoelectric Energy Harvesters in Pavement with Passing Vehicles

By

Farjana Faisal

A thesis submitted to
the Faculty of Graduate Studies
in partial fulfilment of
the requirements for the degree of
Master of Science

Department of Mechanical Engineering
Faculty of Engineering
University of Manitoba
Winnipeg, Manitoba

December 2016

© Copyright
2016, Farjana Faisal

Abstract

Piezoelectric energy harvesters in the road pavement are developed and studied to collect energy from the passing vehicles. A numerical model based on the Westergaard's stress model is proposed to calculate the three dimensional stress distribution in the pavement and the power generation from the piezoelectric harvesters placed inside the pavement. Piezoelectric patch, plate and beam harvesters are designed. Based on proposed numerical models, simulations are conducted to reveal the effects of vehicle velocity as well as the location and size of the Piezo-electric harvesters on the generated power. Optimally designed plate energy harvester attached with four cantilever harvesters generates up to around 28 W electrical power with the assumption of continuum vehicle passing the pavement by 22.2 m/s. This power can be used to collect enough energy in 2 hours to raise the ice temperature with the thickness of 1 cm, covering a 5 m wide road by 20 degree Celsius.

Acknowledgements

I would like to take this opportunity to thank my supervisor, Dr Nan Wu for helping me throughout my study period here in University of Manitoba. I have learnt a lot from him. He is very wise, kind, nice and helpful person. Dr Nan tries his best to train his students and always makes sure that they can understand and learn. I am blessed and honoured to have a supervisor like him. Without his constant support and guidance it would not be possible for me to complete the thesis.

I have also learnt a lot from the graduate courses which I took during my M.Sc. program. I am grateful to all my course instructors, Dr Igor Telichev, Dr Chuang Deng and Dr Urs P. Wyss. I am also thankful to my research group for their support and encouragement.

Finally, I would like to thank my loving parents, my sister and my husband for supporting me and always encouraging me. Without my family's unconditional love and support I would not be able to fulfill my degree.

Contents

Abstract	ii
Acknowledgement.....	iii
Table of Contents.....	iv
List of Tables.....	vii
List of Figures.....	ix
List of Symbols.....	xiii

Chapter

1

1.1 Background.....	1
1.2 Literature Review.....	3
1.2.1 Energy harvesting by using piezoelectric materials.....	5
1.2.2 Pavement Energy harvesting processes for deicing roads and bridges.....	12
1.2.3 Pavement energy harvesting by using piezoelectric energy harvesters....	13
1.3 Thesis Objectives.....	17
1.4 Thesis Outline.....	18

Chapter

2

2.1 Semi-analytical Model of pressure distribution in pavement under distributed load	19
2.1.1 Validation of the Model (through ANSYS Workbench Modeling).....	32
2.1.2 Comparison of results between ANSYS and MATLAB simulation.....	40
2.2 Simulations and Discussions.....	42
2.2.1 Impact of velocity on electric power generation.....	43

2.2.2	Impact of changing depth of the Piezoelectric Patch on power output.....	44
2.2.3	Power from different loads on wheel.....	47
2.2.4	Optimum Length of each piezoelectric Patch in Pavement.....	48
2.3	Conclusions.....	52
 Chapter		
3		
3.1	Schematic diagram of the piezoelectric composite plate harvester.....	55
3.2	Methodology and Numerical Model of plate deflection under pressure bulb in pavement.....	58
3.3	Simulations and Discussions.....	68
3.3.1	Impact of depth of the harvester in pavement on average power output	69
3.3.2	Relation between thickness of piezoelectric layer and average power output.....	72
3.3.3	Relation between thickness of substrate layer and average power output	75
3.3.4	Average power output with varying length of the harvester.....	78
3.3.5	Average power output with varying width of the harvester.....	81
3.3.6	Impact of vehicle velocity on average power output.....	85
3.4	Conclusions.....	88
 Chapter		
4		
4.1	Methodology and Numerical Model of cantilever composite piezoelectric energy harvester under base motion.....	89
4.2	Simulations and Discussions.....	100

4.2.1 Impact of length of the cantilever harvester on average power generation.....	101
4.2.2 Impact of thickness of the piezoelectric layer of the cantilever harvester on average power generation.....	104
4.2.3 Impact of thickness of the substrate steel layer of the cantilever harvester on average power generation.....	107
4.3 Conclusions.....	111

Chapter

5

Conclusions and Future works.....	112
References.....	116

List of Tables

Table 2-1	Comparison of results between ANSYS and MATLAB simulation.....	40
Table 2-2	Comparison of results between ANSYS and MATLAB simulation for single point load model.....	41
Table 2-3	Percentage of average power output at different depth inside the pavement (starting from the first depth value as 6 cm).....	46
Table 2-4	Average electrical power output from one single piezoelectric patch with different vehicles passing the pavement.....	48
Table 3-1	Properties of the piezoelectric composite plate harvester and the passing vehicle, which are kept constant during the calculation.....	68
Table 3-2	Impact of depth of the harvester in pavement on average power output.....	70
Table 3-3	Change in average power output from the piezoelectric composite plate harvester with the variation of the thickness of the piezoelectric layer.....	73
Table 3-4	Change in average power output from the piezoelectric composite plate harvester with the variation of the thickness of the substrate layer.....	76
Table 3-5	Change in average power output from the piezoelectric composite plate harvester with the variation of the length of the harvester.....	79
Table 3-6	Change in average power output from the piezoelectric composite plate harvester with the variation of the width of the harvester.....	82
Table 3-7	Change in average power output from the piezoelectric composite plate harvester with the variation of the velocity of the passing vehicle.....	86
Table 3-8	Dimension of the piezoelectric composite plate harvester after the optimisation	87
Table 4-1	Material properties of the cantilever composite piezoelectric harvester	100

Table 4-2 Change in average power generation from the cantilever composite harvester with the variation of length..... 102

Table 4-3 Change in average power generation from the cantilever composite harvester with the variation of thickness of the piezoelectric layer..... 105

Table 4-4 Change in average power generation from the cantilever composite harvester with the variation of thickness of the substrate steel layer..... 108

Table 4-5 Dimension of the piezoelectric cantilever composite harvester after the optimisation..... 110

List of Figures

Figure 1-1	The piezoelectric coupled cantilever beam subjected to a dynamic loading...	6
Figure 1-2	Analytical model of the piezoelectric coupled cantilever attached by a mass subjected to a base motion to represent the harvester on a high-rise building	7
Figure 1-3	Piezoelectric harvester subjected to wind load.....	8
Figure 1-4	Schematic diagram and geometries of the piezoelectric energy harvester.....	11
Figure 2-1	A structure of the flexible pavement and the methodology of study in this paper for optimum design of a piezoelectric patch.....	22
Figure 2-2	Pavement structure for CBR 2%. μ is the Poisson's ratio of the layers.....	23
Figure 2-3	Contact of the tyre and pavement and interaction with point P , where stress is to be found.....	24
Figure 2-4	Distribution of force over contact area to find stress at point P	25
Figure 2-5	Variation of pressure distribution at the middle point of the piezoelectric patch with varying edge length of small squares from 0.001 m to 0.02 m.....	26
Figure 2-6	2-D top view of the loading/contact area on the pavement.....	28
Figure 2-7	The pressure bulb formed due to circular loading on pavement.....	29
Figure 2-8	The strain Bulb showing strain distribution on piezoelectric layer at different depths.....	30
Figure 2-9	3D-modeling of the pavement consisting of five different layers.....	33
Figure 2-10	3D-modeling of the pavement showing the mesh in four layers (below the first layer) inside the pavement.....	34
Figure 2-11a	Stress distribution inside the pavement due to the applied pressure of the passing vehicle through the contact area.....	35

Figure 2-11b	Formation of the pressure bulb inside the pavement due to the applied pressure of the passing vehicle through the contact area.....	36
Figure 2-12a & 2-12b	Cross-section of the pressure bulb inside the pavement due to the applied pressure of the passing vehicle through the contact area with and without mesh respectively.....	37
Figure 2-13a & 2-13b	Stress distribution in the second layer of the pavement with and without mesh respectively.....	38 & 39
Figure 2-14	Impact of velocity of moving vehicle on the output power from one single piezoelectric patch for depth 15cm and patch length of 25cm.....	43
Figure 2-15	Output power with changing depth of piezoelectric patch in flexible pavement.....	45
Figure 2-16	Power output from one piezoelectric patch versus length of piezoelectric patch with different depth of the piezoelectric layer and a fixed vehicle velocity of 45 kmph.....	49
Figure 2-17	Power output from one piezoelectric patch versus length of piezoelectric patch with different vehicle velocities and a fixed depth of the piezoelectric layer of 6 cm.....	50
Figure 2-18	Power output from one piezoelectric patch versus length of patch with different loads of wheels at fixed values of the depth of the piezoelectric patch as 6 cm and vehicle velocity as 45Kmph.....	51
Figure 3-1	Schematic diagram of the piezoelectric composite plate harvester.....	55
Figure 3-2	Piezoelectric composite plate harvester placed inside the pavement and under dynamic loading.....	57

Figure 3-3 Variation of pressure distribution at the middle point of the piezoelectric composite plate with varying edge length of small squares from 0.001 to 0.05 m with an increase of 0.0002 m..... 62

Figure 3-4 Power output with changing depth of the piezoelectric composite plate with length and width as 0.2m. The thickness of the piezoelectric layer and substrate layer are 0.0005 m and 0.003 m, respectively, and the velocity is kept constant at 22.2 m/s..... 69

Figure 3-5 Power output with changing thickness of piezoelectric layer with the length and width of the piezoelectric composite plate of $L=W=0.2\text{m}$, the depth of the harvester of $Z=0.12\text{m}$ and the thickness of the substrate layer of the composite plate of $H_2=0.003\text{m}$ 72

Figure 3-6 Power output with changing thickness of substrate layer with the length and width of the piezoelectric composite plate of $L=W=0.2\text{m}$, the depth of the harvester of $Z=0.12\text{m}$ and the thickness of the piezoelectric layer of the composite plate of $H_1=0.0006\text{m}$ 75

Figure 3-7a Power output with changing length of the piezoelectric plate harvester, where the width of the piezoelectric composite plate is 0.2m. The depth is $Z=0.12\text{m}$, thickness of PZT coating layer is $H_1=0.0006\text{m}$ and thickness of steel substrate is $H_2=0.002\text{m}$ 78

Figure 3-7b Power output with changing width of the piezoelectric plate where the length of the piezoelectric composite plate is 0.2m, the depth of the harvester is $Z=0.12\text{m}$ and the thickness of the PZT layer and substrate layer of the composite plate are $H_1=0.0006\text{m}$ and $H_2=0.002\text{m}$, respectively..... 81

Figure 3-8 Power output with changing velocity of the vehicle with the length and width of the piezoelectric composite plate harvester of $L=W=0.2\text{m}$, the depth of the harvester of $Z=0.12\text{m}$ and the thickness of the piezoelectric and substrate layer of the composite plate of $H_1 =0.0006\text{m}$ and $H_2 =0.002\text{m}$ respectively..... 85

Figure 4-1 Piezoelectric composite plate harvester considering vibration due to base excitation..... 89

Figure 4-2 Central deflection of the composite plate structure during passing of vehicle wheels..... 92

Figure 4-3 Mode 1, 2 and 3..... 95

Figure 4-4 Power generation with changing length of the cantilever composite harvester. The thickness of the piezoelectric layer and substrate layer are 0.001 m and 0.002 m, respectively, and the velocity of the passing vehicle is kept constant at 22.2 m/s..... 101

Figure 4-5 Power generation with changing thickness of the piezoelectric layer of the cantilever composite harvester with fixed length of 0.13 m. The thickness of the substrate layer is kept fixed at 0.002 m and the velocity is kept constant at 22.2 m/s..... 104

Figure 4-6 Power generation with changing thickness of the substrate layer of the cantilever composite harvester with fixed length of 0.13 m. The thickness of the piezoelectric layer is kept fixed at 0.0007 m and the velocity is kept constant at 22.2 m/s..... 107

Figure 4-7 Deflection curve of the optimized cantilever composite harvester at different time points..... 110

List of Symbols

- L : Length of the piezoelectric composite plate harvester
- B : Width of the piezoelectric composite plate harvester
- h_1, h_2 : Depths of the homogeneous layers in pavement
- H_1 : Thickness of the piezoelectric layer of the composite plate harvester
- H_2 : Thickness of the substrate layer of the composite plate harvester
- A : Contact Area
- F : Applied Force
- P : Pressure of tyre
- N : Number of small square areas in the contact area
- f_1, f_2 : f_1 and f_2 are the edge length of each small square area of the contact radius
- σ_z : Stress along the depth direction of the pavement generated by one of the point load on the n^{th} small square
- Q : Point load
- Z : Depth of the harvester placement inside the pavement
- r : Radial distance of any point in study box from loading point in contact area inside the pavement
- μ : Equivalent Poisson ratio
- u_1 : Poisson's ratio of the first layer
- u_p : Poisson's ratio of the piezoelectric layer
- h_p : Thickness of the piezoelectric layer of the patch
- s_1, s_2 : s_1 and s_2 are the edge length of each small square area of the plate
- w : Deflection of the harvester

- m, n : m and n are the number of modes
- X, Y : Position of the small square areas in the plate along x and y direction
- i, j : Number of the small areas that are subjected to one of the point loads from the pressure bulb along length and width directions of the plate
- i^*s_1, j^*s_2 : Positions of the small area subjected to one of the transverse point loads
- D : Moment of inertia constant
- E_p, E_{PZT} : Young's modulus of the piezoelectric layer
- E, E_s : Young's modulus of the substrate layer
- M_x, M_y : M_x and M_y are the bending moment along x and y directions, respectively
- S_x, S_y : Stress values along x and y directions, respectively
- SS_x, SS_y : Strain values along x and y directions
- D_x, D_y : Surface charge density at (X, Y) position along x and y direction
- Q_x, Q_y : Total charge distribution along x and y direction
- Q_t : Total charge generated on the harvester
- T : Any time
- C : Capacitance of the piezoelectric composite plate harvester
- T : Total time of vehicle passing through the harvester
- I : Current generated by the harvester
- V : Voltage generated by the harvester
- ϵ : Di-electric constant
- K : Static electricity constant
- P_{avg} : Average power output
- V_{rms} : Root mean square (RMS) value of the voltage

- I_{rms} : Root mean square (RMS) values of the current
 $W_n(x)$: nth mode shape function
 $q_n(t)$: Generalized coordinate in the nth mode ($n=1, 2, \dots, \infty$)
 ω : Natural frequency
 l : Length of the cantilever composite harvester
 b : Width of the cantilever composite harvester
 h : Thickness of the substrate layer of the cantilever harvester
 h_{PZT} : Thickness of the PZT layer of the cantilever harvester
 ρ_s : Density of the steel layer
 ρ_{PZT} : Density of the PZT coating layer
 A_s : Area of the substrate steel layer
 A_{PZT} : Area of the PZT coating layer
 $\frac{dW(x)}{dx}$: Slope
 $\frac{d^2W(x)}{dx^2}$: Bending moment
 $\frac{d^3W(x)}{dx^3}$: Shear force
 $m(x)$: Mass per length of the cantilever at the position x ($0 \leq x \leq l$)
 f : Distributed force on the cantilever composite harvester
 I_s : Moment of inertia of the substrate steel layer
 I_{PZT} : Moment of inertia of the PZT coating layer
 $Q_n t$: Generalized force corresponding to $q_n t$
 b'' : Constant

- Q : Generated electric charge on piezoelectric layer
- e_{31} : Piezoelectric constant
- C_v : Electrical capacity of the PZT coating layer
- C_v'' : Electrical capacity per unit width of the PZT layer

Chapter 1

The following chapter 1 is an introduction describing the background of energy harvesting, the research works that has been done in the field of energy harvesting in pavement followed by research objectives and outline of this thesis.

1.1 Background

In today's era electricity has become one of the basic necessities of human life, our comfort in our day to day activities is directly or indirectly dependent on electricity. It can be stated that a nation's prosperity can be judged on the parameter that how much capable it is to meet its power supply requirements to give a quality life to its people. Energy is needed everywhere for example for lighting our houses, to drive cars, heating and air conditioning, using internet and all the technology we use are dependent on energy. The production of our food and cloths also require significant amount of energy supply. There are non-renewable energy sources, such as natural gas and fuels and renewable/alternative sources of energy to produce electricity. Fossil fuels, as traditional energy resources, are the main drivers behind the world's economic engine, which are accounting for more than 80% of the total world energy consumption in 2010 [1]. It was reported by Le et al. (2009) that 29 percent increase in global CO₂ emissions has occurred from fossil fuel between 2000 and 2008 [2]. Jacobson and Delucchi mentioned that over the last 50 years, 43% global CO₂ emissions from burning fossil fuels remained in the atmosphere leading to the greenhouse effect. Because of the adverse effects of fossil fuels, the development of clean and renewable energies has become more important for sustainability [3]. With time the amount of reserve of fuels and natural gas is decreasing. Due to that reason over the last few decades, a special attention has been given globally towards renewable/alternative sources of energy for a sustainable development of

human society without harming the environment. Renewable/alternative sources means that they are environment friendly. Renewable energy sources are required also to keep the reserve of natural gas and fuels and provide our future generation with clean and habitable environment. Solar, Wind and Tidal are the prime renewable sources of energy to generate electricity without polluting the surroundings. Solar energy is a good example of alternative energy, in which heat energy from sunrays is converted to electrical energy by solar panels. Wind and wave are also excellent sources from where renewable energy can be harvested. Now a days energy harvesting especially from the renewable energy resources is getting more and more attention because of the increasing demand of energy required for electronics and also different types of wireless sensors.

In this research the concentration is given in energy harvesting from pavement. The harvested energy can be used in various sectors for example illuminating road lights, signalization, identifying overloaded vehicles and various other sectors. However, the most important use of the generated power can be snow melting of roads and bridges of cold countries by converting the generated energy into heat. Snow melting on the public traffic facilities is one of the biggest challenges faced by the cold countries. In 2013, Vancouver spent about \$1.7-million on snow removal. Dealing with the ice storm and also snow removal cost Ottawa \$11.7-million [4]. Road accidents take place due to the heavy snow and the slippery road condition. Plowing snow can temporarily clear the highways but the plowed snows are kept on two sides of the roads which cause problems for pedestrians. Besides that it requires a lot of money to buy and maintain those snow removing tools and to pay the salary of the workers. The workers also found it very difficult to work in such kind of adverse weather condition.

Generally main roads gets the first priority to clean up the snow. Different types of methods are used to remove snow from highways and roads however the chemical method is widely used. The chemical method, by using sodium chloride and calcium chloride, has been used for preventing the buildup of ice and snow on roads and thus controlling the slippery road conditions. Salt is used to melt snow in lower temperature. However, bad corrosion of the underbodies of trucks, passenger cars etc. can also take place by using the chemical method. However, these salts are soluble in water, so there is no disposal problem but sometimes they can cause water pollution by getting mixed with underground water. They can make ground water salty and harm aquatic plants and animals when salt mixed with lake, river or other sources of water. The salty water can cause health issue for people on restricted-sodium diets and a taste problem for everyone else. Even after having various environmental and health problems associated with the use of salts continuous improvement in the salt spreading equipment and techniques are taking place. If energy can be generated from passing vehicles from the pavement then that energy can be converted to heat energy and by proper collecting technique this snow removal problem can be reduced to a certain extent. As a result it is very important to think of effective ways of energy generation from pavement which will be economic and environment friendly. The generated energy from pavement by passing vehicles can be a great source of energy as the amount of vehicles moving on roads are increasing day by day.

1.2 Literature Review

The process of deriving electricity from external ambient sources is known as energy harvesting. Energy can be harvested in different methods. Some most common types of vibration based energy harvesting techniques are electrostatic, electromagnetic and piezoelectric.

In electrostatic effect of energy harvesting a variable capacitor structure is used to generate charges from a relative motion between two plates. Despesse et al. (2005) worked on energy scavenging from mechanical vibrations and fabricated prototype structures. It was found by experiments that 0.584 mW/mm^3 of power can be obtained [5]. Electromagnetic energy harvesting technique is based on electromagnetic induction where an electromotive force is generated from a relative motion between coil and a magnet. Glynne-Jones et al. (2004) determined an electromagnetic generator which after placing in a car engine compartment can generate $157 \text{ }\mu\text{W}$ of power [6]. Saha et al. (2006) conducted their research on modeling of an electromagnetic-based generator which can generate power from ambient vibrations. The optimization of the generator was also done and they found that the energy density of the electromagnetic energy harvester was around 4.375 mW/mm^3 [7]. Jeon et al. (2005) designed thin film piezoelectric energy generator which can generate electric power from the ambient vibration. It was reported an energy density of 37 mW/mm^3 can be obtained by the piezoelectric effect [8]. Based on the above representative works, it can be concluded that the energy density of piezoelectric generator is much higher than both electrostatic and electromagnetic generators. That is the reason why piezoelectric materials are receiving a large amount of attention these days. The application of piezoelectric materials provide a possible alternative source for electrical power generation. Piezoelectric materials have the property of generating charge when stress is applied on it. This charge can be used to generate electricity and for many other purposes. Piezoelectric materials can be used for effective energy harvesting and generating by simply attaching them on the host structures under elastic strains. The harvested energy can be used for various applications and one of the most important application of piezoelectric energy harvesting can be from pavement, by using the piezoelectric energy harvester inside the pavement. Stress will be produced inside the pavement due to the

moving vehicle, generating charge on piezoelectric material which can be used to harvest energy. The harvested energy can be used for ice melting in cold countries.

1.2.1 Energy harvesting by using piezoelectric materials

Since piezoelectric materials have advantages over other traditional energy conversion methods and because of their electromechanical coupling effect that means the ability to produce electrical charge when subjected to an external load and alternately ability to produce a mechanical deformation when under an electric field, they have drawn a lot of attention now a days. Piezoelectric materials are being used a lot as sensors and actuators. One of the most significant reasons of the recent popularity of piezoelectric materials is also because of their electromechanical coupling effect can be changed significantly. In 1880, Pierre Curie and Jacques Curie first demonstrated the direct piezoelectric effect that is internal generation of electric charge by applying mechanical force. Years of study led to the new lead zirconate titanate materials, also referred as PZT materials, which are among the most commonly used piezoelectric materials now a days.

Because of the high coupling effects among all the piezoelectric ceramics PZT (lead zirconate titanate) is most commonly used. PZT materials can be mainly divided into two groups. One is hard and another is soft. Soft PZT materials are used where large response is required.

Researchers have been using piezoelectric materials for energy harvesting for a long time. Ajitsaria et al. (2007) analytically modeled a PZT bender for generating voltage and power generation from transforming ambient vibrations into electrical energy. In that research they have also done experimental testing of a prototype structure which can generate microwatt range of power [9]. Wang and Wu (2012) developed a numerical model to design a piezoelectric coupled

beam for power harvesting aim. They also studied the effect of size and location of the piezoelectric patch to calculate maximum power generation to achieve highest efficiency. In that research they used a host beam coupled with the piezoelectric patch and used the generated voltage, due to the electromechanical coupling effect of the piezoelectric patch when the host beam is subjected to dynamic loading, to produce power.

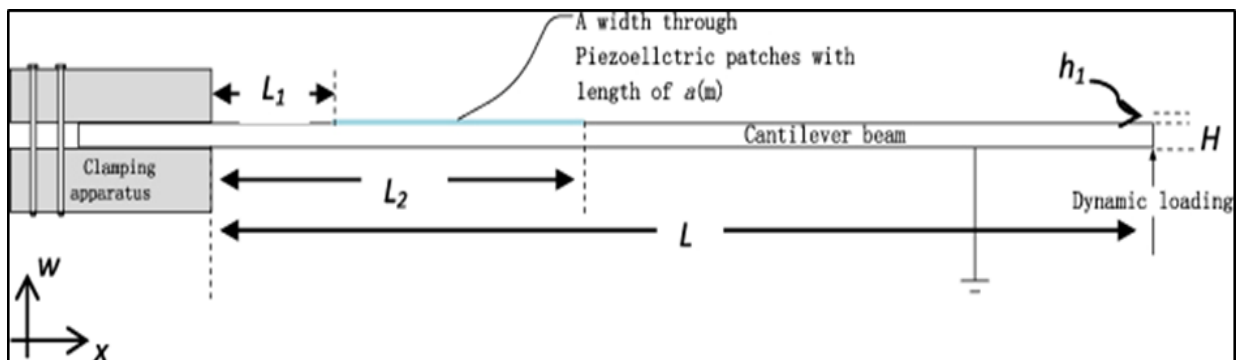


Figure 1-1 The piezoelectric coupled cantilever beam subjected to a dynamic loading [10].

The model is also validated by experimental study. It is also observed from simulation results that to increase the power harvesting efficiency of the harvester the piezoelectric patches should be placed close to the fixed end of the cantilever and by keeping the excitation angular frequency of the piezoelectric coupled harvester close to the resonant frequency [10]. Piezoelectric materials can also be used to harvest energy from high rise buildings when subjected to dynamic motion. Xie et al. (2013) developed a mathematical model to calculate generation of electrical charge and voltage from high rise buildings by using a piezoelectric coupled cantilever with a proof mass. For the optimization the effect of length and location of the piezoelectric patch, excitation frequency and also thickness ratio of the piezoelectric patch to the host beam were investigated.

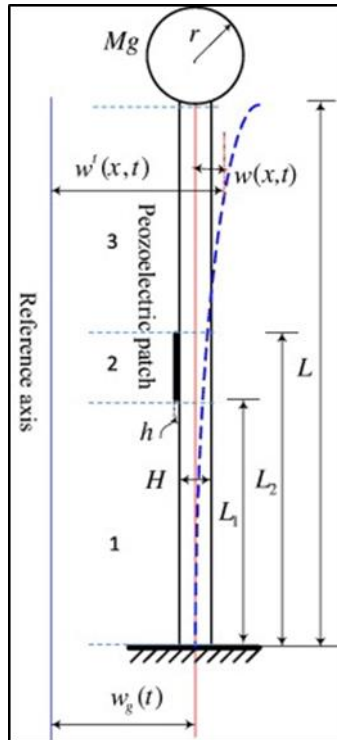


Figure 1-2 Analytical model of the piezoelectric coupled cantilever attached by a mass subjected to a base motion to represent the harvester on a high-rise building [11].

In this research it is found that with an optimum design of the harvester 28% energy harvesting efficiency can be obtained. They also found that the energy harvesting efficiency can be increased by placing the piezoelectric patch close to the fixed end of the cantilever and also when the excitation frequency is close to resonant frequency [11].

Researchers also used piezoelectric energy harvesters for wind energy harvesting. Besides wave energy wind energy can also play a vital role to meet the necessities of human life power requirement. The flowing power of winds is usually from a typical intensity of 0.1–0.3 kW/m² to 0.5 kW/m² on the earth surface along the wind direction, while the flowing power of ocean wave is round 2–3 kW/m² under the ocean surface along the direction of the wave propagation [12]. Wu et al. (2013) introduced a wind energy harvester consisting of a cantilever attached with

piezoelectric patches and a proof mass. They calculated the charge and voltage generation from the piezoelectric patches with the help of theoretical model. The concept of that research was to utilize the cross wind induced vibration of the piezoelectric patches attached to the cantilever because of the vortex shedding phenomenon.

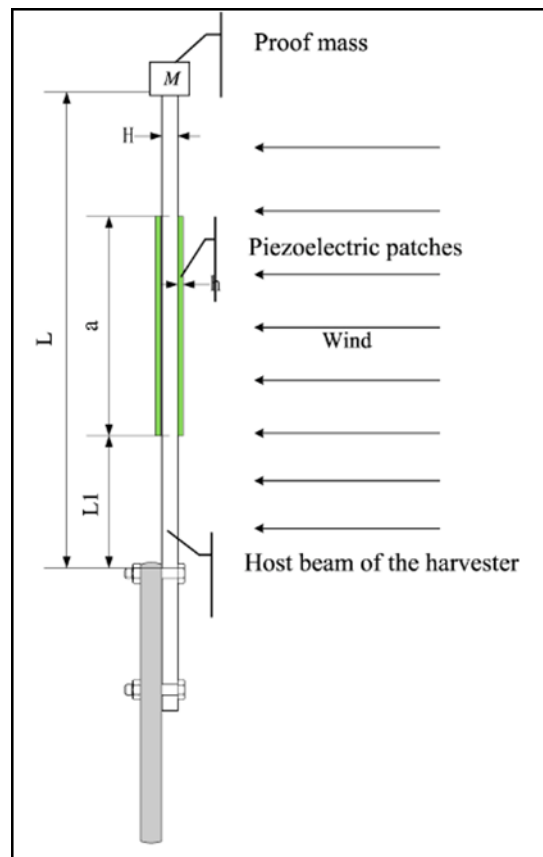


Figure 1-3 Piezoelectric harvester subjected to wind load [13].

In that research the influence of the length and location of the piezoelectric energy harvester on power generation is conducted. Research findings shows that it is possible to generate about 2 W of power from a harvester by optimizing various parameters [13]. Priya (2005) described a theoretical model about harvesting energy from piezoelectric bimorph transducers mounted on a windmill in low frequency range. A prototype piezoelectric windmill consisting of ten piezoelectric bimorph transducers were operated and it was found that 7.5 mW of power can be

obtained with the wind speed of 10 mph [14]. Li et al. (2011) studied and tested the conversion of wind energy to electrical energy by using a bioinspired piezo-leaf architecture by wind-induced fluttering motion. They found that one single leaf can generate about 600 μ W of power [15].

With regards to renewable energy resources, the hydro power, wind and solar energy have been well studied [16] and widely used taking up 3.34%, 0.51% and 0.062% of the total world energy consumption, respectively. However the utilization of ocean energy is still in the early stage (0.001% of the total world energy). It should be noted that abundant ocean energy is available at most coastal area of the world. For example, the ocean wave energy was measured at about 100 kW/m of wave front on the Pacific coast in Canada [17]. In 2009 the total investment in renewable energy capacity (excluding large hydro) was about \$150 billion [18].

One of the technical barriers for ocean wave energy harvesting is the lack of highly efficient, robust and cost effective energy harvesting devices. Conventional devices, i.e. oscillating buoys that drive magnetic-electric generators received few attention from the industry, partially due to the difficulty in deployment, high cost for maintenance, and relatively low efficiency of energy conversion [19]. The development of ocean wave energy harvesting techniques could be able to provide an alternative solution to the electricity requirement. Piezoelectric plates can be used to harvest energy from ocean waves. Taylor et al. (2001) developed a new energy harvester named 'eel', consisting of long strips of piezoelectric polymer, which can convert the mechanical energy of water in ocean or river flows into electricity. It is found that when the 'eel' harvester is under oscillating motion it can generate a power of 1 W in a nominal 1 m/s water flow [20]. Gao et al. (2013) developed a flow energy harvester having piezoelectric cantilever with a cylindrical extension. This flow harvester can harvest energy from ambient flows for example wind and water streams because of the flow-induced vibration of the cylindrical extension makes the piezoelectric

cantilever to vibrate. They made prototypes and tested them [21]. Xie et al. (2014) used piezoelectric patch to harvest energy from transverse ocean waves where they developed a mathematical model to calculate voltage and generation of charge by the harvester. The findings of the research is that under certain specified conditions it is possible to get around 30 Watt of power generation from a harvester [22]. Zurkinden et al. (2007) worked on harvesting wave energy from wave motions and designed a piezoelectric polymer energy harvester. In that research they investigated the power generation that can be found by using that kind of energy harvester, however the generation is small [23].

The ratio of the mechanical energy input to the generation from the piezoelectric energy harvester is a very significant factor to be considered in case of designing a practical energy harvester. That is the reason why optimization of the piezoelectric energy harvester is essential. In recent years some of the research works are conducted to optimize the energy harvesting efficiency from the piezoelectric energy harvester. Sodano et al. (2005) studied the ability of three types of piezoelectric devices to convert the ambient vibration energy into electric energy generation. The three types of harvesters are made from three common types of piezoelectric materials they are, lead zirconate titanate (PZT), bimorph Quick Pack (QP) actuator and the macro-fiber composite (MFC). The research found out that among all the three materials PZT is most suitable for recharging a discharged battery [24]. Xie et al. (2014) developed a ring piezoelectric energy harvester by using magnetic forces and generated power is calculated with the help of a mathematical model. The harvester consists of an outer ring stator and an inner ring rotator. The design involves choosing the optimal length of the piezoelectric harvester and also the optimal rotating speed of the rotator ring.

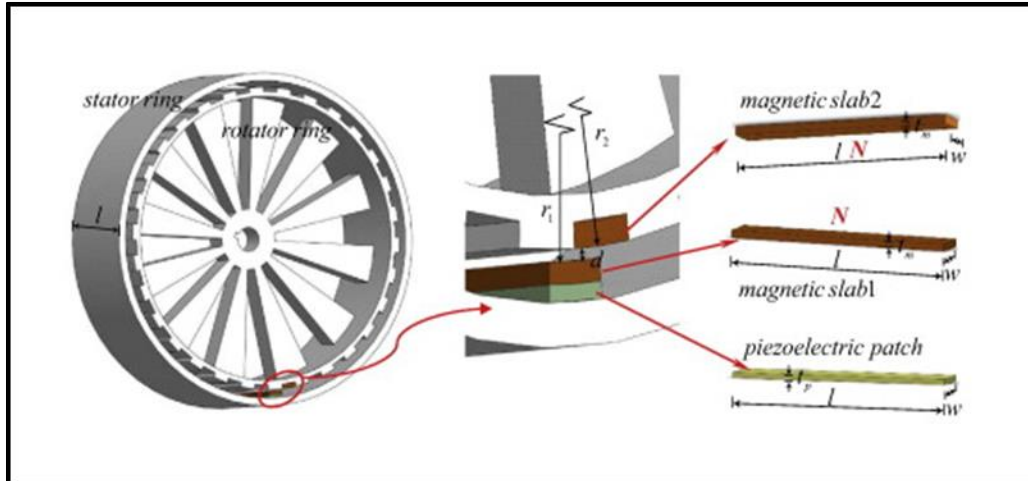


Figure 1-4 Schematic diagram and geometries of the piezoelectric energy harvester [25].

It was found that with specific selection of geometric parameters up to 5274.8 Watt of power generation can be obtained [25].

Minazara et al. (2013) conducted their research about harvesting piezoelectricity from mechanical vibrations of bicycles by using piezoelectric generator on bicycle handlebar. In their research after getting the electrical energy from the piezoelectric energy harvester a static converter was used before supplying it into the electrical device. However, the dynamo they used there breaks easily and the generated power was 3.5 mW which is small [26]. Li and Vladimir (2014) studied modeling of piezoelectric energy harvester and its potential in an educational building, where energy harvesting potential of commercialized piezoelectric tiles were analyzed [27]. Ende et al. (2012) talked about using piezoelectric harvester in tires of automobiles [28]. Malotte (2012) conducted his Master thesis on a research, determining feasibility of using piezoelectric tyre for energy harvesting in bicycles having no emission. In that research they made a tyre prototype and attached the piezoelectric harvester outside the tyre and inside the tyre the energy storage device was kept. However, it has less power generation, costly and fragile [29]. Danesh et al. (2011) in his paper

talked about different approaches to form mathematical methods to conceptualize the potential of generating piezo-electricity but the approach act only as guideline and are based on prominently used mathematical model [30].

1.2.2 Pavement Energy harvesting processes for deicing roads and bridges

Some of the researchers have worked on deicing of roads and bridges. Yehia et al. (1998) studied two large slabs for bridge deck deicing experiment in natural environment where they monitored the power consumption and deicing performance and also the cost estimation was done to see the effectiveness of using concrete overlay on bridge deck. An average power generation of 48 W/m^2 can be generated by using conductive concrete to raise slab temperature from -1.1°C (30°F) to 15.6°C (60°F) in 30 minutes, found on a small scale slab heating experiment [31]. Chang et al. (2009) studied a concrete which is self-heating and containing embedded carbon nanofiber paper where the carbon nanofiber paper acts as electric resistance heating element. They did some laboratory testing for different compositions of concrete, analyze the electrical power consumption, rate of heating and also cost estimation [32]. Gao et al. (2010) studied the slab solar collection (SSC) process which is made of cement concrete and hydronic pipe imbedded in that and stores solar energy in summer to melt ice and snow on the road in winter. In the experiment, they found that in summer the average heat collecting capacity can be up to $150\text{--}250 \text{ W/m}^2$, which is about 30% of the solar heat [33]. Pan et al. (2015) studied snow melting of road by using hydronic asphalt pavement which utilizes the solar radiation and based on the theory that fluid circulating through the pipes network imbedded in the asphalt pavement can capture the solar energy and store for later use. They also conducted numerical simulations. However the use of pipes in pavement can cause harmful effects [34].

It is noted that snow melting by applying the thermos requires continuous electrical energy input. For the public traffic facilities, such as road pavements, that cover large area, the energy supplement for the thermos is always the economy problem that restrict the practical application of the technique. However if energy can be harvested by using piezoelectric energy harvesters inside the pavement, then that harvested energy can be used to produce heat and to melt the snow on roads.

1.2.3 Pavement energy harvesting by using piezoelectric energy harvesters

Researchers have been concentrating on harvesting energy from road pavement to support the on-site electrical devices on the road. The generated energy can also be used to help ice melting in cold countries. Innowattach (an Israel based organization) carried a pilot project with Israel national road company to demonstrate the use of energy harvester below roads using their own designed piezoelectric harvester named IPEG but technical data is not available publicly (Innowattech 2014) [35].

Piezoelectric materials can also be used as sensors inside the pavement to monitor vehicle flow on roads. Li et al (2006) developed a cement based piezoelectric sensor to monitor walking person or passing vehicle. In that research they also carried out experiments for monitoring person flow and also vehicle flow by considering the road made of steel molds and as the passing vehicle they considered handcart with different loads and found that the sensor can reliably detect moving vehicles [36]. Xiang et al. (2013) considered the piezoelectric pavement as a Bernoulli-Euler beam and they made a mathematical model over which after applying complex numeral approaches and boundary conditions relationship between voltage and different parameters were shown but no specific talk about generated power was made in this analysis [37]. Ali et al. (2011) presented the

vibration based model to power wireless devices on bridges using piezoelectric harvester [38]. Tianchen et al. (2014) studied vibration energy harvesting system for railroad safety by using piezoelectric drum transducer during rail movement. The piezoelectric transducer can generate 30 mW power which is relatively small [39].

Zhang et al. (2014) studied piezoelectric cantilever based harvester for energy harvesting from concrete slab-on-girder bridges. They used ANSYS and MATLAB for simulation considering two conditions, one for single vehicle passing through and another for continuous vehicle flow. They also studied the optimum vehicle speed and position of the energy harvester [40]. Duarte et al. (2013) studied pavement energy harvesting system which captures kinetic energy and convert it into electrical energy. They used blocks of different shapes having the mechanism that can generate electrical power with small displacement on the vertical axis each time a person or vehicle moves over the block area. It generates electric energy for public illumination, outdoor advertising, traffic lights, or electrical supply [41]. Xiang et al. (2014) studied theoretical model of piezoelectric energy harvesting from traffic induced deformation of the pavement which can harvest piezoelectricity. They used Fourier transform and the residue theorem. In that research they considered the pavement as Bernoulli–Euler beam on an elastic foundation and the load from the moving vehicle is considered as a moving line load. The power generation of around 5.33 W can be found by the piezoelectric harvester embedded in the pavement with the velocity of the passing vehicle as 150 m/s without considering the damping [42]. Xiong et al.(2012) in their work stated that vehicle induce deformation in pavement and that deformation in pavement can harvest piezoelectricity, they discussed about power generation based on vibration induced in pavement by moving vehicles and gave a review about the optimum power collection system to give usable power [43]. Zhao et al. (2010) designed a Cymbal piezoelectric transducer for harvesting energy

from asphalt pavement where they used finite element analysis (FEA) for the calculations. In that research they suggested an optimum sized Cymbal energy harvester and they found out that the potential electric energy harvested from pavement increases with the increase in diameter of the Cymbal but the efficiency decreases with the increase in size of the harvester. It was reported that the maximum electric power generation by using such an optimum sized harvester is 1.2 mW at 20 Hz vehicle load frequency [44]. Tao et al. (2014) developed one prototype pavement generator consisting of PZT piles which can harvest more than 50 KW/h from one lane 1 kilometer highway if there is heavy vehicle movement on pavement by placing the harvester at a depth of 4 cm from the surface layer of the pavement. After considering the stress, displacement, stability and also the cost of the harvester, 8-16 round shaped PZT piles are suggested for one energy harvester. They used finite element method to determine the performance of seven typical transducers [45]. Zhao et al. (2012) discussed about the energy harvesting efficiency of some piezoelectric transducers like multilayer, MFC (Macro-Fiber Composite), Moonie, Cymbal, Bridge, and THUNDER) and they did a comparison among them by using finite element analysis (FEA). In that research for energy harvesting from asphalt pavement with reasonable efficiency and moderate stiffness the Cymbal and Bridge type transducers were suggested. The lifetimes of those energy harvesters are also reasonable but when the applied stress exceeds a certain value then the bridge fails because of stress concentration between end cap and PZT at the inner corner of contact area [46].

Based on the literature review described above, the researches that has been done so far on harvesting piezoelectricity from roads mainly consider the harvester as Euler beam or induced vibration on harvester and cost approximation. The accurate stress distribution model in pavement with passing vehicles to guide the proper design of the piezoelectric harvester for obtaining more electrical energy has not been well studied. One of the most important motivation of my research

is considering the moving vehicle load as distributed load, because most of the research works on harvesting energy from piezoelectric energy harvester inside the pavement considered the moving vehicle as a point load and calculated stress distribution inside the pavement based on that point load. Another motivation of my research is that in most of the research they followed one model to get the results without validating the results by using another modeling technique. Moreover, optimization of the piezoelectric harvester for highest amount of energy harvesting in the pavement has not been well studied and the power generation they got was actually not sufficient for melting ice/snow on roads in cold countries.

1.3 Thesis Objectives

The primary objective of that research is to harvest energy from piezoelectric energy harvesters placed inside the pavement during vehicles passing through the harvester embedded pavement. In order to realize that objective the following tasks have been conducted,

- Developing accurate stress distribution model in pavement with passing vehicles.
- Designing piezoelectric energy harvesters in road pavement.
- Calculating the maximum power generation from the harvester by optimizing parameters like depth, thickness, length, width and velocity.
- Validation of the mathematical results found from MATLAB simulation with the FEA results obtained in ANSYS.
- To utilize the vibration produced by the passing vehicle in the piezoelectric plate as a base motion for the attached cantilever energy harvester to increase the power generation further.
- Brief study of the possibility of ice melting with the power generated by the piezoelectric harvester in pavement.

1.4 Thesis Outline

The following thesis has been divided into four sections. The outline of the thesis is given below.

- First chapter describes the introduction, literature review and then the knowledge gap and motivation of my research followed by thesis objective.
- Second chapter propose an accurate semi-mathematical model of the pressure bulb in pavement. An energy harvesting process is described with passing vehicle, when a single piezoelectric patch energy harvester is placed inside the pavement. The effects of changing vehicle velocity, load on the tyre of the vehicle wheel, length of the patch and location of the Piezo-electric patch placement inside the flexible pavement on the generated power are also discussed.
- In chapter three an improved design of the piezoelectric patch harvester is proposed which is a piezoelectric composite plate harvester to increase the average power generation. Impact of various parameters like depth of the harvester placement inside the pavement, velocity of the passing vehicles and changing dimension of the harvester are also discussed, followed by an optimum design of the harvester.
- To increase the power harvesting efficiency furthermore in chapter four a cantilever energy harvester is attached inside the composite plate harvester box model to utilize the vibration produced by the passing vehicle in the piezoelectric plate as the base motion for the cantilever.
- Conclusions and future works.

Chapter 2

This chapter discusses about harvesting piezoelectricity from roads with piezoelectric patches based on a new semi-mathematical model of pressure bulb in the pavement. A concept of harvesting energy from the piezoelectric material layer embedded in the flexible pavement is studied. For the first time, a numerical model based on the Westergaard's stress model is proposed to calculate the three dimensional (3D) stress distribution in the pavement and to find the potential of energy harvesting from the piezoelectric layers placed inside the pavement. Based on the proposed numerical model, simulations are conducted to reveal the effects of changing vehicle velocity and location of the piezoelectric patch inside the flexible pavement on the generated power. Moreover, an attempt for designing an optimum piezoelectric unit in piezoelectric layer is done to obtain maximum power generation. Significant increase in traffic at present time shows a potential of larger scope of power generation by the piezo-electric layer in pavement.

2.1 Semi-analytical Model of pressure distribution in pavement under distributed load

When load is applied over the soil mass, pressure is transferred to the soil mass causing deflection/deformation in it. Soil itself is a complex structure which vary from place to place. In general to avoid complexities, for small deformation conditions, soil is assumed to be an elastic medium, and stress and strain can be calculated accordingly in soil mass. Boussinesq and Westergaard are the most commonly used equations to describe the stress flow based on the simplification that they offer an approximation of stress. Westergaard's is an accepted equation for approximation of stress distribution in soil, and it also gives us an approximate idea about the stress on piezoelectric layer to realize the corresponding power harvesting. Westergaard's assumptions are -

- The stiff layers are spaced very closely such that the compound material has the characteristics of a homogeneous material.
- The thickness of the stiff layers are negligible compared to that of the soft materials.
- The stiff material is inextensible and thus prevents any horizontal strain in both the soft and stiff layers.

In Boussinesq equations they mainly consider loading at a point and used for homogeneous and isotropic materials [47]. However soil is neither isotropic nor homogeneous. In calculation by using Boussinesq equations modulus of elasticity and Poisson's ratio are not required. However, stress distributes in soil medium in the shape of a bulb, which is called pressure bulb and is also referred as stress isobars. Westergaard's model assumes soil to be an elastic medium of semi-infinite extent but containing numerous, closely placed, horizontal sheets of negligible thickness of infinite rigid materials, which permits only downward deformation of the mass as a whole without allowing it to undergo any lateral strain as also mentioned by Punmia et al. (2005, p.316) [48]. Taking Westergaard's assumptions is more reasonable for this study because piezoelectric ceramic layers can be considered as one layer in the stratified soil mass, and only vertical loading on the piezoelectric layer is considered because it is the most significant load in pavement vehicle interaction. Westergaard's is an accepted equation for approximation of stresses and it also gives us an approximate idea about the stress to realize the corresponding power. The pavement considered in this research is asphalt pavement. The Westergaard's model of three dimensional pressure distribution is not suitable for concrete pavement. In case of concrete pavement the stress distribution model inside the pavement will be different because concrete pavement is not flexible. In this research piezoelectric patch, plate and beam models are designed and temperature effects on pavement materials property variation is not considered.

When vehicle moves over the pavement, applied load from the wheel is propagated in soil mass through the contact area between the vehicle tyres and the pavement. The contact area of a vehicle tyre with road is complicated to be traced, but for most study and analysis it is assumed to be circular and the contact radius is given by Equation (1) (Moazami et al. 2011) [49],

$$a = \sqrt{\frac{F}{\pi P}} \quad (1)$$

where ‘ a ’ is contact radius, ‘ F ’ is applied force and ‘ P ’ is Pressure of tyre. In general pressure of tyre for heavy vehicles is 120-130 pounds per square inch (P.S.I) and for car tires it is 35-44 P.S.I.

Design of flexible pavement is done in equivalence to standard axle load, which is 80 KN (Indian Road Standard, IRC 37-2001, pavement interactive 2014). In this study for defining a path we have carried out simulations with standard axle load which is 40KN over each wheel, but the proposed mathematical model for finding generated power can also be used for other wheel loads (discussed in results section).

In this study, a layer of 2 cm thick piezoelectric material is placed below the road surface in pavement structure. Piezoelectric layer extends in horizontal plane at fixed depth, which are arranged to form a continuous layer. It is also noted that the piezoelectric layer in the pavement is not a whole large layer or patch but composed by many small piezoelectric patches, which are available in the market. We assume the thickness of piezoelectric patches in the piezoelectric layer as 2 cm, which is the reasonable size of piezoelectric patch structures available in the market. The proposed model can give power approximation for any thickness or size of piezo patch/tile/stack structures.

Figure (1)

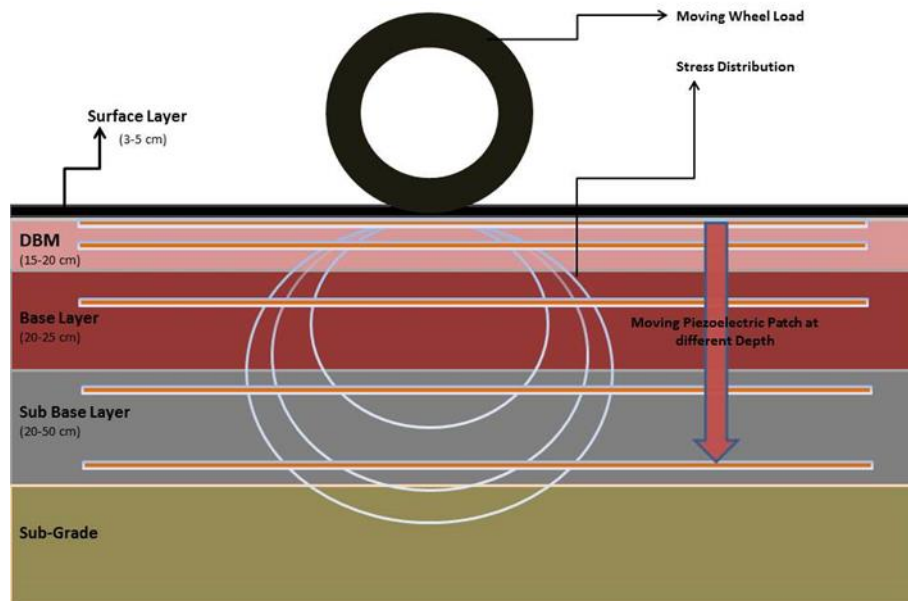


Figure 2-1 A structure of the flexible pavement and the methodology of study in this paper for optimum design of a piezoelectric patch. Load from the tyre distributes in soil mass and the piezoelectric layer is taken at different depths from the surface to find stress and corresponding power produced at every depth.

Figure 2-1, shows the structure of the flexible pavement. The piezoelectric layer can be located at any depth inside the pavement. Pavement design considered in this study is shown in Figure 2-2, it is designed for California bearing ratio (CBR) value of 2% with IRC recommendation for 150 million axle load for serving life of 15 years. The primary objective of this research is to design piezoelectric energy harvester models inside the pavement and not the pavement design.




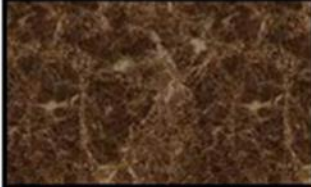
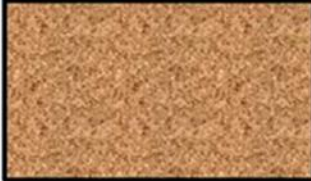
	5cm , $\mu= 0.35$
	20cm , $\mu= 0.35$
	25cm , $\mu= 0.4$
	46cm , $\mu= 0.4$
	$\mu= 0.45$

Figure 2-2 Pavement structure for CBR 2%. μ is the Poisson's ratio of different layers.

When a tyre moves over a flexible pavement, force is subjected from tyres to the pavement and the layers below pavement, which results certain strain in soil mass and the corresponding subjected stress. The total force by each tyre is considered as 40KN. In general, the tyre pressure for such load is 130 P.S.I (max), which is 900 kPa. From Equation (1) the contact radius is found to be 12cm. Westergaard's model in Equation (2) gives the value of stress at any point in the pavement subjected to a point load at radial distance of r from the center of the contact area between the tyre and the pavement surface as shown in Figure 2-3.

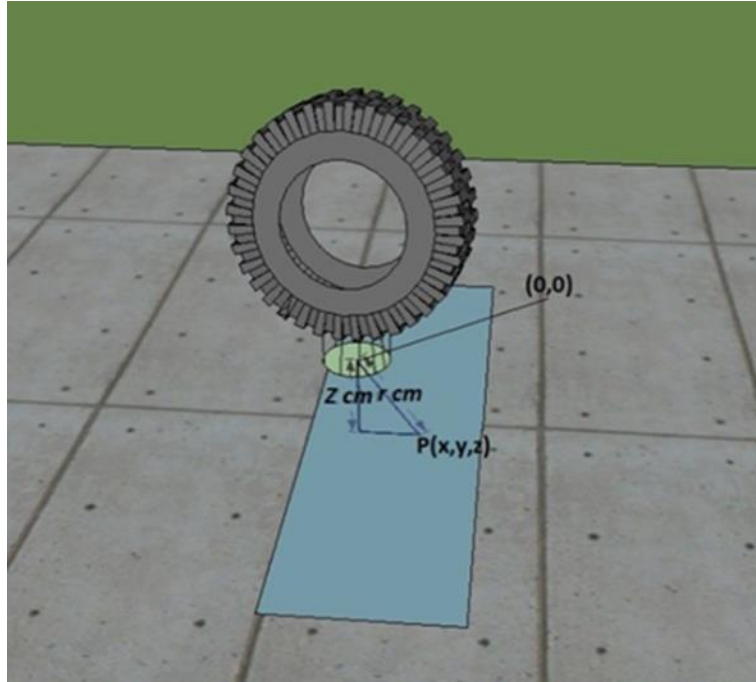


Figure 2-3 Contact of the tyre and pavement and interaction with point P, where stress is to be found (based on Westergaard's model).

Based on the finite element numerical method, the circular contact with radius of 0.12 m is divided into N small squares with edge length of 0.001m, and the total load of 40KN is distributed evenly over the small squares.

Considering each square as a point load as shown in Figure 2-4, for each point load of the n th small square, the value of stress at every point in the pavement below the loading area and on the piezoelectric layer is calculated till 6 metre length and width and 1.5 metre depth from centre of the contact area with Equation (2) (6m x 6 m x 1.5m is a box, in which pressure bulb is calculated and studied under influence of the load from the wheel).

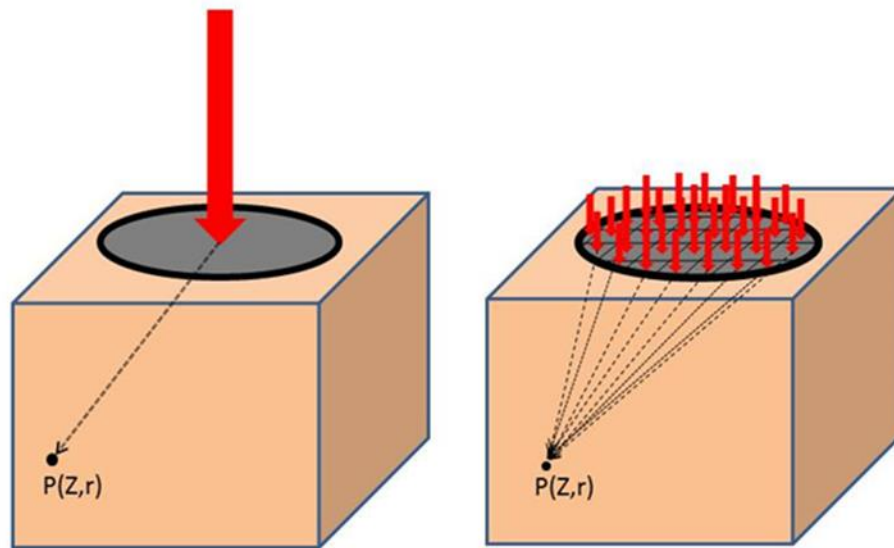


Figure 2-4 Distribution of force over contact area to find stress at point P . (contact area is divided into N equal parts and force is distributed equally above it and the resultant of all the point forces at any point gives total stress).

In order to determine the accuracy of the assumption of dividing the contact radius into small areas having edge length of 0.001 m, the convergence calculation is conducted. For the convergence test, the edge length of the small squares are changed from 0.001 m to 0.02 m. For that calculation, the position of the vehicle wheel is considered at the middle of the contact area between the tyre and the pavement. The calculation is done for a certain point which is the middle point of the piezoelectric patch in the pavement.

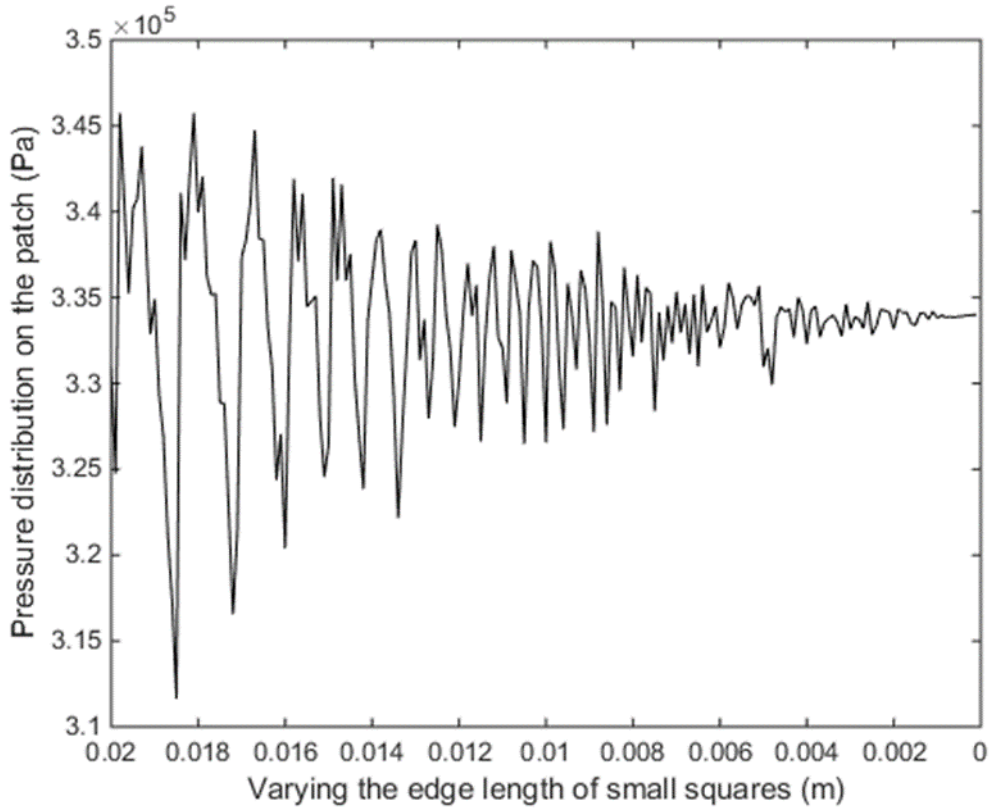


Figure 2-5 Variation of pressure distribution at the middle point of the piezoelectric patch with varying edge length of small squares from 0.001m to 0.02 m.

The plot given in Figure 2-5 shows the convergence study in area of the small squares. It is seen that the pressure value converges with very tiny variation when the edge length of each small square area is smaller than 0.002m. Therefore it can be stated that the assumption of taking the value of the edge length of each small square as 0.001m is correct.

To calculate the stress distribution in the pavement due to one point load, Westergaard's equation is given as,

$$\sigma_z = \frac{Q}{2\pi n^2 Z^2 \left(1 + \left(\frac{r}{nZ}\right)^2\right)^{3/2}} \quad (2)$$

where σ_z is the stress along the depth direction of the pavement, generated by one point load on the n^{th} small square ($\frac{KN}{m^2}$); Q is the point load (KN), and Z (m) and r (m) are the depth and radial distance of any point in the pavement from loading point of the contact surface as shown in Figure 2-3.

$$n = \sqrt{\left(\frac{1-\mu}{2-2\mu}\right)} \quad (3)$$

μ is the equivalent Poisson's ratio. The factors r and Z in the Equation (2) are shown in Figure 2-3 and Figure 2-4.

Equivalent Poisson's ratio is the weighted arithmetic mean of the Poisson's ratio of each layer of the pavement,

$$\mu = \frac{\mu_1.h_1 + \mu_2.h_2}{H} \quad (4)$$

where h_1 and h_2 are the depths of the homogeneous layers in pavement and H is the total depth from surface ($H=h_1+h_2$). To minimize the error in the calculation we have used the "equivalent Poisson's ratio" which is the weighted mean of all layers in the strata. With this assumption, it will be possible to calculate stress at different layers and its behavior at junctions, as isobars of stress would not be continuous. Poisson's ratio of different layers varies from 0.3 to 0.45 (0.3 is for PZT layer). Since the variation in Poisson's ratio is small, the error caused by assuming the equivalent Poisson's ratio after placing the piezoelectric patches inside the pavement will not be significant. With the variation of the depth, Poisson's ratio and radial distance of different layers average power generation will be different but the trends of the results will be similar.

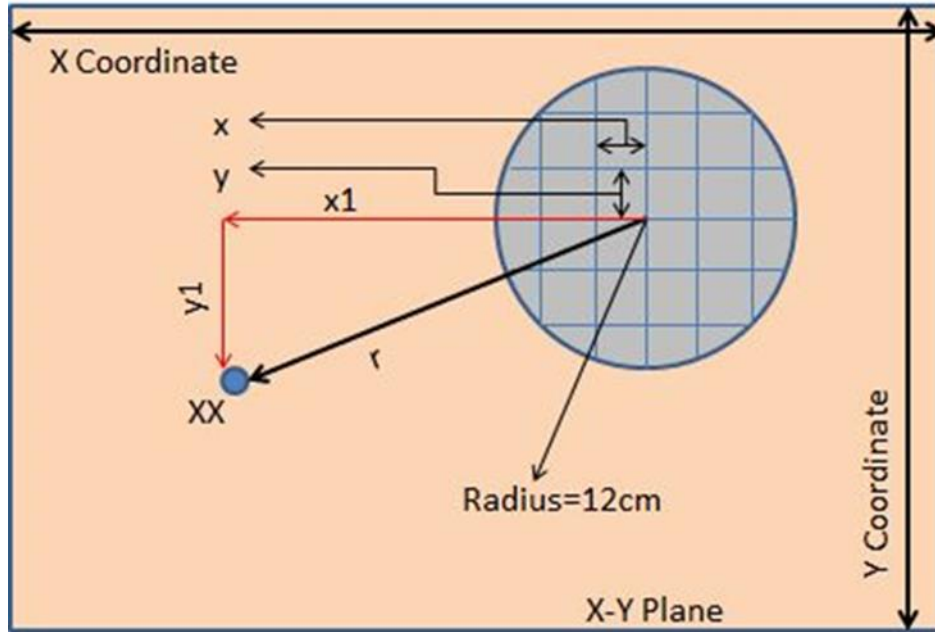


Figure 2-6 2-D top view of the loading/contact area on the pavement.

Figure 2-6 shows the two dimensional top view of the loading area on the pavement. XX is a study point in the box shown in Figure 2-6, on which total stress is computed due to all loading points in contact area.

We assume the loading area is in x - y coordinate plane. Radius of contact area is 12 cm. Illustrating for a point say XX in study area at depth Z and distance of $x1$ and $y1$ from the center of the circular contact area between the tyre and the pavement surface, the distance from XX to the center point of the loading area is $\sqrt{(x1)^2 + (y1)^2}$ cm. For any n th ($1 \leq n \leq N$) loading point in the circular contact area, radial distance at the study point XX is given as $r = \sqrt{(x1 - x)^2 + (y1 - y)^2}$ cm, where x and y are the horizontal and vertical distances from the n th loading point to the centre of the contact area (x, y shows mapping of point load in circular loading/contact area). x & y changes by 0.1 cm by all possible combinations, in such a way that all loading points in circular contact area i.e. $\sqrt{x^2 + y^2} \leq 12$ will be considered to calculate the stress distributed at point XX. With

Equation (2), the total stress generated at the study point XX can be calculated as $\sigma_z = \sum_{n=1}^N \sigma_{zn}$ with a fixed Z and varying r .

It is noted that the equivalent Poisson's ratio depicts significance of thickness of each layer in pavement for the amount of stress.

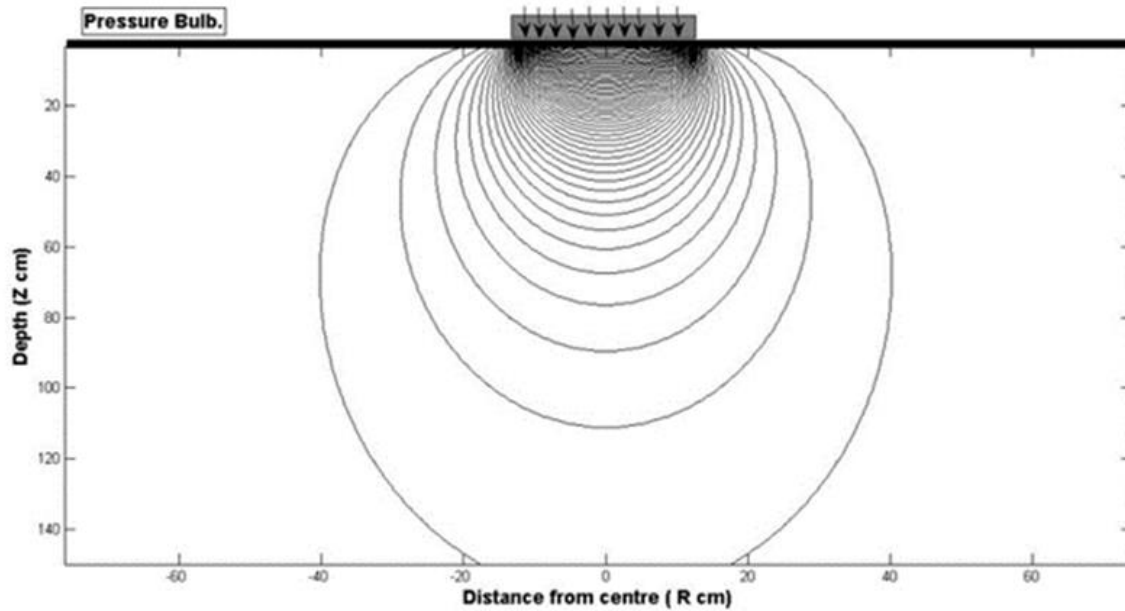


Figure 2-7 The pressure bulb formed due to circular loading on pavement.

The final result that we are looking from the Westergaard's model is the stress in the layer of piezoelectric patch at different depths, which is in the pressure bulb as shown in Figure 2-7. Based on Westergaard's assumption that only vertical load acts significantly in pavement stress distribution, we get strain as

$$\epsilon_z = \sigma_z / E \tag{5}$$

Strain value is obtained on piezoelectric patch corresponding to stress. E is Young's modulus of the piezoelectric material taken as $7.8 * 10^{10} \frac{N}{m^2}$. The strain bulb is formed to show the strain distribution over the piezoelectric patch/layer located at different depths as shown in Figure 2-8.

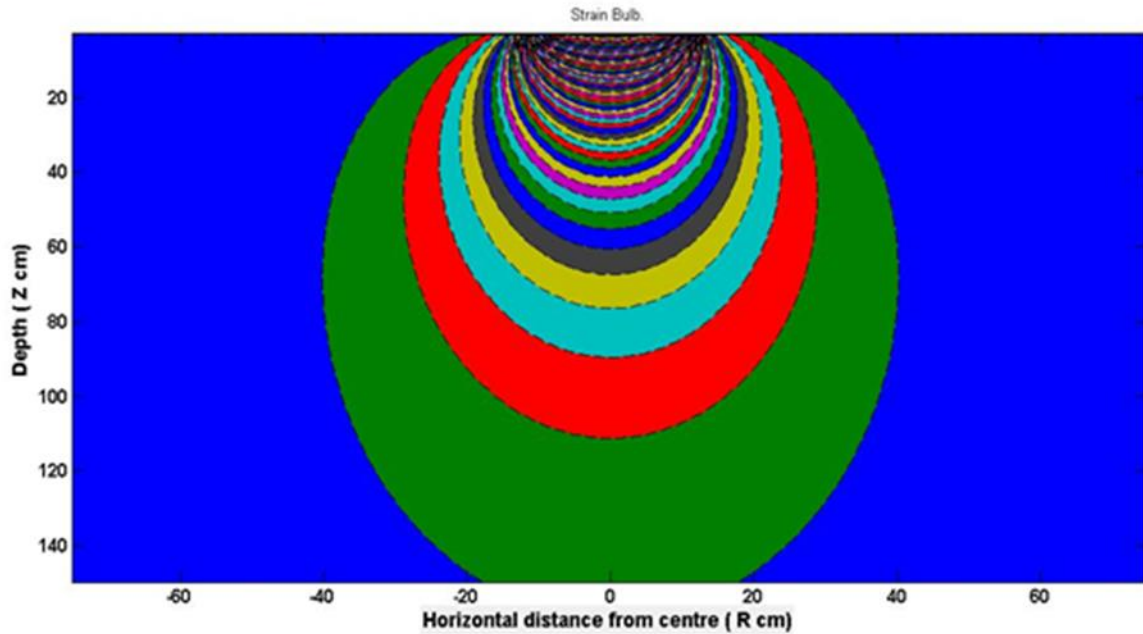


Figure 2-8 The strain Bulb showing strain distribution on piezoelectric layer at different depths.

Knowing strain distribution over the piezoelectric patch, the surface charge can be computed as,

$$D(t) = \varepsilon z(t) \cdot e_{33} \tag{6}$$

where e_{33} is the piezoelectric constant; D is the surface charge density ($\frac{C}{m^2}$) at any time t .

T is defined as the total period, in which vehicle approaches the pavement with piezoelectric layer from 1 metre distance, passes over it and is at 1 meter distance away. Here distance 1 meter is taken because at distance greater than 1 meter, the stress applied on the piezoelectric layer due to the influence of tyre load is very small and negligible. When the tyre of the vehicle approaches,

stress distribution on the piezoelectric layer starts to increase, t is any time in time period T , the charge distribution can be found over the piezoelectric patch as,

$$Qg(t) = D(t).A \quad (7)$$

where A is the area of the electrode of one piezoelectric patch in the whole piezoelectric layer.

When a vehicle moves over the piezoelectric layer embedded pavement with certain velocity, at any time t , it produces charges on the piezoelectric patches, which is located at a certain depth inside the pavement. Current and voltage generated on a piezoelectric patch can be computed as,

$$I(t) = \frac{dQg}{dt} \quad (8a)$$

$$V(t) = \frac{Qg(t)}{C} \quad (8b)$$

C is the capacitance of one piezoelectric patch, which is given as,

$$C = \frac{\epsilon a.b}{4\pi kh} \quad (9)$$

where a and b are the length and width of the piezoelectric patch, $A=a*b$, ϵ is di-electric constant and K is static electricity constant. h is the height/thickness of the piezoelectric patch (here it is taken as 2cm for the study). We can conceptualize the piezoelectric patch of length say a cm, width as b cm and h as 2 cm is a collection of thin piezoelectric material strips or a homogeneous piezoelectric material electroplated to form the dimension of the patch.

The final generation we are looking for is the average electrical power generated by one piezoelectric patch. The average power generation would be maximum with the optimal design of the patch. In this study, the average electric power generated from the piezoelectric patch is defined by the multiplication of root mean square (RMS) values of the voltage and current generated from

the piezoelectric patch and given as below. The average power generated by a single piezoelectric patch given by this model is calculated in the period T , when a single wheel approaches the piezoelectric patch from 1 metre distance; passes over a piezoelectric patch and is 1 metre away from the piezoelectric patch.

$$P_{avg} = V_{rms} \cdot I_{rms} \quad (10)$$

where V_{rms} and I_{rms} are found by using the V and I in Equations. (8a) and (8b). The following two equations demonstrate how the root mean square values are calculated from the I and V values, which are actually a function of time, t .

$$V_{rms} = \sqrt{\frac{1}{T} \int_0^T V^2(t) dt} \quad (11)$$

$$I_{rms} = \sqrt{\frac{1}{T} \int_0^T I^2(t) dt} \quad (12)$$

2.1.1 Validation through finite element analysis (FEA)

To validate the stress distribution results in the pavement found from proposed mathematical model based on the Westergaard's theory, in this section the results from MATLAB code are compared with FEA results obtained in ANSYS. A model of the pavement is designed using ANSYS workbench design modeler. The pavement has the same material properties as of the pavement mentioned in the numerical modeling section. The Poisson's ratio at first and second layer is kept as 0.35, for third and fourth layer the value is 0.4 and for fifth layer inside the pavement the value of Poisson's ratio is 0.45.

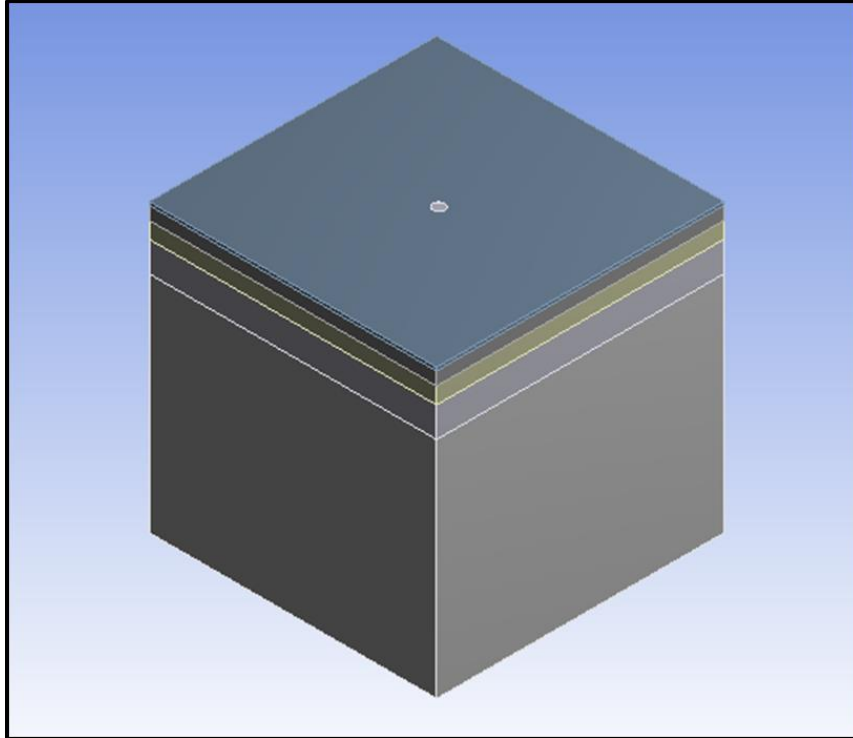


Figure 2-9 3D-modeling of the pavement consisting of five different layers.

Figure 2-9 shows five different layers of the considered pavement having different material properties for each layer. The box considered here having length and width of 440 cm and 440 cm depth. Therefore, the pressure bulb is calculated and studied within a box (4.4 m * 4.4 m * 4.4 m) under the influence of the load from the wheel of the passing vehicle through the contact area. The contact between the tyre and pavement is considered as a circular area and kept same as the one in the mathematical model and MATLAB calculation having radius of 0.12 m. The layers are bonded with each other and closely packed. The amount of pressure distributed over the contact area is considered as 880 KPa with the total load applied on the contact surface of 40KN and the bottom surface is kept fixed.

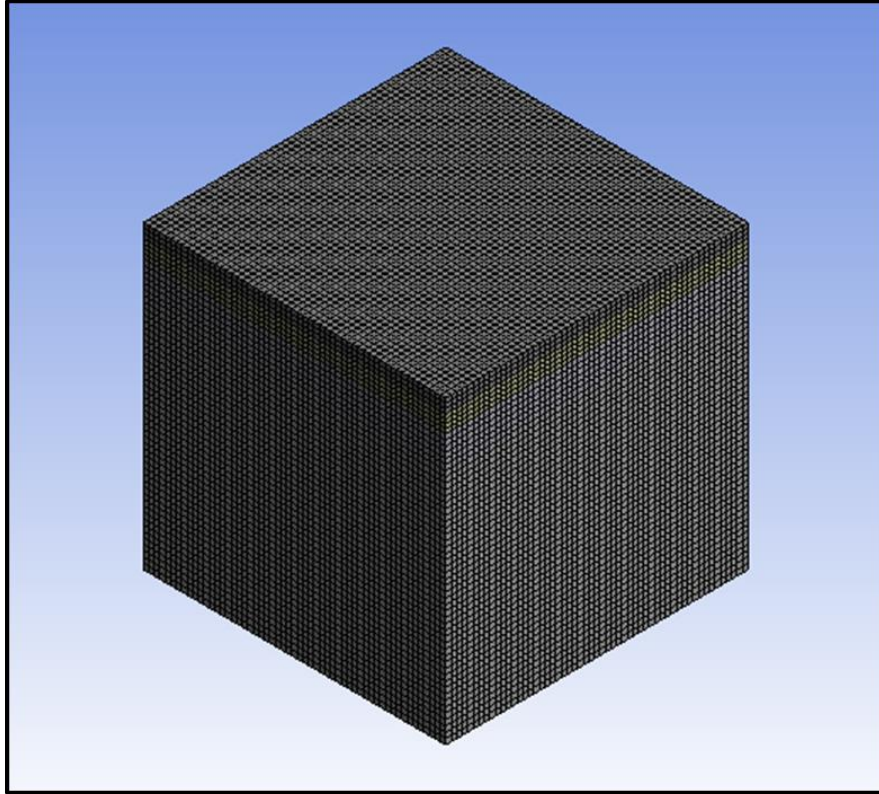


Figure 2-10 3D-modeling of the pavement showing the mesh in four layers (below the first layer) inside the pavement.

Figure 2-10 shows mesh in four different layers of the pavement except the first layer. First layer is not shown here because the piezoelectric energy harvester will be placed below the first protection layer of the pavement. This is the minimum depth where the piezoelectric harvester can be placed without the risk of breaking which is 5 cm. The depth of the harvester placement inside the pavement is made 5 cm in the MATLAB code to compare with the ANSYS results as well. The stresses inside the pavement from both mathematical model and the ANSYS simulations are compared.

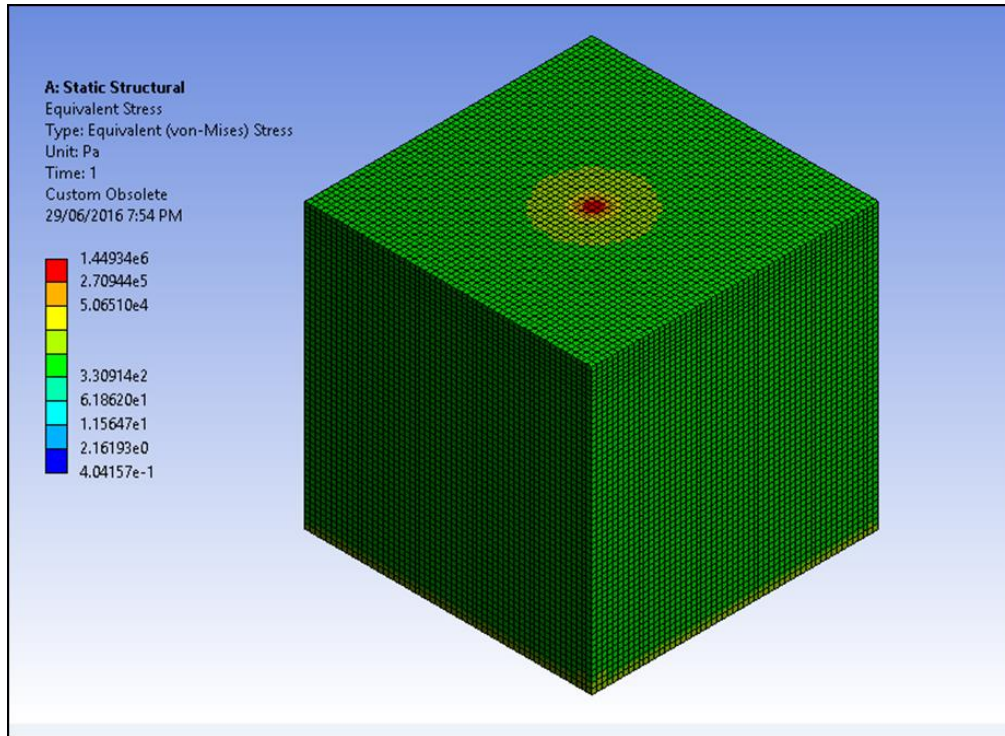


Figure 2-11a Stress distribution inside the pavement due to the applied pressure of the passing vehicle through the contact area.

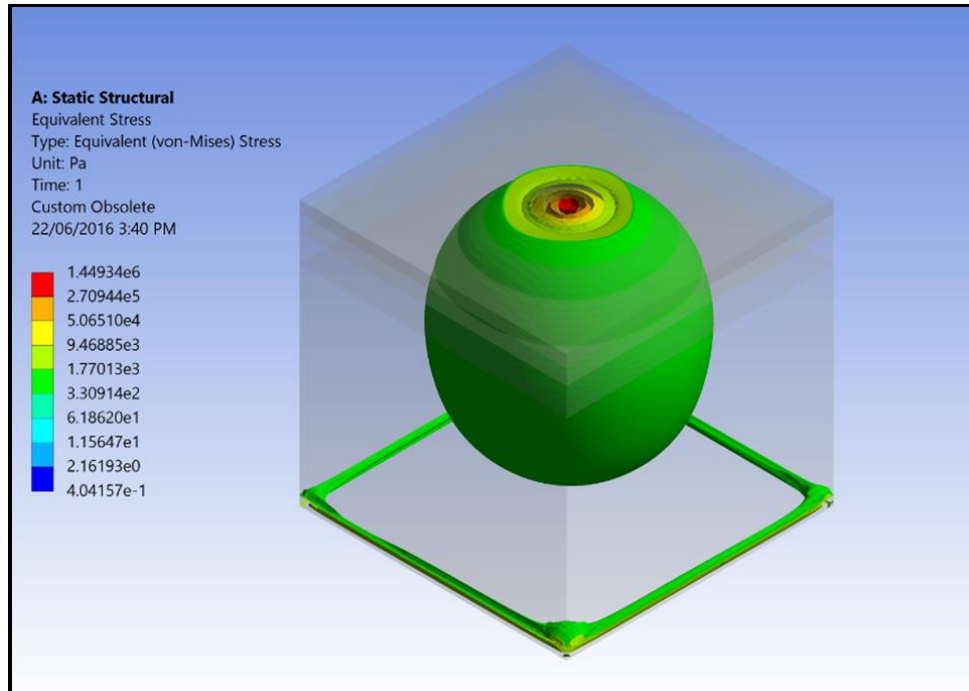


Figure 2-11b Formation of the pressure bulb inside the pavement due to the applied pressure of the passing vehicle through the contact area.

Figure 2-11b, illustrates the FEA 3-D stress distribution inside the pavement which is in the shape of a bulb. It can be seen that the highest stress generates just below the contact area. The undeformed model is also shown in that figure.

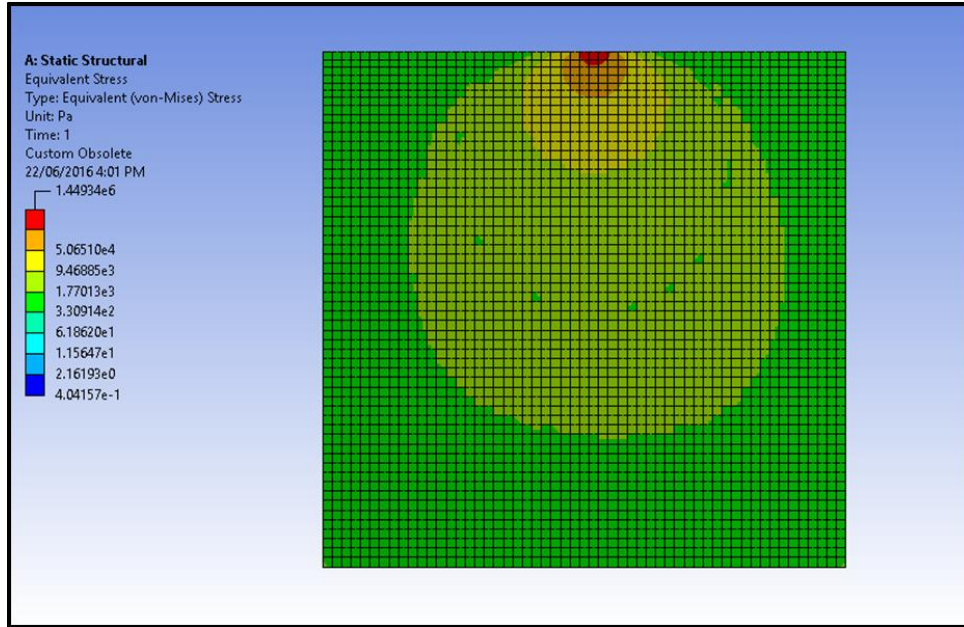


Figure 2-12a

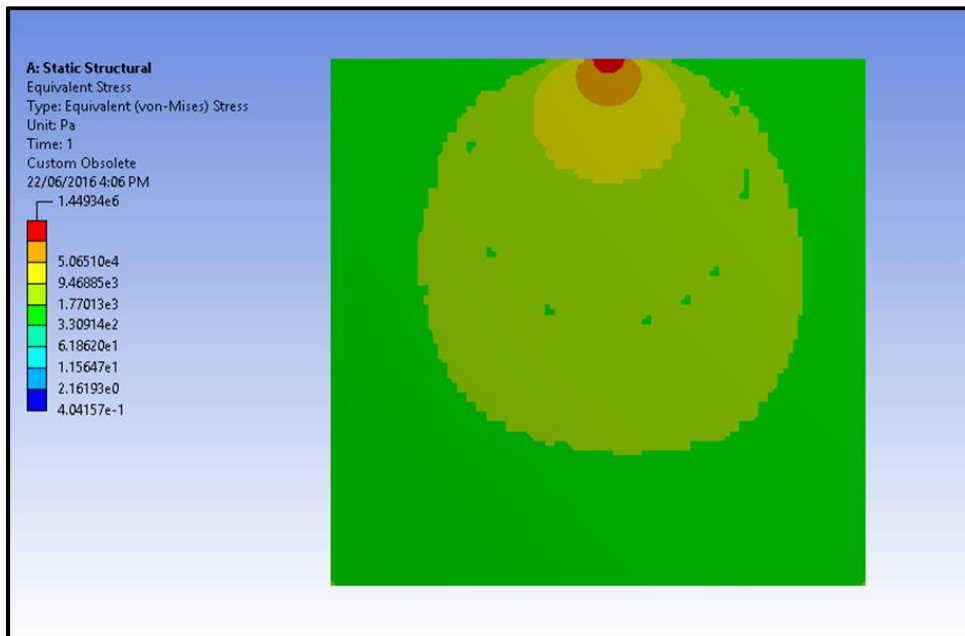


Figure 2-12b

Figure 2-12a and 2-12b Cross-section of the pressure bulb inside the pavement due to the applied pressure of the passing vehicle through the contact area with and without mesh respectively.

Figure 2-12a and **2-12b** illustrates the stress distribution inside the pavement at different layers. We need to consider the stress values in the second layer of the pavement because we have considered that the piezoelectric energy harvester will be placed inside the pavement below the first layer.

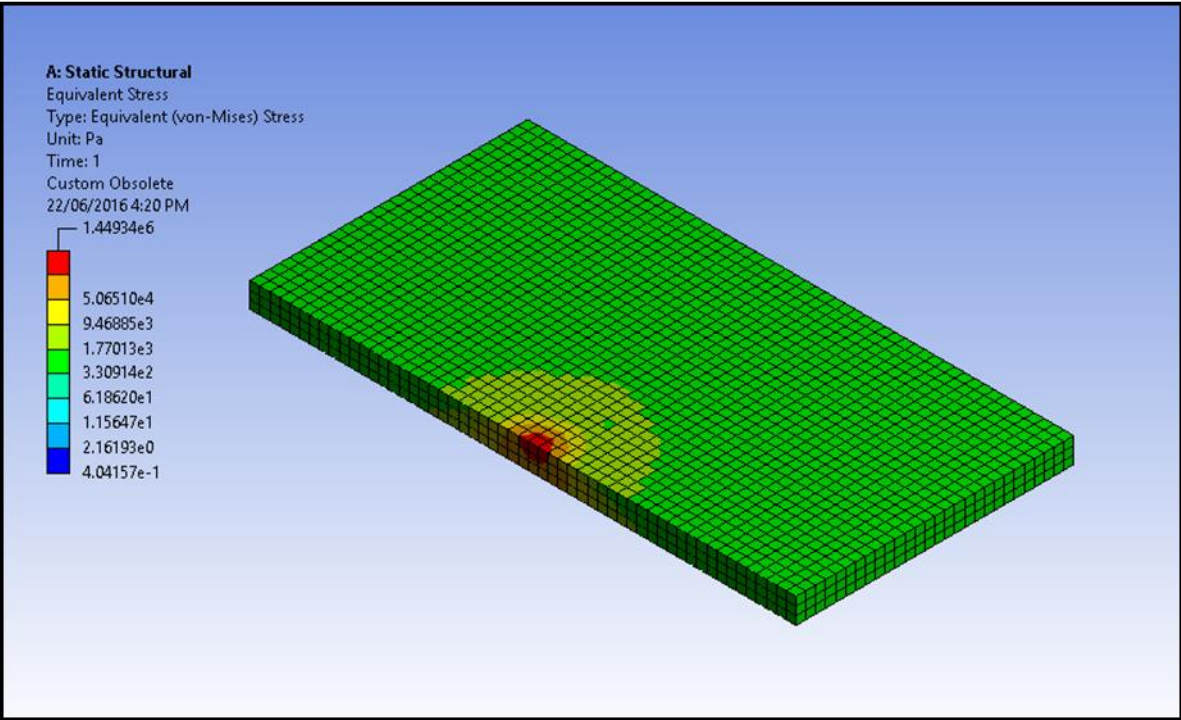


Figure 2-13a

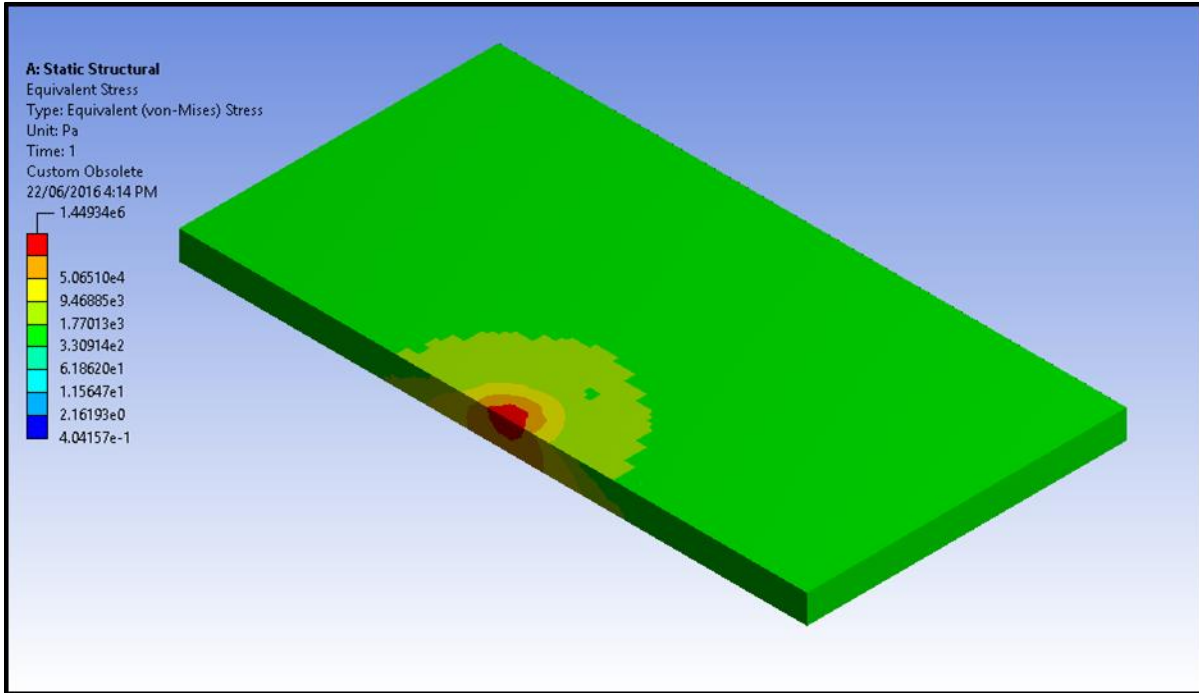


Figure 2-13b

Figure 2-13a & 2-13b Stress distribution in the second layer of the pavement with and without mesh respectively.

2.1.2 Comparison of results between ANSYS and MATLAB simulation for the distributed and single point load model

Following Table 2-3 describes the stress values inside the pavement at different positions located at 5 cm depth from the top of the pavement from both ANSYS and MATLAB simulation results for the distributed load model. The points considered inside the pavement at 5 cm depth from ANSYS simulation results are then compared with the stress values at the same positions found from MATLAB simulation results.

Table 2-1 Comparison of results between ANSYS and MATLAB simulation for distributed load model,

Position of the point considered (Distance from centre) (cm)	Stress data (Pa) (ANSYS)	Stress data (Pa) (MATLAB)	Difference (%)	Average difference (%)
4	6.97E+05	6.9612 E+05	0.126 %	
12	3.54 E+05	3.3719 E+05	4.749 %	
18	5.394 E+04	5.2614 E+04	2.458 %	3.646 %
26	1.314 E+04	1.1949 E+04	9.064 %	
34	5.294 E+03	5.1972 E+03	1.832 %	

From Table 2-1, it is seen that the difference in stress values at different points inside the pavement at 5 cm depth is not obvious. After taking five different points into consideration at 5 cm depth

inside the pavement in ANSYS simulation and comparing with MATLAB simulation results the average error percentage is only 3.646%, which is acceptable. Therefore, it can be concluded that the proposed mathematical model is accurate and efficient to calculate the stress distribution in a pavement with evenly distributed load applied on certain area of the pavement.

Following Table 2-2 describes the stress values inside the pavement at different positions located at 5 cm depth from the top of the pavement from both ANSYS and MATLAB simulation results by considering a single point load. The points considered inside the pavement at 5 cm depth from ANSYS simulation results are then compared with the stress values at the same positions found from MATLAB simulation results.

Table 2-2 Comparison of results between ANSYS and MATLAB simulation for single point load model,

Position of the point considered (Distance from centre) (cm)	Stress data (Pa) (ANSYS)	Stress data (Pa) (MATLAB)	Difference (%)	Average difference (%)
4	6.97E+05	1.5057E+06	116%	
12	3.54 E+05	8.3483E+04	76.42 %	
18	5.394 E+04	2.7764E+04	48.53%	57.62%
26	1.314 E+04	9.1073E+03	30.69%	
34	5.294 E+03	4.4215E+03	16.48%	

From Table 2-2, it is seen that the difference in stress values at different points inside the pavement at 5 cm depth is very large. After taking five different points into consideration at 5 cm depth inside the pavement in ANSYS simulation and comparing with MATLAB simulation results for a single point load, the average error percentage is 57.62 %, which is not acceptable for the accurate consideration of the stress distribution on the piezoelectric energy harvester in the pavement. Therefore, it can be concluded that considering the moving vehicle load as a single point load is not accurate practical. The comparison also prove the accuracy and necessary of the distributed load model.

2.2 Simulations and Discussions

In this section, by using the developed mathematical model, effects of changing vehicle velocity and the depth location of the piezoelectric layer on the generated power from one signal piezoelectric patch are discussed. In addition, the average electrical power from one signal piezoelectric patch is computed for different sizes of piezoelectric patch to obtain an optimum design that can be used in flexible pavement to get maximum power generation from the whole piezoelectric layer.

In this research, entire layer of the piezoelectric material in pavement is actually a setup of several piezoelectric patches with the same dimension that are kept together. A moving vehicle produces moving pressure bulb over the piezoelectric layer, due to which there is changing charge distribution and electrical power generation over the piezoelectric patches.

2.2.1 Impact of velocity on electric power generation

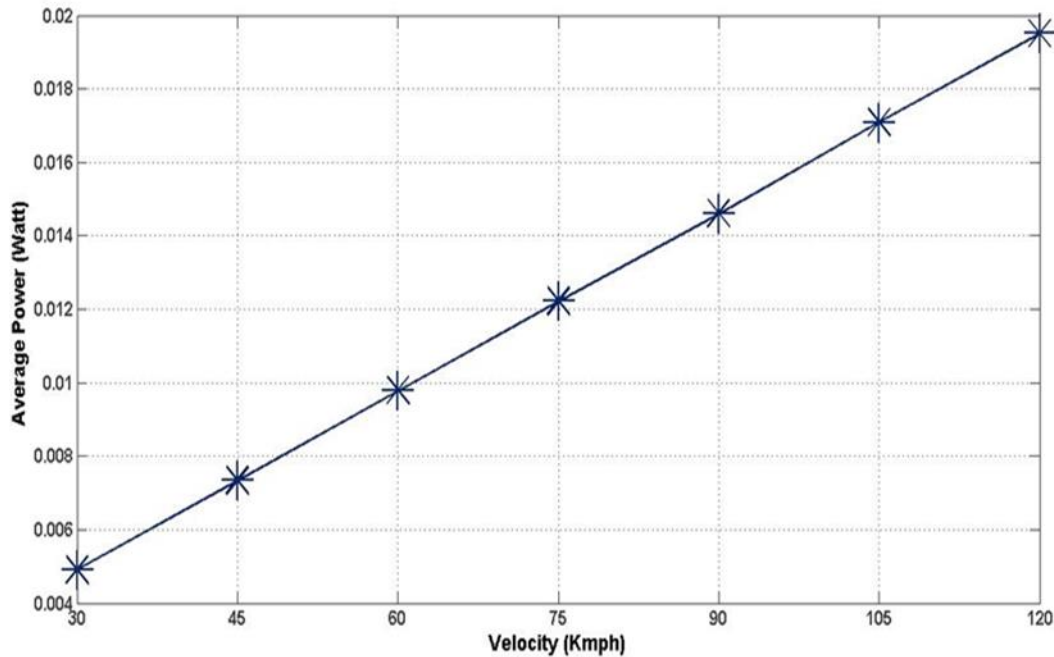


Figure 2-14 Impact of velocity of moving vehicle on the generated power from one single piezoelectric patch for depth 15 cm and patch length of 25 cm.

Fig. 2-14 shows, change in average power generation from a spare piezoelectric patch with the length of 25 cm and depth of 15 cm from pavement surface with changing velocity of the moving vehicle wheel. A linear increasing relationship is observed between the resulting average power and velocity of the vehicle. It can be explained that with higher vehicle velocity, there is decrease in period taken by the wheel of the vehicle to pass over the patch. As a result of this a certain amount of charge is generated on the piezoelectric patch surface within shorter charging period leading to higher current generation from the piezoelectric patch and increase in average generated power. When the depth increases, the average power generation decreases.

For rest of the calculations in this paper velocity is taken as 45kmph, which is more common in urban scenarios, Figure 2-14 shows that double resultant power can be found for vehicle moving at 90 kmph compared to 45kmph.

2.2.2 Impact of changing depth of the piezoelectric patch on power generation

In the pavement, load is transferred from the top layer to the bottom layer of the pavement, stress in the bottom layer is negligible as they are distributed over larger area with very small value, so with lower depth value i.e. close to the surface more power can be obtained as generated power from the piezoelectric layer/patches with higher stress.

In this research, piezoelectric patch is placed at different depth below the pavement till 150 cm depth. Piezoelectric ceramic should not be kept at the top most layer because direct forces exerted by the vehicles produce shear and tensile forces of varying magnitude and can lead to the cracking of the piezoelectric ceramic. With the dimension of safety, our simulation is carried by keeping the piezoelectric ceramic patch below the first layer of surface asphalt as shown in Figure 2-1.

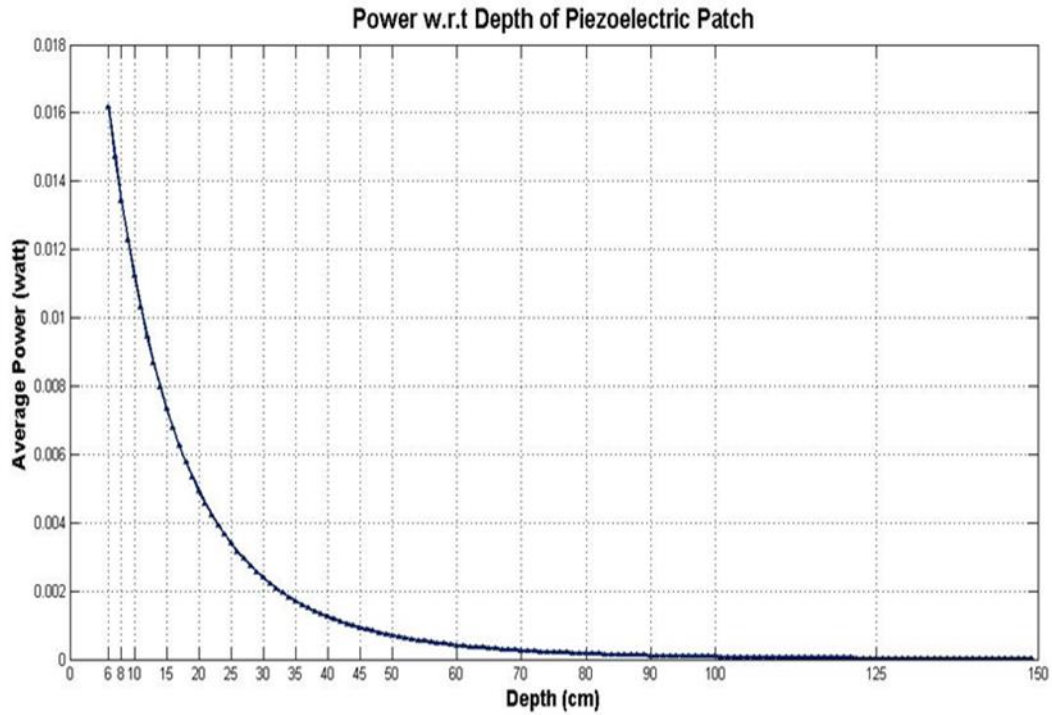


Figure 2-15 Generated power with changing depth of piezoelectric patch in flexible pavement.

Figure 2-15 shows, average power generation from one single piezoelectric patch for different depths in flexible pavement; velocity of vehicle is fixed at 45 kmph and length of each unit of the piezoelectric patch (square in shape) is 25 cm.

The result gives us a range of depth in flexible pavement where some optimum values of power generation results can be expected without damaging the piezoelectric patch.

From Figure 2-15, it is seen that when piezoelectric patch is located just below the surface layer, power of 0.016 Watt, by single wheel of moving standard axle load vehicle over one piezoelectric patch of 25 cm length, can be realized. This depth is our most shallow one where piezoelectric patch can be kept safely, so it is even considered as 100% generated power that we could expect

from one piezoelectric patch for this case in this model. Table 2-3 shows more detailed results of Figure 2-15.

Table 2-3 Percentage of power at different depth inside the pavement from the first depth value of 6 cm.

Depth (cm)	Pavg (Watt)	Percentage of power generation (%)	Depth (cm)	Pavg (Watt)	Percentage of power generation (%)
6	0.016	100	34	0.0018	11.26
7	0.014	91.12	36	0.0015	9.88
8	0.013	83.15	38	0.0014	8.7
9	0.012	75.98	40	0.0012	7.68
10	0.011	69.53	42	0.0010	6.8
11	0.010	63.71	44	0.00097	6.04
12	0.0094	58.45	46	0.00086	5.37
13	0.0086	53.69	48	0.00074	4.79
14	0.0079	49.36	50	0.00069	4.29
15	0.0073	45.44	52	0.00062	3.84
16	0.0067	41.88	54	0.00055	3.45
17	0.0062	38.64	56	0.00050	3.11
18	0.0057	35.68	58	0.00042	2.66
19	0.0053	32.98	60	0.00040	2.53
20	0.0049	30.52	70	0.00025	1.57

22	0.0042	26.2		80	0.00016	1
24	0.0036	22.57		90	0.00011	0.69
26	0.0031	19.51		100	0.00007	0.48
28	0.0027	16.93		110	0.00005	0.34
30	0.0023	14.73		120	0.00003	0.25
32	0.0020	12.86		140	0.00002	0.14

The power generation keep decreasing with the increase of depth. For depth value of 7cm to 20 cm the average power generation keep decreasing from 0.014 Watt to 0.0049 Watt. It is seen that for a very deeper position when depth is 140 cm then the average power generation is very small which is 0.00002 Watt. The value of average power generation found here is only 0.14%. From Table 2-3, we find that in 36 cm below surface average power is very low. It is optimum selection to keep the piezoelectric patch just below the Asphalt surface layer, but placing piezoelectric patch over the base layer of the pavement, which refers to depth of 26 cm will also give reasonable results for power generation.

2.2.3 Power from different loads on wheel

A reference loading of 80KN, which is standard axle load as prescribed and also used by IRC, is taken for calculations in this study. In designing of flexible pavement all loads are converted in equivalence of standard axle load. As a general idea, weight of buses and trucks are around standard axle load and cars weight 0.2 to 0.5 times the standard axle load, and there are heavy movers on road weighing more. Using this numerical model, as discussed in paper, potential of power generation is determined for other weight vehicles and are depicted in Table 2-4.

Table 2-4 Average electrical power generation from one single piezoelectric patch with different vehicles passing the pavement. (Velocity of vehicle is 45 kmph and length of patch is 25 cm)

Vehicle	Light vehicles	Cars	Standard load	Heavy buses
Weight on each tyre	5 KN (500 kg)	10 KN (1000 kg)	40 KN (4000 kg)	70 KN (8000 kg)
Tyre Pressure	35 P.S.I	37 P.S.I	130 P.S.I	130 P.S.I
Average Power mW	0.31	1	15	29

From Table 2-4 it can be seen that for light vehicles the average power generation is very small that is 0.31 mW due to smaller load on tyre and smaller tyre pressure. Moreover for cars and standard load vehicles the average power generation is 1 mW and 15 mW respectively. However it is also found that for heavy buses it is possible to get about 29 mW of power generation.

2.2.4 Optimum length of each piezoelectric patch in pavement

In this research, entire layer of piezoelectric material in pavement is actually a setup of several piezoelectric patches with the same dimensions that are kept together.

It is known from Equations (9) and (10) that the charging and power generation of piezoelectric layer is dependent on its dimensions. It is seen that more the average distribution of charge over the piezoelectric layer more is the generation of power that we can expect. With increased dimension of patch, current increases due to the large charging, but capacitance increases as well leading to the decrease of the voltage. Therefore, due to this coupling effect, we see peak power generation with an optimal dimension of the square patch. Here, piezoelectric patch is not taken

of any other shape because of efficient joining of adjacent units which can be realized in square shape, furthermore, better understanding of charge distribution can be seen when patch is symmetrical in shape.

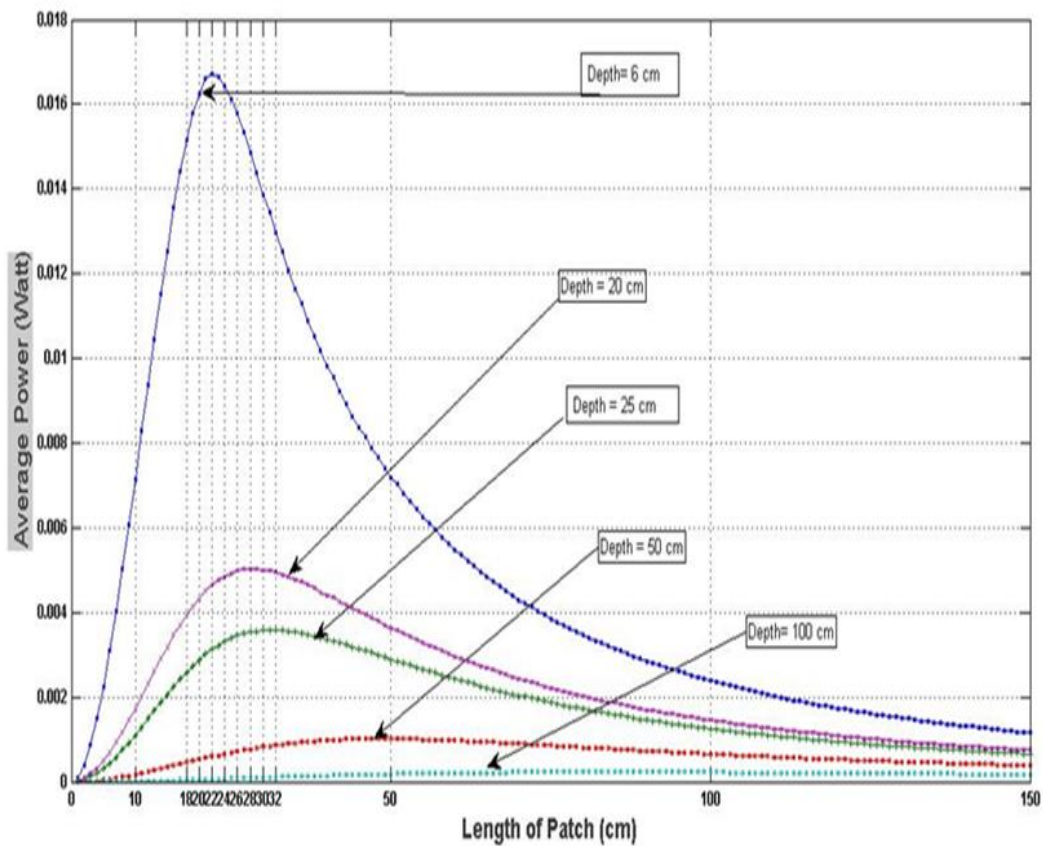


Figure 2-16 Power generation from one piezoelectric patch versus length of piezoelectric patch with different depth of the piezoelectric layer and a fixed vehicle velocity of 45 kmph.

Figure 2-16, makes this obvious that initially as the area of piezoelectric patch is increased, there is an increase in the generated power, but after particular value of dimension, it shows a decrement in the generated power giving us a peak average power with an optimal design of the piezoelectric patch. It can be seen that with increasing depth; the optimal length of patch tends to increase; this

can be explained referring Figure 2-1. Stress distributes over a larger area on the piezoelectric layer with lower density, when depth of the piezoelectric layer is increased. In this case to incorporate larger charge corresponding to stress, we see a little increase in optimal patch length corresponding to maximum generated power.

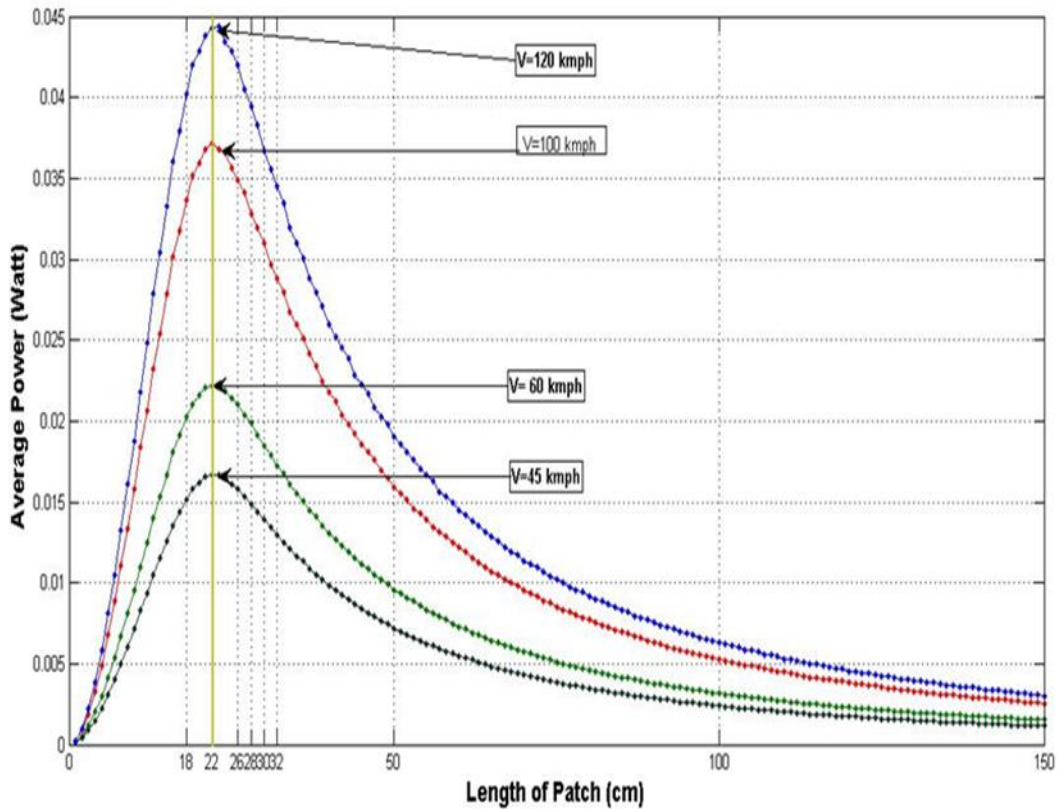


Figure 2-17 Power generation from one piezoelectric patch versus length of piezoelectric patch with different vehicle velocities and a fixed depth of the piezoelectric layer of 6 cm.

Figure 2-17, shows the relation of the optimal patch length with velocity, and it can be seen that optimal patch length is not affected by the velocity, but the generated power tends to increase with the velocity by the linear factor, which has been discussed in section 2.3.1.

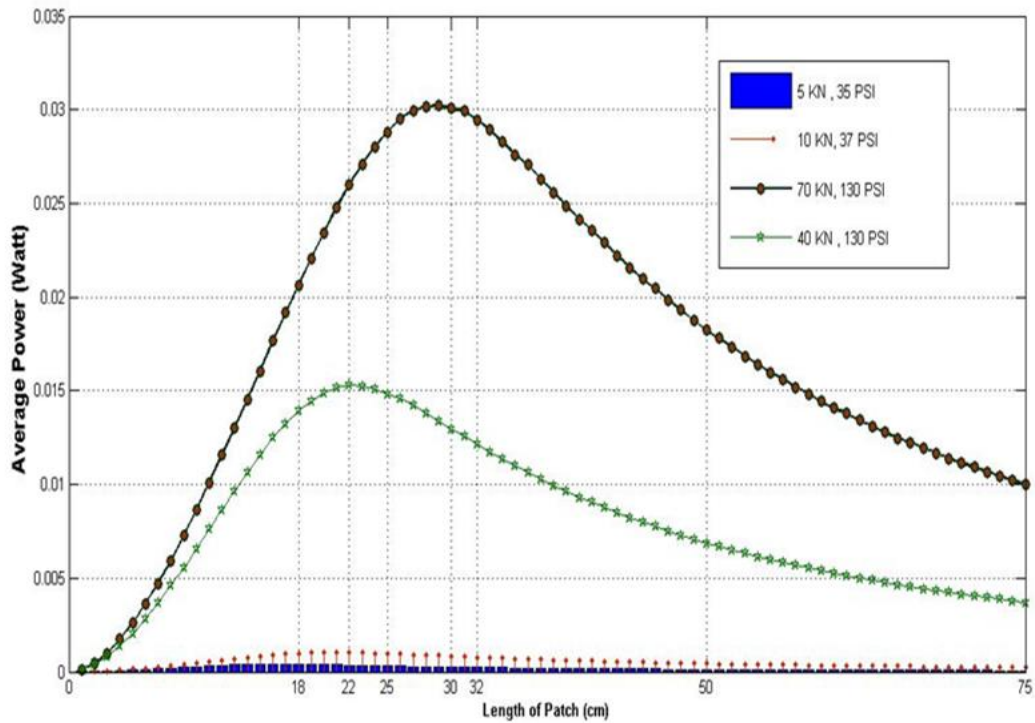


Figure 2-18 Power generation from one piezoelectric patch versus length of patch with different loads of wheels at fixed values of the depth of the piezoelectric patch as 6 cm and vehicle velocity as 45 Km/h.

Figure 2-18 shows a relation of different wheel loads with the optimal patch length. It is noted for higher loads, the high stress is distributed in a relatively larger area in the above layers, and therefore, the optimal length of piezoelectric patch to accumulate the maximum charge is comparatively larger than that for lower layers with lower values of load.

From figures 2-16, 2-17 and 2-18 we can see that there is a particular window of patch length ranging from 18 to 30 cm, between which a generated power is close to maximum for different depths, velocities and loads. Therefore, it can be justified that a piezoelectric patch of dimension

25 x 25 cm² can be a reasonable and optimal choice of piezoelectric patch dimension below the pavements to give us efficient energy generation from the piezoelectric layer.

2.3 Conclusions

An approach to design a simple piezoelectric harvester for flexible pavement is discussed taking the effects of size of piezoelectric harvester unit, depth of piezoelectric harvester located in the pavement and velocity of vehicle passing the pavement. An idea about expected power generation for different types of vehicle with different loads on wheels is also given using the numerical model. Optimal design of the piezoelectric patch (size and location) is found from the numerical simulations. A two centimeter thick piezoelectric layer is placed below the flexible pavement and it is noted with higher loading from the vehicle and deeper position the corresponding optimal patch size in the piezoelectric layer will be larger. Modeling of piezoelectric patch takes into account the effect of velocity of the vehicle, effect of different depth of piezoelectric patch and of different loads applied on the pavement to get an idea about optimum design of the piezoelectric patch. Results shows that placing piezoelectric layer below the asphalt/bitumen coating (5-10 cm from surface) with each unit in piezoelectric layer as a square piezoelectric patch with length of 25 cm is suggested considering practical application for energy harvesting from the pavement with the maximum electrical power generation. Using the proposed model, the optimum designing of piezoelectric harvester in flexible pavement can be done even for specific cases. Piezoelectric harvester is placed below pavement layers rather than directly on surface to ensure that piezoelectric ceramic does not go any fatal failure due to complex forces induced on pavement. Life of piezoelectric harvester will be affected adversely if placed directly on surface, so placing in below the surface coating of bitumen/asphalt and to the top of base layer is a reasonable choice.

By this model it can be summarized that for a flexible pavement, a single axle moving truck has a potential to generate 30 mW of power from one single optimum sized (25 cm * 25 cm) piezoelectric patch under the pavement. Significant increase in traffic at present time shows a potential of larger scope of power generation by piezo-electric harvester below road pavements.

The model is also validated by comparing the stress generation results found from MATLAB simulation results with the ANSYS simulation results. The pressure bulb model takes into consideration only Poisson's ratio of different layers of the pavement, but the effect of Young's modulus of different layers on stress distribution in pavement is not considered. This will cause some error. The average error percentage found by comparing the stress values from ANSYS and MATLAB simulations among 5 data points at 5 cm depth inside the pavement is only 3.646%, which certainly validates the MATLAB simulation results and describes that the stress distribution results inside the pavement found from MATLAB simulation is accurate. Designing of network to collect this power with best efficiency for different applications and experimental testing of the numerical model in practical field are among the future scope of this work.

Chapter 3

This chapter discusses about harvesting piezoelectricity from roads with piezoelectric composite plate harvester based on the same semi-mathematical model of pressure bulb inside the pavement described in chapter 2. In this chapter also Westergaard's stress model is proposed to calculate the three dimensional (3D) stress distribution in the pavement and to find the potential of energy harvesting from the piezoelectric plate harvester placed inside the pavement. In this chapter the design of the piezoelectric patch harvester developed previously in chapter 2 is improved in order to increase the power generation. The power generation we found by using a single optimum sized piezoelectric patch in chapter 2 is only 30 mW if the load on each tyre of the passing vehicle is 40 KN and the velocity is 45 km/hr. In this chapter instead of a piezoelectric patch the design is modified by making it a composite plate harvester. The reason behind making the harvester as a composite plate is to provide better protection to the piezoelectric layer from tensile force induced failures due to the application of larger loads and also to provide larger strain to the piezoelectric layer. It is known that piezoelectric materials can sustain large amount of compressive force but it is very fragile for larger tensile force, so a substrate layer is provided under the piezoelectric material layer to protect the harvester from failure under higher applied load. The hollow space over the base support allows the structure to bend and thus it provides larger strain and as a result of that higher power generation can be obtained.

3.1 Schematic diagram of the piezoelectric composite plate harvester

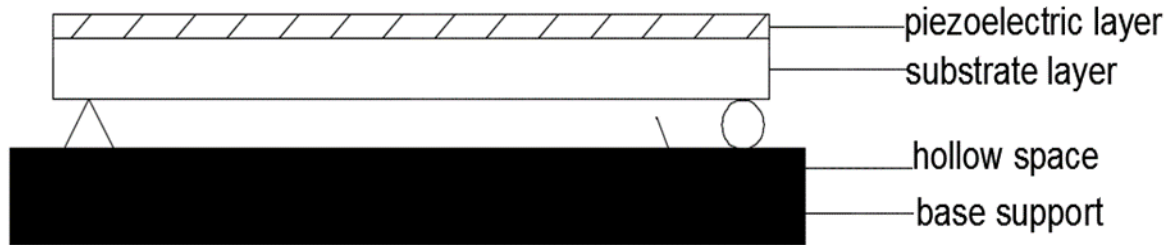


Figure 3-1 Schematic diagram of the piezoelectric composite plate harvester.

In the proposed model with the new design, a piezoelectric composite plate harvester embedded in the pavement is designed to collect the piezoelectricity, when vehicle is passing through the pavement. Due to the deflection of the piezoelectric layer, the stress and strain produced in the piezoelectric layer are high so the average power generation is relatively high in our composite plate structure. The maximum stress that can be sustained by the PZT material and the host plate structure is considered to restrict the maximum deflection of the plate harvester. Extra current generated by the harvester can be stored and used, when there will be less vehicle movement on the road. The piezoelectric composite plate harvester has two layers, the coating layer as PZT material and the substrate layer as A514 steel, which are mounted on a hollow space so that the structure can bend. The schematic diagram of the piezoelectric composite plate harvester is shown in Figure 3-1, where, the length of the composite plate is taken as L , width as B , thickness of the PZT layer as H_1 and thickness of the substrate steel layer as H_2 . The PZT layer covers all over the substrate assuming that it is perfectly bonded with the substrate layer. This composite plate harvester is placed at different depths inside the pavement to find the optimum depth value. When

a vehicle passes through the pavement, load is applied over the soil mass by the wheel in the contact area between the wheel and pavement. The strains and kinetic energies generated by the loads of the passing vehicles are dissipated as thermal energies. Thus these energies in the pavement went away as waste thermal energy. Therefore, placement of piezoelectric energy harvesters inside the pavement can harvest part of these wasted energy. The load of the passing vehicles generates pressure/stress as well as the deformation and strain in the pavement, which distributes like a bulb shape. The calculation of the pressure bulb is based on the semi-mathematical model of pressure bulb formation in pavement discussed in chapter 2. The pressure bulb can be simulated and calculated using Westergaard's stress distribution model. As the vehicle wheels keep moving on the pavement so the contact area between the pavement and the wheel will keep changing, so the pressure bulb will keep moving with the moving vehicle.

The model assumes soil as an elastic media. The composite plate structure, which is placed inside the pavement at a certain depth, is subjected to a moving pressure bulb and get bended with the passing vehicle. The bending moment as well as plane stress and strain are produced on the composite plate harvester. Due to the plane strain on the PZT layer, charge is generated on the surface of the harvester. From the total charge generated on the harvester, voltage and current can be calculated during the vehicle passing through the harvester position on the pavement. The piezoelectric composite plate in the pavement does not have to be a whole large layer or plate. It can be composed of many small piezoelectric plates, which are available in the market. Our studied model can give approximation of power for any thickness or size of piezoelectric plate harvester.

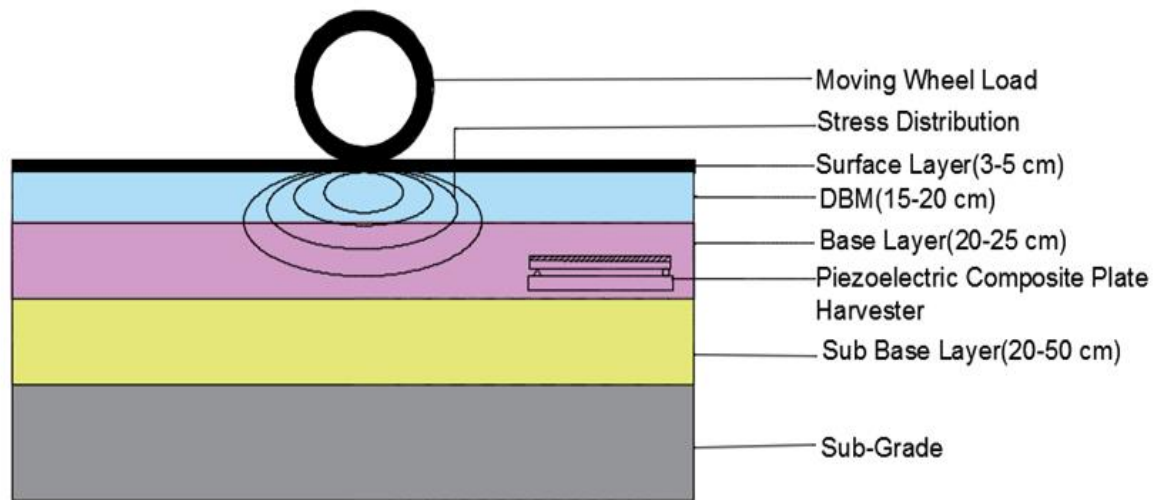


Figure 3-2 Piezoelectric composite plate harvester placed inside the pavement and under dynamic loading.

Figure 3-2, illustrates the piezoelectric composite plate harvester that is placed inside the pavement. Different layers of pavement are also shown in Figure 3-2 with detailed dimensions.

It is assumed, the plate harvester will not vibrate since it is inside the pavement, and it will only undergo deformation, which is induced by the pressure applied on the plate surface because of the pressure bulb generated in the pavement.

3.2 Methodology and Numerical Model of plate deflection under pressure bulb in pavement

In this model of piezoelectric composite plate harvester the formula to get the contact area between the pavement and tyre of the vehicle wheel is same as that used for single piezoelectric patch energy harvester. The contact area between the pavement and tyre is assumed to be circular for the simplicity of calculation (Moazami et al. 2011) [49]. The contact radius is calculated by the formula below which is same as the formula that was used for piezoelectric patch in previous chapter and can be given by,

$$A = \sqrt{\frac{F}{\pi P}} \quad (13)$$

where 'A' is contact radius, 'F' is applied force and 'P' is Pressure of tyre.

Flexible pavement is designed in equivalence to standard axle load, which is 80 KN (Indian Road Standard, IRC 37-2001, pavement interactive 2014). The calculations of that chapter is done with standard axle load of 40KN over each wheel same as that was used in previous chapter in case of piezoelectric patch harvester. However, the mathematical model can be used for any other wheel loads as well. Pavement considered in this study is designed for value of California bearing ratio (CBR) 2% using IRC recommendation for 150 million axle load for design life of 15 years same as that used for the analysis of piezoelectric patch harvester in chapter 2.

The total distance covered by the vehicle is considered as 3.8 m which means the average power generation calculation is done when the vehicle wheels are within 3.8 m range from the harvester. Therefore the vehicle wheels will come from 1.9 m distance from the piezoelectric harvester,

passes through it and will go away up to 1.9 m distance. This range of distance is studied because outside of that range the stress generation by the wheels will be very small and the average power generation will be small as well. After the contact area is determined, then the point load is calculated due to the contact between the pavement and the tyre. In general, the tyre pressure for such load is 130 p.s.i (max), which is 900 kPa. Here we have used the tyre pressure as 880 KPa. By using Equation (13), the contact radius can be determined which is 0.12m.

Based on the finite element numerical method, the circular contact with radius of 0.12 m is divided into N small squares with the edge length of $f_1 * f_2$ m, where f_1 and f_2 are the edge length of each small square. The values of f_1 and f_2 are considered as 0.001m. The convergence calculation for that calculation is mentioned in chapter 2.

The total load of 40KN is distributed evenly over the small squares. Then, each small square area is considered as a point load. For each point load the value of stress at every point on the piezoelectric composite plate harvester below the loading area in the pavement is calculated.

The Westergaard's stress equation is,

$$\sigma_{zn} = \frac{Q}{2\pi n^2 Z^2 (1 + (\frac{r}{nZ})^2)^{3/2}} \quad (14)$$

where, σ_z is the stress along the depth direction of the pavement generated by the point load on the n^{th} small square ($\frac{KN}{m^2}$); Q is the point load (N) and Z (m) and r (m) are depth and radial distance of any point in study box from loading point in contact area of the pavement. By using that equation, the values of stress at any point inside the pavement can be found and here,

$$n = \sqrt{((1 - 2\mu)/(2 - 2\mu))} \quad (15)$$

where, μ is the equivalent Poisson's ratio. The depth of the first layer of the pavement is considered 0.25 m. Here also to minimize the error in the calculation we have used the "equivalent Poisson's ratio" which is the weighted mean of all layers in the strata. Without this assumption it will not be possible to calculate stress at different layers and its behavior at junctions, as isobars of stress would not be continuous. This assumption is same as that used in chapter 2 in case of piezoelectric patch harvester calculation. Poisson's ratio of different layers varies from 0.3 to 0.45 (0.3 is of PZT). As the difference in Poisson's ratio is not very large then the error caused by assuming that the stress distribution after placing the piezoelectric patches inside the pavement remains continuous will not be significant.

The point load can be calculated by the formula below,

$$Q = \frac{F}{\pi A^2 * f_1 * f_2} \quad (16)$$

where, F is the applied force, A is the contact radius, f_1 and f_2 are the edge length of each small square areas of the contact radius, respectively.

The equivalent Poisson's ratio is calculated from the following formula,

$$\mu = \frac{(u_1 * (Z - \left(\frac{H_1}{2}\right)) + \left(\frac{H_1}{2}\right) * u_p)}{Z} \quad (17)$$

where, u_1 and u_p are the Poisson's ratio of the first layer and piezoelectric layer in the pavement respectively, H_1 is the thickness of the piezoelectric layer and Z is the depth of the piezoelectric composite plate harvester.

Thus, the stress distribution due to entire loaded area in the pavement and pressure bulb is found. Then, the calculation for piezoelectric composite plate harvester, which is placed in the pavement inside the pressure bulb at a certain depth, is done. To simulate the maximum deflection, the unevenly distributed pressure applied on the composite plate surface by the pressure bulb is broken down and simulated as many point loads. Based on the finite element numerical method, the composite plate is divided into N_I small square areas having edge length of $s_1 * s_2$ m. s_1 and s_2 are the edge length of each small square area of the plate where the value of s_1 and s_2 are considered as 0.005 m.

In order to determine the accuracy of the assumption of dividing the composite plate harvester into small square areas having edge length of 0.005 m, the convergence calculation is conducted. For the convergence test the edge length of the small squares are changed from 0.001 m to 0.05 m with an increase of 0.0002 m. For the convergence calculation, the position of the vehicle wheel is considered at the middle of the contact area between the tyre and the pavement. The calculation is done for a certain point which is the middle of the piezoelectric composite plate in the pavement.

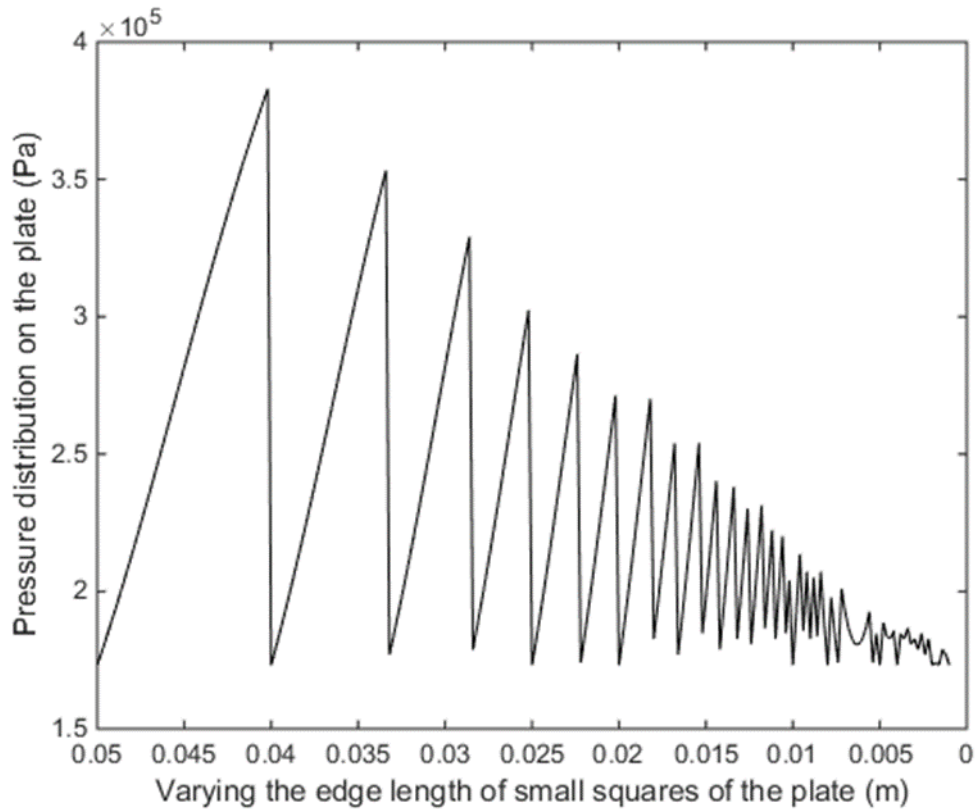


Figure 3-3 Variation of pressure distribution at the middle point of the piezoelectric composite plate with varying edge length of small squares from 0.001 to 0.05 m with an increase of 0.0002 m.

The plot given in Figure 3-3 shows the convergence study in area of the small squares of the plate. It is seen that the pressure value convergences with very tiny variation when the edge length of each small square area is smaller than 0.005 m. Therefore it can be said that the assumption of dividing the small square areas of the plate harvester with edge length of 0.005m is a reasonable choice.

The point loads induced by the pressure bulb are applied on different small areas of the plate. Each point load will generate a deflection curve of the plate, and the total deflection can be calculated

by combining the deflection curves induced by each point loads, due to the superposition principle. The plane strain generated at each small square of the composite plate harvester for each point load of the contact radius is then calculated.

The deflection of the harvester subjected to a point load is calculated by the formula below,

$$w_{i,j}(X, Y) = \frac{4Q}{\pi^4 DBL} \sum_{m=1}^{\alpha} \sum_{n=1}^{\alpha} \frac{\sin(m\pi i s_1/L) \sin(n\pi j s_2/B) \sin(m\pi X/L) \sin(n\pi Y/B)}{((m/L)^2 + (n/B)^2)^2} \quad (18)$$

where, w is the deflection of the harvester, m and n are the number of modes, L is the length, B is the width of the piezoelectric composite plate harvester. Q is the point load, X and Y give the position of the small square areas in the plate along x and y direction, α is the mode number, which is 3 for our calculation, i and j are the number of the small areas that are subjected to one of the point loads from the pressure bulb along length and width directions of the plate. $i*s_1$ and $j*s_2$ are the positions of the small area subjected to one of the transverse point loads. D is the moment of inertia constant of the composite plate and is given by-

$$D = \frac{1}{3} Ep \left(\left(\frac{H_1 + H_2}{2} \right)^3 - \left(\frac{H_2 - H_1}{2} \right)^3 \right) + \frac{1}{3} E \left(\left(\frac{H_2 - H_1}{2} \right)^3 - \left(\frac{-H_2 - H_1}{2} \right)^3 \right) \quad (19)$$

where, H_1 and H_2 are the thickness of the piezoelectric layer and substrate layer respectively and Ep and E are the Young's modulus of the piezoelectric layer and the substrate layer (A514 steel), respectively.

Total deflection produced by all the point loads can be simulated by the following formula,

$$w(X, Y) = \sum_{i=1}^{L/s_1} \sum_{j=1}^{B/s_2} w_{i,j}(X, Y) \quad (20)$$

The bending moment in the x direction produced by single point load is calculated as,

$$Mx_{i,j}(X, Y) = \frac{4Q}{\pi^2 BL} \sum_{m=1}^{\alpha} \sum_{n=1}^{\alpha} \left(\left(\frac{m}{L} \right)^2 + up \left(\frac{n}{B} \right)^2 \right) \frac{\sin\left(\frac{m\pi is_1}{L}\right) \sin\left(\frac{n\pi js_2}{B}\right) \sin\left(\frac{m\pi X}{L}\right) \sin\left(\frac{n\pi Y}{B}\right)}{\left((m/L)^2 + (n/B)^2 \right)^2} \quad (21)$$

The total bending moment in the x direction produced by all the point loads is calculated as,

$$Mx(X, Y) = \sum_{i=1}^{L/s_1} \sum_{j=1}^{B/s_2} Mx_{i,j}(X, Y) \quad (22)$$

The bending moment in the y direction produced by single point load is calculated as,

$$My_{i,j}(X, Y) = \frac{4Q}{\pi^2 BL} \sum_{m=1}^{\alpha} \sum_{n=1}^{\alpha} \left(up \left(\frac{m}{L} \right)^2 + \left(\frac{n}{B} \right)^2 \right) \frac{\sin(m\pi is_1/L) \sin(n\pi js_2/B) \sin(m\pi X/L) \sin(n\pi Y/B)}{\left((m/L)^2 + (n/B)^2 \right)^2} \quad (23)$$

The total bending moment in the y direction produced by all the point loads is calculated as,

$$My(X, Y) = \sum_{i=1}^{L/s_1} \sum_{j=1}^{B/s_2} My_{i,j}(X, Y) \quad (24)$$

where Mx and My are the bending moment along x and y directions, respectively, up is the Poisson's ratio of the piezoelectric layer, L and B are the length and width of the composite plate

harvester respectively, Q is the point load, X and Y give the position of the small square areas in the plate along x and y direction, α is the mode number, which is 3 for our calculation, i and j are the number of the small areas that are subjected to one of the point loads from the pressure bulb along length and width directions of the plate. $i*s_1$ and $j*s_2$ are the positions of the small area subjected to one of the transverse point loads.

Then the stress values along x and y direction are also calculated as,

$$S_x(X, Y) = \frac{6}{(H_1 + H_2)^2} M_x(X, Y) \frac{H_2}{H_1 + H_2} \quad (25)$$

$$S_y(X, Y) = \frac{6}{(H_1 + H_2)^2} M_y(X, Y) \frac{H_2}{H_1 + H_2} \quad (26)$$

where S_x and S_y are stress values along x and y directions and M_x and M_y are the bending moment generated along x and y directions, H_1 and H_2 are the thickness of the PZT coating layer and substrate layer respectively.

Based on Westergaard's assumption that says, in case of pavement stresses, only vertical load is significant to be considered, at any point. The strain value is calculated from the formula below,

$$SS_x(X, Y) = \frac{S_x(X, Y)}{E_p} \quad (27)$$

$$SS_y(X, Y) = \frac{S_y(X, Y)}{E_p} \quad (28)$$

where E_p is the modulus of elasticity of the PZT layer, and SS_x and SS_y are the strain values along x and y direction respectively.

After the calculation of strain distribution, the charging density along x and y direction are calculated by using the formula below,

$$Dx(X, Y) = SSx(X, Y) \cdot e_{31} \quad (29)$$

$$Dy(X, Y) = SSy(X, Y) \cdot e_{31} \quad (30)$$

where Dx and Dy are the surface charge density ($\frac{C}{m^2}$) at (X, Y) position along x and y direction; e_{31} is piezoelectric constant, at any time (t) .

Then the total charge distribution along x and y direction is calculated by,

$$Qx = \int_0^L \int_0^B Dx(X, Y) \cdot dXdY \quad (31)$$

$$Qy = \int_0^L \int_0^B Dy(X, Y) \cdot dXdY \quad (32)$$

where Qx and Qy are total charge distribution along x and y direction and $dXdY$ is the area of the rectangular piezoelectric composite plate harvester. Then the total charge (Q_t) on the plate harvester at any time point, t , is calculated by the following formula,

$$Q_t = Qx + Qy \quad (33)$$

When a vehicle moves over piezoelectric composite plate harvester embedded pavement with a certain velocity, at any time t , it produces charge on the PZT layer, which is located at a certain depth inside the pavement. Current and voltage generated on a piezoelectric composite plate harvester are computed as,

$$I(t) = \frac{dQ_t}{dt} \quad (34)$$

$$V(t) = \frac{Q_t}{C} \quad (35)$$

C is the capacitance of the piezoelectric composite plate harvester which is given as,

$$C = \frac{\epsilon * L * B}{4\pi k H_1} \quad (36)$$

where L and B are the length and width of the piezoelectric composite plate harvester, ϵ is dielectric constant, K is static electricity constant, H_1 is the thickness of the piezoelectric layer.

The average electric power generated from the piezoelectric composite plate harvester is defined by the multiplication of root mean square (RMS) values of the voltage and current generated from the PZT layer and is calculated as below,

$$P_{avg} = V_{rms} \cdot I_{rms} \quad (37)$$

The following two equations demonstrate how the root mean square values are calculated from I and V values, which are actually functions of time, t . The values of I and V used here are the values when the tyre of the vehicle is at different distances from the composite plate harvester embedded pavement at different time point, t .

$$V_{rms} = \sqrt{\frac{1}{T} \int_0^T V^2(t) dt} \quad (38)$$

$$I_{rms} = \sqrt{\frac{1}{T} \int_0^T I^2(t) dt} \quad (39)$$

where V and I are the generated voltage and current given in Equations (35) and (34) respectively.

Table 3-1 Properties of the piezoelectric composite plate harvester and the passing vehicle, which are kept constant during the calculation.

Parameters	Host beam (A514 steel)	Piezoelectric layer (PZT)
Young's modulus, E (Pa)	$E=200*10^9$	$E_p= 78*10^9$
Piezoelectric constant, e_{31}	----	$e_{31} = -2.8$
Dielectric constant, ϵ	----	$\epsilon= 300$
Static electricity constant, K	----	$K = 9*10^9$
Yield strength	700 MPa	950 MPa
Axle load on tire, F	40 KN	40 KN
Tire pressure, P	900 KPa	900 KPa

3.3 Simulations and Discussions

Numerical simulations are conducted based on the proposed theoretical model calculating the average power generation from a composite plate harvester by placing it inside the pavement. Here, along with the simulation results, optimal design of the piezoelectric plate harvester is presented. During the simulation, the design of the pavement itself is kept fixed and given in Figure 2-2, which also gives the thickness values of different layers. Material properties of the piezoelectric composite plate harvester used for conducting the simulations are given in Table 3-1. The parameters of the vehicle passing through the pavement are given in Table 3-1 as well.

3.3.1 Impact of depth of the harvester in pavement on average power generation

Figure 3-4 below demonstrates the impact of position of placement of the piezoelectric composite plate harvester inside the pavement on average power generation.

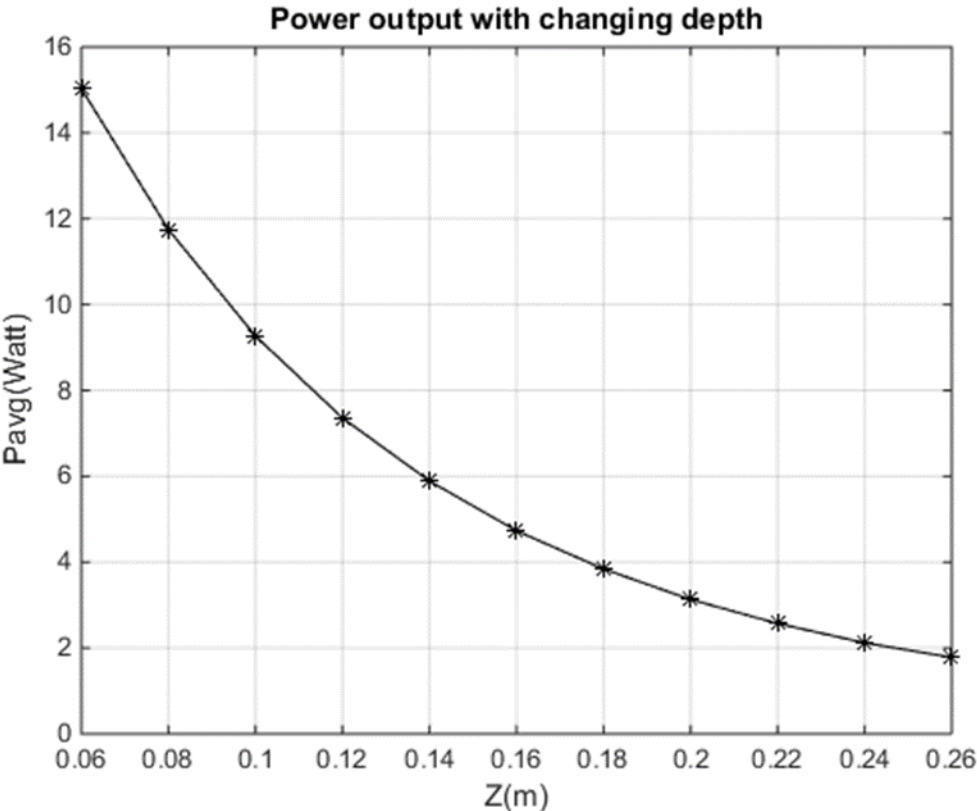


Figure 3-4 Power generation with changing depth of the piezoelectric composite plate with length and width as 0.2m. The thickness of the piezoelectric layer and substrate layer are 0.0005 m and 0.003 m, respectively, and the velocity is kept constant at 22.2 m/s.

Table 3-2 Change in average power generation from the piezoelectric composite plate harvester with the variation of depths.

The length and width of the harvester is kept constant as 0.2 m, the thickness of the PZT layer and the substrate layer are chosen as 0.0005 m and 0.003 m, respectively, and the velocity of the passing vehicle is kept constant at 22.2 m/s.

Depth (m)	Average power generation (Watt)	Highest stress (MPa)	Maximum deflection (m)
0.06	15.03	502	0.0071
0.08	11.76	449	0.0063
0.1	9.27	402	0.0056
0.12	7.36	360	0.0050
0.14	5.89	323	0.0045
0.16	4.74	291	0.0041
0.18	3.84	262	0.0037
0.2	3.13	237	0.0033
0.22	2.57	215	0.0030
0.24	2.12	195	0.0027
0.26	1.78	179	0.0025

Figure 3-4 illustrates the change in average power generation from the harvester, when the piezoelectric composite plate harvester is placed at different depths from 0.06 m to 0.26 m. The detailed values of change in average power generation, highest stress generation and maximum deflection with changing depth of the harvester placement inside the pavement are shown in Table 3-2. The width and length of the harvester are fixed at $L=B=0.2$ m. The thickness of the PZT layer and the substrate layer are chosen as 0.0005 m and 0.003 m, respectively, and the velocity of the passing vehicle is kept constant at 22.2 m/s. The figure shows that, average power generation is 15.03 Watt, when the harvester is placed at the depth of 0.06 m. However, the average power generation keep decreasing, while the depth is increased to a higher value. For example, for a deeper position of the harvester with $Z=0.26$ m, the average power generation is only 1.78 Watt. It is noted that, the average power generation is really high at a very shallow position in the pavement. However, placement of the harvester close to the pavement surface leads to significant shear forces of varying magnitudes from the passing vehicle, which may break the PZT material. Therefore, the smallest value of the depth is set as 0.06 m during the simulation. The largest deflection values of the plate harvester changes from 0.0071m to 0.0025m, respectively. The highest stress values generated in the plate harvester by the passing vehicle (constant vehicle parameters are given in Table 3-1) at depths varying from 0.06 m to 0.26 m changes from 502 MPa to 179 MPa, respectively. The power generations at those positions hence decreases from 15.03W to 1.78 W, respectively. The decreasing trend of the average power generation with increasing depth can be explained as below. At higher depth, the stress in the pavement produced by the passing vehicle is distributed over a larger area so that the actual pressure applied on the plate surface becomes small leading to smaller deflection and average power generation. Based on the material strength of the plate harvester given in Table 3-1, for safety the depth of the plate

harvester placement without possible breaking of the harvester is chosen as 0.12 m. At that position, the highest stress value in the harvester generated by the passing vehicle is 360 MPa, and power generation is 7.36 W. The maximum deflection value at the depth of 0.12m is 0.005m, which can be considered as a safe value.

3.3.2 Relation between thickness of piezoelectric layer and average power generation

Figure 3-5 below demonstrates the impact of thickness of the piezoelectric layer of the composite plate harvester on average power generation.

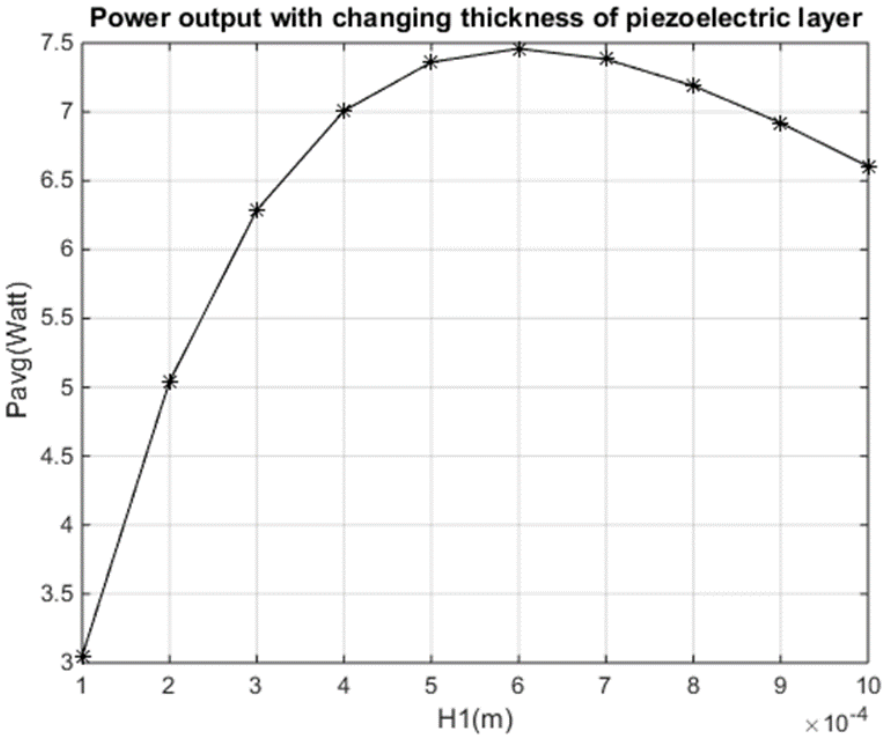


Figure 3-5 Power generation with changing thickness of piezoelectric layer with the length and width of the piezoelectric composite plate of $L=W=0.2\text{m}$, the depth of the harvester of $Z=0.12\text{m}$ and the thickness of the substrate layer of the composite plate of $H_2=0.003\text{m}$.

The following Table 3-3 shows the change in average power generation from the piezoelectric composite plate harvester with the variation of the thickness of the piezoelectric layer.

Table 3-3 Change in average power generation from the piezoelectric composite plate harvester with the variation of the thickness of the piezoelectric layer.

The length and width of the piezoelectric composite plate harvester are considered as $L=B=0.2\text{m}$, the depth of the harvester as $Z=0.12\text{m}$ and the thickness of the substrate layer of the composite plate as $H_2=0.003\text{m}$. The velocity is kept constant at 22.2 m/s for that calculation.

Thickness of PZT layer (m)	Average power generation (Watt)	Highest stress (MPa)	Maximum deflection (m)
0.0001	3.05	519	0.0062
0.0002	5.04	472	0.0059
0.0003	6.29	430	0.0056
0.0004	7.01	393	0.0053
0.0005	7.36	360	0.0050
0.0006	7.46	331	0.0047
0.0007	7.38	305	0.0045
0.0008	7.19	282	0.0042
0.0009	6.92	260	0.0039
0.001	6.60	241	0.0037

Figure 3-5 illustrates the change in average power generation with the varying thickness of the piezoelectric layer of the composite plate harvester. The length and width of the piezoelectric composite plate harvester are considered as $L=B=0.2\text{m}$, the depth of the harvester as $Z=0.12\text{m}$ and the thickness of the substrate layer of the composite plate as $H_2=0.003\text{m}$. The velocity is kept constant at 22.2 m/s for that calculation. In the graph, it is seen that, the average power generation increases with the increase in thickness of piezoelectric layer up to certain value followed by a decreasing trend. From the equation of capacitance, it is seen that, capacitance is inversely proportional to the thickness of the piezoelectric layer. If the thickness of the PZT coating layer increases, then capacitance will decrease, which leads to an increment in voltage generation. As a result of that, the power generation will increase as well. However, after reaching a certain value, it again starts to decrease. The lowest value of average power generation from the plate harvester is 3.05 Watt when thickness is 0.0001m . The highest stress at that point is 519 MPa and the maximum deflection value is 0.0062 m . For the thickness values varying from 0.0002 m to 0.001m , the highest stress values changes from 472 MPa to 241 MPa , respectively. The average power generation at those points varies from 5.04 W to 6.60 W , respectively. The maximum deflection values decreases with the increase in thickness of the PZT layer (H_1) and reaches the lowest value of 0.0037m when H_1 is 0.001m .

It can be concluded that, the maximum value of the average power generation obtained is 7.46 Watt for $H_1=0.0006\text{ m}$, where the highest stress is 331 MPa , which is lower than the yield strength of the substrate layer and the PZT layer (values are given in Table 3-1). The deflection at the thickness of 0.0006 m is 0.0047m , which is reasonable and no risk of breaking the harvester. However, based on the material strength of the plate harvester given in Table 3-1, the optimum value of the thickness of the piezoelectric layer can be chosen as 0.0006m .

3.3.3 Relation between thickness of substrate layer and average power generation

Figure 3-6 below demonstrates the impact of thickness of the substrate layer of the harvester on average power generation.

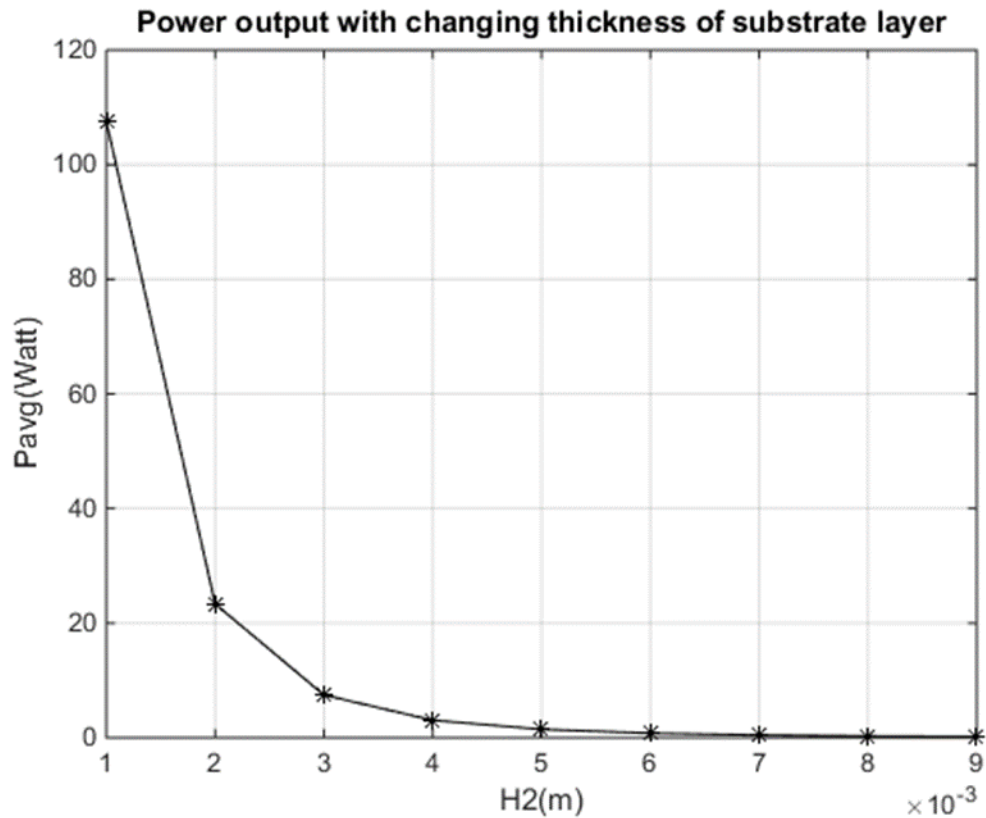


Figure 3-6 Power generation with changing thickness of substrate layer with the length and width of the piezoelectric composite plate of $L=W=0.2\text{m}$, the depth of the harvester of $Z=0.12\text{m}$ and the thickness of the piezoelectric layer of the composite plate of $H_1=0.0006\text{m}$.

Table 3-4 Change in average power generation, highest stress and maximum deflection from the piezoelectric composite plate harvester with the variation of the thickness of the substrate layer.

The length and width of the piezoelectric composite plate harvester are taken as $L=B=0.2\text{m}$, the depth as $Z=0.12\text{m}$ and the thickness of the piezoelectric layer as $H_1=0.0006\text{m}$. The velocity is kept constant at 22.2 m/s for that calculation.

Thickness of substrate layer (m)	Average power generation (Watt)	Highest stress (MPa)	Maximum deflection (m)
0.001	107.53	1257	0.0605
0.002	23.36	586	0.0133
0.003	7.46	331	0.0047
0.004	3.05	212	0.0022
0.005	1.46	147	0.0012
0.006	0.79	107	0.0007
0.007	0.46	82	0.0005
0.008	0.29	65	0.0003
0.009	0.19	52	0.0002

Figure 3-6 describes the change in average power generation with the varying thickness of the substrate layer of the plate harvester. The length and width of the piezoelectric composite plate

harvester are taken as $L=B=0.2\text{m}$, the depth as $Z=0.12\text{m}$ and the thickness as $H_1=0.0006\text{m}$. The figure shows that, with the increase in thickness of the substrate layer, the average power generation decreases. For thickness values varying from 0.001m to 0.009m , the highest stress generated on the plate harvester decreases from 1257MPa to 52MPa , respectively. The average power generation is highest when the thickness of the substrate layer is 0.001m . The maximum deflection of the plate harvester at that thickness is 0.0605m with the highest stress of 1257MPa . Therefore, the thickness value of 0.001m with the highest power generation of 107.5Watt , cannot be taken because of the high stress and deflection value at that point can break the harvester.

When the thickness value is 0.002m the P_{avg} is 23.36Watt , the highest stress is 586MPa and maximum deflection is 0.0133m which can be considered as safe value. However, based on the material strength of the plate harvester given in Table 3-1, the optimum value of the thickness of the substrate layer can be chosen as 0.002m .

3.3.4 Average power generation with varying length of the harvester

Figure 3-7a below demonstrates the impact of length of the harvester on average power generation.

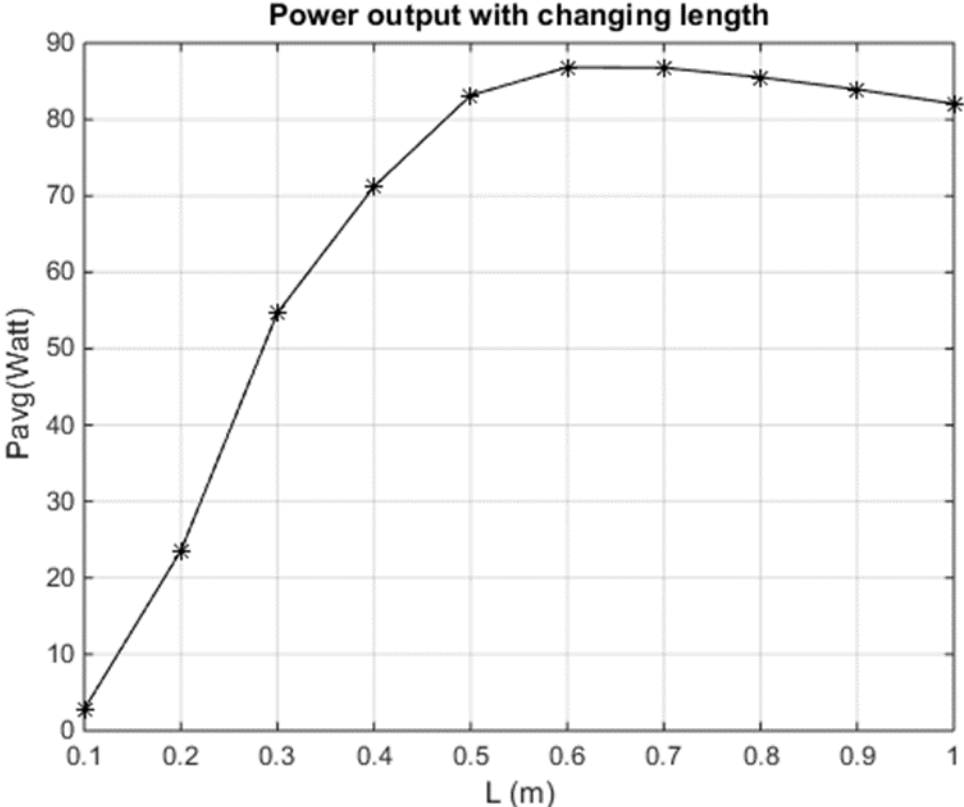


Figure 3-7a Power generation with changing length of the piezoelectric plate harvester, where the width of the piezoelectric composite plate is 0.2m. The depth is $Z=0.12\text{m}$, thickness of PZT coating layer is $H_1=0.0006\text{m}$ and thickness of steel substrate is $H_2=0.002\text{m}$.

The following Table 3-5 shows the change in average power generation, highest stress and maximum deflection of the piezoelectric composite plate harvester with the variation of the length of the harvester,

Table 3-5 Change in average power generation, highest stress and maximum deflection of the piezoelectric composite plate harvester with the variation of the length of the harvester.

The depth of the harvester used for the calculation is $Z=0.12\text{m}$ and the thickness of the piezoelectric layer and the substrate layer are chosen as $H_1=0.0006\text{m}$ and $H_2=0.002\text{m}$, respectively. The width of the harvester is fixed at $B=0.2\text{m}$. The velocity of the vehicle passing through the plate harvester is kept constant at 22.2 m/s .

Length (m)	Average power generation (Watt)	Highest stress (MPa)	Maximum deflection (m)
0.1	2.16	155	0.0022
0.2	23.36	586	0.0133
0.3	54.28	920	0.0233
0.4	74.93	1067	0.0279
0.5	84.23	1118	0.0295
0.6	86.84	1128	0.0300
0.7	86.77	1119	0.0298
0.8	85.52	1099	0.0294
0.9	83.94	1072	0.0288
1	82.07	1041	0.0281

Figure 3-7a, describes the change in average power generation with varying length of the composite plate harvester. The velocity of the vehicle passing through the plate harvester is kept constant at 22.2 m/s, the depth of the harvester used for the calculation is $Z=0.12\text{m}$ and the thickness of the piezoelectric layer and the substrate layer are chosen as $H_1=0.0006\text{m}$ and $H_2=0.002\text{m}$, respectively. The width of the harvester is fixed at $B=0.2\text{m}$.

From the Figure 3-7a, it is seen that the average power generation increases gradually with increasing length of the composite harvester and reaches its maximum value of power generation at the length of 0.6 m, which is 86.84 Watt. With larger length over 0.6m, the average power generation start decreasing. However, the highest stress generated on the plate harvester at the length of 0.6 m is 1128 MPa and maximum deflection is 0.0300 m. Both of the stress and deflection values are too large for our composite plate structure to be sustained (Material properties of the composite harvester are given in Table 1). At length of 0.2m, the P_{avg} is 23.36 Watt. The highest stress value at that point is 586 MPa and the largest deflection is 0.0133 m, which is acceptable with the power generation of 23.36 Watt and also no risk of breaking the harvester.

It is seen that, for higher length values, the average power generation by the composite plate harvester can be very high up to 86.83 Watt but then higher stress and deflection will be generated, which can break the structure. After considering all those factors, the optimum value for the length of the composite harvester can be selected as 0.2m.

3.3.5 Average power generation with varying width of the harvester

Figure 3-7b below demonstrates the impact of width of the harvester on average power generation.

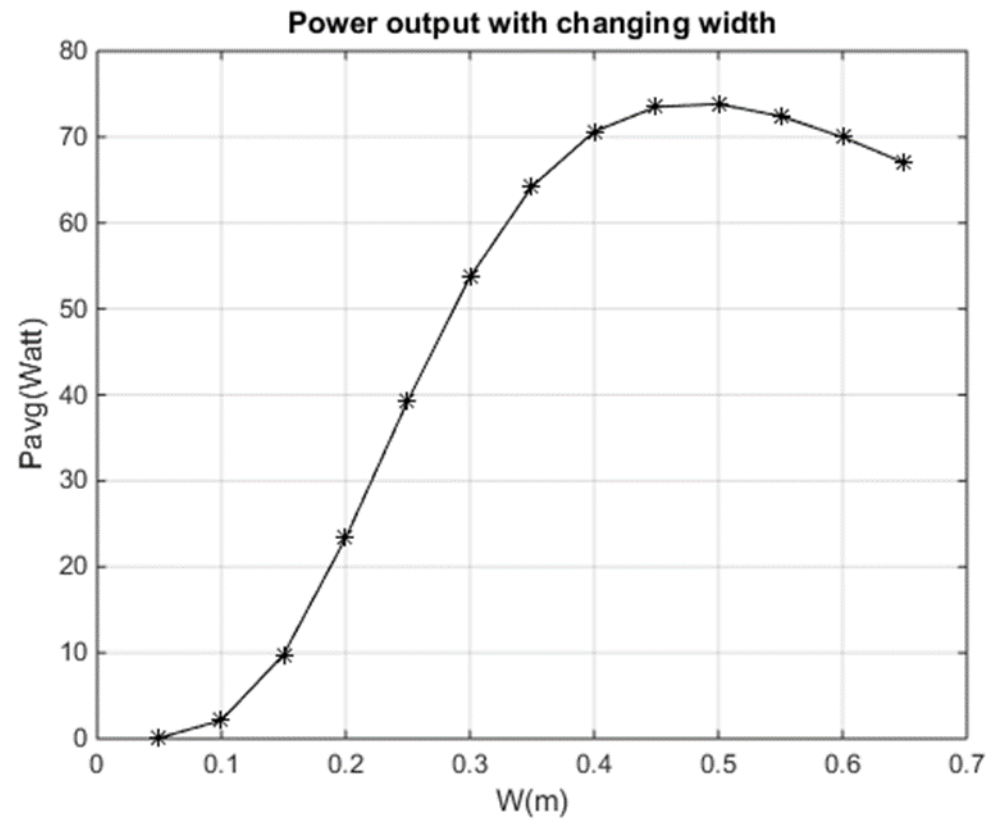


Figure 3-7b Power generation with changing width of the piezoelectric plate where the length of the piezoelectric composite plate is 0.2m, the depth of the harvester is $Z=0.12\text{m}$ and the thickness of the PZT layer and substrate layer of the composite plate are $H_1=0.0006\text{m}$ and $H_2=0.002\text{m}$, respectively.

The following Table 3-6 shows the variation in average power generation, highest stress and maximum deflection from the piezoelectric composite plate harvester with the variation of the width of the harvester,

Table 3-6 Variation in average power generation, highest stress and maximum deflection from the piezoelectric composite plate harvester with the variation of the width of the harvester.

For this calculation, the length of the composite plate harvester is chosen as 0.2m, depth as $Z=0.12\text{m}$ and the thickness of the piezoelectric layer and substrate layer as $H_1=0.0006\text{m}$ and $H_2=0.002\text{m}$, respectively. The velocity of the vehicle passing through the plate harvester is kept constant at 22.2 m/s.

Width (m)	Average power generation (Watt)	Highest stress (MPa)	Maximum deflection (m)
0.05	0.098	40	0.0002
0.1	2.14	155	0.0022
0.15	9.79	357	0.0071
0.2	23.36	586	0.0133
0.25	39.32	780	0.019
0.30	53.70	920	0.0233
0.35	64.25	1011	0.0261
0.4	70.63	1067	0.0279

0.45	73.51	1100	0.0289
0.5	73.83	1118	0.0295
0.55	72.44	1126	0.0298
0.6	70.00	1128	0.0300
0.65	66.98	1125	0.0299

Figure 3-7b, demonstrates the change in average power generation from the composite plate harvester with varying width. For this calculation, the length of the composite plate harvester is chosen as 0.2m, depth as $Z=0.12\text{m}$ and the thickness of the piezoelectric layer and substrate layer as $H_1=0.0006\text{m}$ and $H_2=0.002\text{m}$, respectively. The length of the harvester is fixed at $L=0.2\text{m}$. The velocity of the vehicle passing through the piezoelectric composite plate is kept constant at 22.2 m/s. From the graph, it is noticed that, the average power generation starts increasing from 0.05m width and then keep rising up to $P_{avg}=73.83$ Watt with $B=0.5\text{m}$, where the highest stress generated is 1118 MPa. That stress value is very large and may cause breakage of the structure. However, this is the highest value of power generation and the maximum deflection at that point is 0.0295m which is also large. When the width keeps increasing from $B=0.5\text{m}$, the average power generation starts to decrease. From equations (34-37), it is known that, the average power generation is dependent on the dimension of the composite plate harvester. Therefore, if the length and width increases, then the distribution of the total charge over the composite plate will be higher and so current and P_{avg} will be higher. However, with the increase in dimension, capacitance also increases, which decreases the generated voltage. That is why, an optimum value of length and

width needs to be selected for which the power generation will be higher with reasonable stress and deflection.

However, if the deflection is very high, then the pavement may get deformed and other layers of the pavement will get harmed. The maximum deflection value for width varying from 0.25 m to 0.45 m changes from 0.019 m to 0.0289 m, respectively. The highest stress values increases from 780 MPa to 1100 MPa, which are more than the yield strength of the steel substrate layer (700MPa). Considering these factors, those width values cannot be taken even after having higher power generation. Keeping the safety factor in consideration, the value of width can be chosen as 0.2 m with power generation of 23.36 Watt. The highest stress value is 586 MPa, and the maximum deflection is 0.0133 m, which is reasonable.

3.3.6 Impact of vehicle velocity on average power generation

The figure 3-8 below demonstrates the impact of vehicle velocity on average power generation.

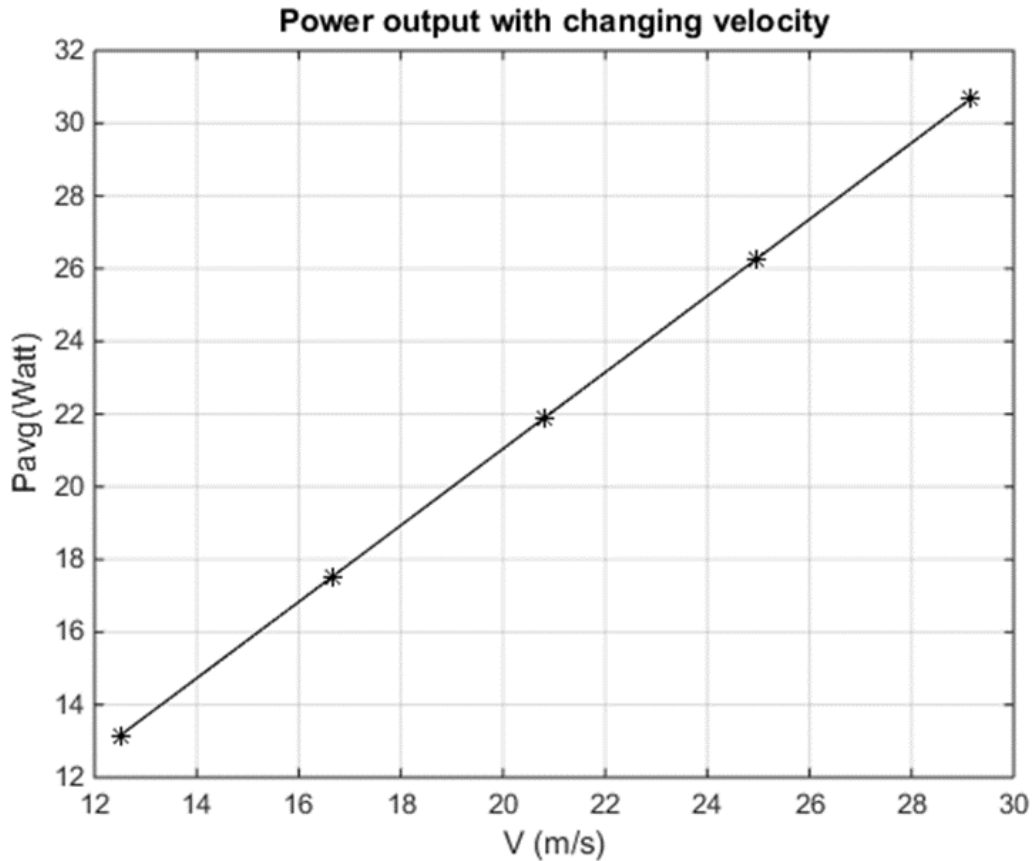


Figure 3-8 Power generation with changing velocity of the vehicle with the length and width of the piezoelectric composite plate harvester as $L=W=0.2\text{m}$, the depth of the harvester as $Z=0.12\text{m}$ and the thickness of the piezoelectric and substrate layer of the composite plate of $H_1=0.0006\text{m}$ and $H_2=0.002\text{m}$ respectively.

The following Table 3-7 shows the change in average power generation, highest stress and maximum deflection from the piezoelectric composite plate harvester with the variation of the velocity of the passing vehicle,

Table 3-7 Change in average power generation, highest stress and maximum deflection from the piezoelectric composite plate harvester with the variation of the velocity of the passing vehicle.

The length and width of the piezoelectric composite plate harvester is considered as $L=B=0.2\text{m}$, depth Z equals to 0.12m , and the thickness of the piezoelectric and substrate layer of the harvester are $H_1=0.0006\text{m}$ and $H_2=0.002\text{m}$, respectively, for the calculation.

Velocity (m/s)	Average power generation (Watt)	Highest stress (MPa)	Maximum deflection (m)
12.5	13.15	586	0.0133
16.66	17.53	586	0.0133
20.82	21.91	586	0.0133
24.98	26.28	586	0.0133
29.14	30.66	586	0.0133

Figure 3-8, demonstrates the change in average power generation from the harvester with the varying vehicle velocity. The length and width of the piezoelectric composite plate harvester is considered as $L=B=0.2\text{m}$, depth Z equals to 0.12m , and the thickness of the piezoelectric and substrate layer of the harvester are $H_1=0.0006\text{m}$ and $H_2=0.002\text{m}$, respectively, for the calculation.

It is seen that, a linear increasing relationship exists between the velocity of the passing vehicle and the average power generation. When the velocity is 12.5 m/s , the average power generation is 13.15 Watt , and then it increases linearly up to 30.66 Watt for velocity 29.14 m/s . For velocities 16.66 m/s , 20.82 m/s and 24.98 m/s the average power generations are 17.53 W , 21.91 W and

26.28 W, respectively. The maximum deflection at all the velocities is constant at 0.0133 m. The highest stress generated by the plate harvester remains same with changing velocity of the vehicle, which is 586 MPa. The increasing average power generation with the increase in vehicle velocity can be described as follows. When the vehicle velocity increases, it takes less time for the wheels to pass through the piezoelectric composite plate harvester. As a result of this, a certain amount of charge is generated on the surface of the harvester with less charging time, which actually increases the current produced by the harvester. Thus, an increase in average power generation takes place.

Table 3-8 Dimension of the piezoelectric composite plate harvester after the optimisation

Parameters	Host beam (A514 steel)	PZT layer
$L (m)$	0.2	0.2
$B (m)$	0.2	0.2
$H (m)$	$H_1=0.002$	$H_2= 0.0006$

3.4 Conclusions

In this chapter, a piezoelectric composite plate energy harvester in the road pavement is designed and studied to collect energy from the passing vehicles. Numerical simulations have been carried out and calculations are done by MATLAB coding to calculate the power generation by the piezoelectric composite plate harvester. The optimization of the piezoelectric composite plate harvester is done by keeping into mind the maximum stress that can be sustained by both the piezoelectric material and the substrate material used. It is calculated that, the optimum dimension of the harvester is $0.2 \text{ m} * 0.2 \text{ m} * 0.0026 \text{ m}$. When the optimum sized harvester is under dynamic loading and the velocity of the vehicle passing through is 22.2 m/s , then it can generate up to 23.36 W . This power generation can be used to collect enough energy within 2.5 hours to raise the temperature of the ice with the thickness of 1 cm , covering a 5 m wide road by $20 \text{ degree Celsius}$. The power generation with optimal design can be sufficient for ice melting, if there is continuum moving vehicle on the road passing the pavement and the rest of the energy can be stored for future use. The harvested energy can also be used for different other purposes like road lighting and signalization. In addition, more power can be generated by using materials with higher Young's modulus and yield strength. Designing of network to collect this power with best efficiency for different applications and experiment testing of the numerical model in practical field are among the future scope of this work, which can guide us to the path of alternate energy from vehicles in highways, urban and rural roads.

Chapter 4

In this chapter, to increase the average power generation produced by the composite plate harvester, a cantilever composite harvester is attached inside the composite plate harvester by modifying its design. The modification of the design is done in order to utilize the deflection of the composite plate harvester as base motion for the attached cantilever harvester.

4.1 Methodology and Numerical Model of cantilever composite harvester under base motion

Figure 4-1 shows the schematic diagram of the modified design of the piezoelectric composite plate harvester with attached cantilever composite harvester. The cantilever harvester is under vibration subjected to the base excitation because of the dynamic deformation of the plate due to the passing vehicle.

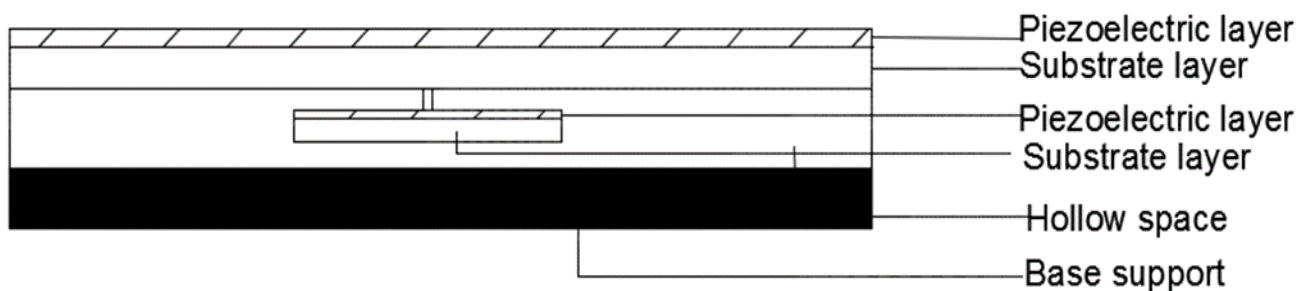


Figure 4-1 Piezoelectric cantilever composite harvester.

As shown in figure 4-1, we have considered the vibration of the cantilever composite harvester consisting of two layers, the coating layer as PZT material and the substrate layer as A514 steel and that is made as a cantilever. The cantilever plate model is placed inside the hollow space of

the box composite plate structure. When the box rectangular composite plate harvester having an optimum size plate of 0.2 m * 0.2 m * 0.0026 m dimension is placed inside the pavement then it is subjected to the stress bulb, during the vehicle wheel moving through the pavement embedded with that harvester, which is calculated by the Westergaard's stress model described in chapter 2 in detail. The box composite plate harvester alone has an average power generation of 23.36 Watt. In the aim of increasing the average power generation furthermore the cantilever composite harvester is attached inside the hollow space of the box structure. The cantilever composite harvester will undergo vibration while the plate harvester is under dynamic deformation.

The length and width of the composite cantilever harvester is considered to be as $l * b = 0.13 \text{ m} * (0.14 - l) * 2 \text{ m}$ respectively. To fit the cantilever inside the square composite plate harvester the width of the cantilever harvester must meet the dimension of $(0.14 - l) * 2 \text{ m}$. The thickness of the PZT coating is chosen as $h_{PZT} = 0.001 \text{ m}$ and the thickness of the steel substrate layer as $h = 0.002 \text{ m}$. Young's modulus of the piezoelectric layer is $E_p = 78 * 10^9 \text{ Pa}$ and Young's modulus of the substrate layer (A514 steel) is $E = 200 * 10^9 \text{ Pa}$. The density of the substrate layer is 7850 kg/m^3 and the density of the coating layer is 7750 kg/m^3 .

The deflection of the composite plate harvester with the passing of the vehicle wheels can be given as,

$$w_{i,j}(X, Y) = \frac{4Q}{\pi^4 DBL} \sum_{m=1}^{\alpha} \sum_{n=1}^{\alpha} \frac{\sin(m\pi s_1/L) \sin(n\pi s_2/B) \sin(m\pi X/L) \sin(n\pi Y/B)}{((m/L)^2 + (n/B)^2)^2} \quad (40)$$

where, w is the deflection of the harvester, m and n are the number of modes, L is the length, B is the width of the piezoelectric composite plate harvester. Q is the point load, X and Y give the position of the small square areas in the plate along x and y direction, α is the mode number, which is 3 for our calculation, i and j are the number of the small areas that are subjected to one of the point loads from the pressure bulb along length and width directions of the plate. $i*s_1$ and $j*s_2$ are the positions of the small area subjected to one of the transverse point loads. This equation is also described in chapter 3.

From the deflection equation of the composite plate structure given in equation (40), the calculation of the central deflection of the plate attached with cantilever harvesters can be conducted. After that the calculation of the central velocity and central acceleration of the plate is done. The acceleration found from that calculation will act as the base motion excitation for the composite cantilever harvester.

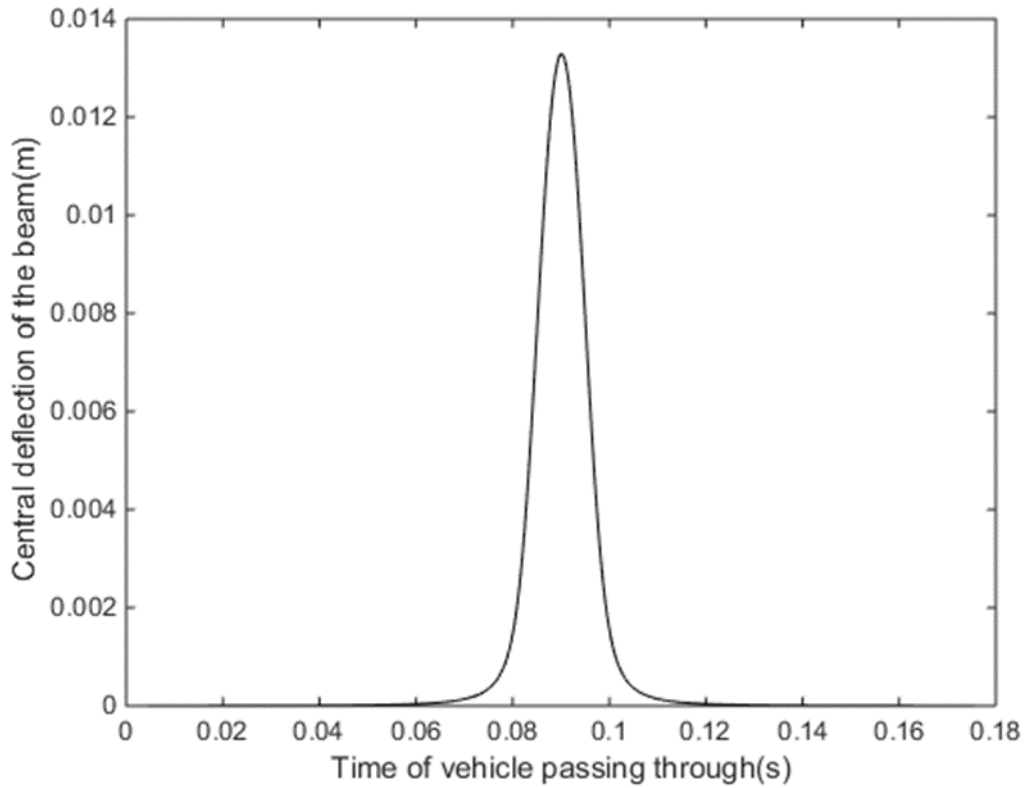


Figure 4-2 Central deflection of the composite plate harvester during passing of vehicle wheels.

From figure 4-2, it can be seen that the deflection of the cantilever composite harvester increases while the vehicle wheel start reaching the middle of the harvester and reaches the highest value while the vehicle wheel is right on top of the composite plate harvester position on pavement.

From the central deflection of the composite plate harvester, the central velocity and central acceleration can be found.

$$\text{Central Velocity}(i - 1) = \frac{\text{Central deflection } w(i) - \text{Central deflection } w(i - 1)}{\Delta t}$$

$$\text{Central Acceleration } (i - 2) = \frac{\text{Central velocity } V(i - 1) - \text{Central velocity } V(i - 2)}{\Delta t}$$

The value of Δt is 0.0005.

The general forced vibration equation can be written as,

$$EI \frac{\partial^4 w(x,t)}{\partial x^4} + \rho A \frac{\partial^2 w(x,t)}{\partial t^2} = f(x, t) \quad (41)$$

The forced vibration solution of a beam can be determined using the mode superposition principle.

The equation involves a fourth order derivative with respect to x so the equation can be solved by four boundary conditions for $w(x, t)$. $f(x, t)$ is the force per unit length.

The deflection of the beam is assumed as,

$$w(x, t) = \sum_{n=1}^{\infty} W_n(x) q_n(t) \quad (42)$$

where $W_n(x)$ is the n th mode shape function and $q_n(t)$ is the generalized coordinate in the n th mode ($n=1, 2, \dots, \infty$). Here three vibration modes are considered for calculation.

Substituting equation (42) into equation (41) we get,

$$EI \sum_{n=1}^{\infty} \frac{d^4 W_n(x)}{dx^4} q_n(t) + \rho A \sum_{n=1}^{\infty} W_n(x) \frac{d^2 q_n(t)}{dt^2} = f(x, t) \quad (43)$$

The solution for $W_n(x)$ is the vibration mode function corresponding with the total length of the beam in space domain and can be obtained as:

$$W_n(x) = A_1 \cos \beta x + A_2 \sin \beta x + A_3 \cosh \beta x + A_4 \sinh \beta x \quad (44)$$

$$\text{Here } \beta^4 = \frac{\rho A \omega^2}{EI} \text{ and } \omega = \beta^2 \sqrt{\frac{E_S I_S + E_{PZT} I_{PZT}}{\rho_S A_S + \rho_{PZT} A_{PZT}}} \quad (45)$$

Here ω is the natural frequency.

ρ_s and ρ_{PZT} are the densities of the steel plate and the PZT coating layer respectively and

A_s and A_{PZT} are the areas of the steel plate and PZT coating layer respectively.

$$\frac{dW(x)}{dx} = -A_1\beta\sin\beta x + A_2\beta\cos\beta x + A_3\beta\sinh\beta x + A_4\beta\cosh\beta x \quad (46)$$

$$\frac{d^2W(x)}{dx^2} = -A_1\beta^2\cos\beta x - A_2\beta^2\sin\beta x + A_3\beta^2\cosh\beta x + A_4\beta^2\sinh\beta x \quad (47)$$

$$\frac{d^3W(x)}{dx^3} = A_1\beta^3\sin\beta x - A_2\beta^3\cos\beta x + A_3\beta^3\sinh\beta x + A_4\beta^3\cosh\beta x \quad (48)$$

Where A_1 , A_2 , A_3 and A_4 can be solved by four boundary conditions.

The boundary conditions for cantilever are-

At (fixed end) $x = 0$: Deflection $W(x) = 0$,

$$A_1 + A_3 = 0 \quad (49)$$

At (fixed end) $x = 0$: slope $\frac{dW(x)}{dx} = 0$,

$$A_2\beta + A_4\beta = 0 \quad (50)$$

At (free end) $x = l$: Bending moment $\frac{d^2W(x)}{dx^2} = 0$,

$$-A_1\beta^2\cos\beta l - A_2\beta^2\sin\beta l + A_3\beta^2\cosh\beta l + A_4\beta^2\sinh\beta l = 0 \quad (51)$$

At (free end) $x = l$: Shear force $\frac{d^3W(x)}{dx^3} = 0$,

$$A_1\beta^3\sin\beta l - A_2\beta^3\cos\beta l + A_3\beta^3\sinh\beta l + A_4\beta^3\cosh\beta l = 0 \quad (52)$$

By using the boundary conditions which leads to four linear equations a matrix can be formed.

$$\begin{bmatrix} 1 & 0 & 1 & 0 \\ 0 & \beta & 0 & \beta \\ -\beta^2 \cos\beta l & -\beta^2 \sin\beta l & \beta^2 \cosh\beta l & \beta^2 \sinh\beta l \\ \beta^3 \sin\beta l & -\beta^3 \cos\beta l & \beta^3 \sinh\beta l & \beta^3 \cosh\beta l \end{bmatrix} \begin{bmatrix} A_1 \\ A_2 \\ A_3 \\ A_4 \end{bmatrix} = \begin{bmatrix} 0 \\ 0 \\ 0 \\ 0 \end{bmatrix} \quad (53)$$

By solving eigenvalue problem of the matrix in Equation (53) by MATLAB coding, the solution of the n th natural frequency of the cantilever beam, ω_n in β_n and its corresponding normal modes can be determined.

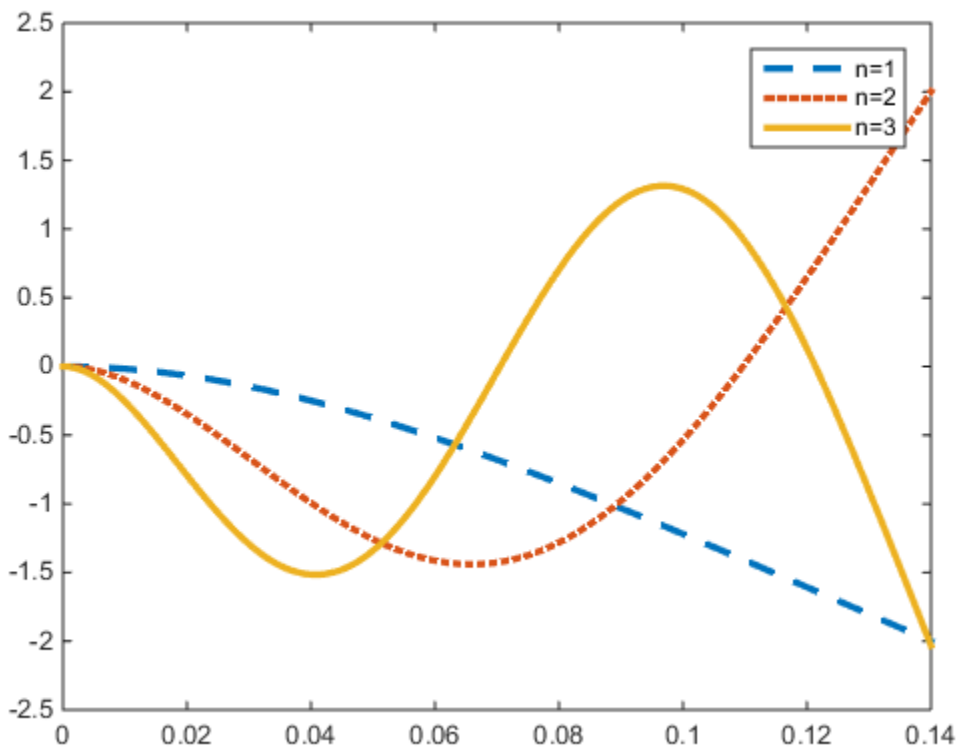


Figure 4.3 Mode 1, 2 and 3.

When the cantilever beam is subjected to the base motion, electric charge and voltage will be generated on the piezoelectric layer attached on it.

For the final response,

$$W(x, n) = A_{n1} \cos \beta_n x + A_{n2} \sin \beta_n x + A_{n3} \cosh \beta_n x + A_{n4} \sinh \beta_n x \quad (54)$$

The forced vibration solution of the piezoelectric bonded cantilever subjected to the harmonic base motion provided by the composite plate harvester due to passing vehicle wheel can be given as below,

$$w(x, t) = \sum_{n=1}^3 W(x, n) q(t) \quad (55)$$

where

$$w(x, n) = W(x, n). \quad \text{at } 0 \leq x \leq l$$

The energy harvesting efficiency of the piezoelectric coupled cantilever under a base excitation is needed to be calculated. The base motion excitation of the piezoelectric coupled cantilever can be expressed as [11],

$$f(x, t) = -m(x) * \text{Acceleration} \quad (56)$$

where $m(x)$ is the mass per length of the cantilever at the position x ($0 \leq x \leq l$), l is the total length of the cantilever harvester and f is the distributed force on the cantilever composite harvester. Here

$$m(x) = \rho_s A_s + \rho_{PZT} A_{PZT} \quad (57)$$

where ρ_s and ρ_{PZT} are the densities of the steel plate and the PZT coating respectively and A_s and A_{PZT} are the areas of the steel plate and PZT coating respectively.

The equation governing the cantilever subjected to base motion which is also called the Euler Bernoulli Beam theory can be given by-

$$[E_s(x)I_s(x) + E_{PZT}(x)I_{PZT}(x)]\frac{\partial^4 w(x, t)}{\partial x^4} + m(x)\frac{\partial^2 w(x, t)}{\partial t^2} = f(x, t) \quad (58)$$

where E_s is the Young's modulus of the substrate steel which is 200×10^9 Pa,

E_{PZT} is the Young's modulus of the PZT coating which is 78×10^9 Pa,

I_s is the moment of inertia of the substrate steel layer which can be derived from the following equation,

$$I_s = \frac{1}{3} \times b \times [(h + h_{PZT})/2]^3 - [(h - h_{PZT})/2]^3 \quad (59)$$

I_{PZT} is the moment of inertia of the PZT coating layer which can be derived from the following equation,

$$I_{PZT} = \frac{1}{3} \times b \times [(h - h_{PZT})/2]^3 - [(-h - h_{PZT})/2]^3, \quad (60)$$

where b is the total width of the cantilever composite harvester, and h and h_{PZT} are the thickness of the substrate A514 steel and the PZT coating layer, respectively.

The generalized coordinate in the n th mode ($n=1, 2, \dots, \infty$) is given as below:

$$q_n t = \frac{1}{b''} \times \frac{1}{(m(x) \times \omega_n)} \times \int_0^t Q_n(\tau) \sin \omega_n(t - \tau) d\tau, \quad (61)$$

$$b'' = \int_0^l (A_1 \cos \beta_n x + A_2 \sin \beta_n x + A_3 \cosh \beta_n x + A_4 \sinh \beta_n x)^2 dx, \quad (62)$$

where $Q_n t$ is the generalized force corresponding to $q_n t$, and b'' is a constant related with n th vibration mode.

$$Q_n t = \int_0^l f \times (A_1 \cos \beta_n x + A_2 \sin \beta_n x + A_3 \cosh \beta_n x + A_4 \sinh \beta_n x) dx \quad (63)$$

When the cantilever composite harvester is under external force due to the moving pressure bulb generated during passing of vehicle wheel, the electrical charge generated on the surface of the piezoelectric coating layer perfectly bonded on the steel substrate layer can be calculated by the formula below, [10]

$$Q(t) = -e_{31} \int_0^l b \left(\left(\frac{h + h_{PZT}}{2} \right) + \left(\frac{h - h_{PZT}}{2} \right) \right) \frac{d^2 w}{dx^2} dx \quad (64)$$

$$Q(t) = -e_{31} * b \left(\left(\frac{h+h_{PZT}}{2} \right) + \left(\frac{h-h_{PZT}}{2} \right) \right) * \left(\frac{dw(x,t)}{dx} \Big|_{x=l} - \frac{dw(x,t)}{dx} \Big|_{x=0} \right) \quad (65)$$

where $Q(t)$ is the generated electric charge on piezoelectric layer, e_{31} is the piezoelectric constant, b is the width of the piezoelectric coating layer, h_{PZT} is the thickness of the PZT coating layer and h is the thickness of the steel substrate layer, w is the deflection of the harvester.

When a vehicle moves over piezoelectric harvester embedded pavement with certain velocity, at any time t , it produces charge on the piezoelectric layer of the cantilever composite harvester, which is located at a certain depth inside the pavement. Current generated on the piezoelectric layer can be computed as,

$$I(t) = \frac{dQ(t)}{dt} \quad (66)$$

The corresponding voltage generated from the PZT coating layer, $V(t)$, can be written as [11],

$$V(t) = \frac{Q(t)}{C_v} = -\frac{e_{31}((h+h_{PZT})+(h-h_{PZT}))}{2C_v} * \left(\frac{dw(x,t)}{dx} \Big|_{x=l} - \frac{dw(x,t)}{dx} \Big|_{x=0} \right) \quad (67)$$

C_v is the capacitance of the cantilever harvester which is given as,

$$C_v = \frac{\epsilon * l * b}{4\pi k h_{PZT}} \quad (68)$$

where l and b are the length and width of the cantilever composite harvester, ϵ is dielectric constant, K is static electricity constant, h_{PZT} is the thickness of the piezoelectric layer.

$C_v'' = \frac{C_v}{b}$ is the electrical capacity per unit width of the PZT layer.

The average electric power generated from the piezoelectric cantilever harvester is defined as the multiplication of root mean square (RMS) values of the voltage and current generated from the piezoelectric layer and given as below,

$$P_{avg} = V_{rms} \cdot I_{rms} \quad (69)$$

The following two equations demonstrate how the root mean square values are calculated from I and V values, which are actually functions of time, t . The values of I and V used here are the values when the tyre of the vehicle is at different distances from the piezoelectric harvester embedded pavement at different time point, t .

$$V_{rms} = \sqrt{\frac{1}{T} \int_0^T V^2(t) dt} \quad (70)$$

$$I_{rms} = \sqrt{\frac{1}{T} \int_0^T I^2(t) dt} \quad (71)$$

where, I and V are the generated voltage and current given in equation (66) and (67) respectively.

Table 4-1 Material properties of the cantilever composite energy harvester

Parameters	Host beam (A514 steel)	PZT coating
Young's modulus (Pa)	$E=200*10^9$	$E_p=78*10^9$
Density(kg/m^3)	$\rho_s =7850$	$\rho_{PZT}=7750$
$e_{31}(C/m^2)$	----	-2.8
Dielectric constant, ϵ	----	$\epsilon= 300$
Static electricity constant, K	----	$K = 9*10^9$
Yield strength	700 MPa	950 MPa
Axle load on tire, F	40 KN	40 KN
Tire pressure, P	900 KPa	900 KPa

4.2 Simulations and Discussions

Numerical simulations are conducted based on the proposed theoretical model calculating the average power generation from a cantilever composite harvester. Here, along with the simulation results, optimal design of the composite cantilever harvester is presented. During the simulation, the design of the pavement itself is kept fixed and given in Figure 2-2. Material properties of the piezoelectric cantilever harvester used for conducting the simulations are given in Table 4-1.

4.2.1 Impact of length of the cantilever harvester on average power generation

The figure 4-4, demonstrates the impact of length of the composite cantilever harvester, attached inside the plate harvester, on its average power generation. For that calculation the length of the cantilever harvester is changed from 0.1 m to 0.13 m when width also varies by $(0.14-l)*2$ m.

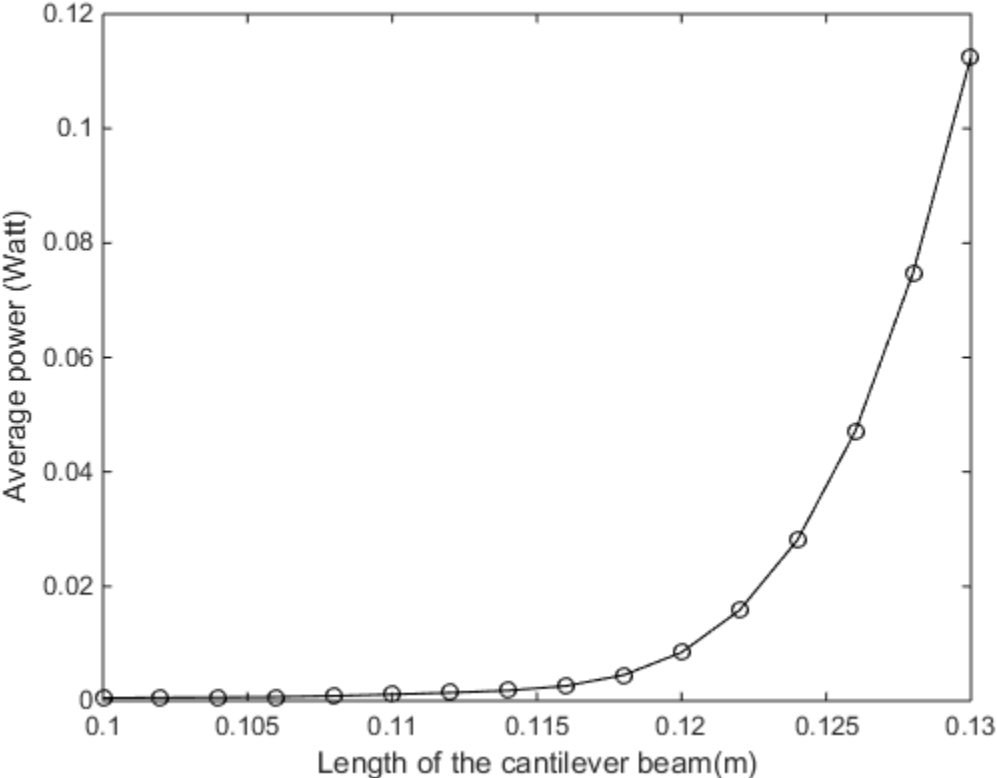


Figure 4-4 Power generation with changing length of the cantilever composite harvester. The thickness of the piezoelectric layer and substrate layer are kept fixed at 0.001 m and 0.002 m, respectively, and the velocity of the passing vehicle is kept constant at 22.2 m/s.

Table 4-2 Change in average power generation from the cantilever composite harvester with the variation of length.

Length of the cantilever harvester (m)	Average power generation (Watt)
0.1000	4.9897 e-04
0.1020	5.7460 e-04
0.1040	6.1297 e-04
0.1060	6.8604 e-04
0.1080	8.6368 e-04
0.1100	0.0011
0.1120	0.0014
0.1140	0.0018
0.1160	0.0026
0.1180	0.0045
0.1200	0.0085
0.1220	0.0158
0.1240	0.0281
0.1260	0.0471
0.1280	0.0748
0.13	0.1126

Figure 4-4, illustrates the change in average power generation from the cantilever composite harvester with the change of length. The detailed values of change in average power generation

with changing length is shown in Table 4-2. During the simulation, the thickness of the piezoelectric layer and substrate layer are kept fixed at 0.001 m and 0.002 m, respectively. It is seen from the figure that with the increase in length of the harvester the average power generation keep increasing. When the length of the cantilever harvester is 0.1 m then the average power generation is very small (4.9897×10^{-4} Watt). However, with the increase in length of the harvester the average power generation keep increasing and reaches the highest value when the length of the harvester is 0.13 m. The average power generation at that length of 0.13 m is 0.1126 Watt. As a result, the optimum value of length for the cantilever can be chosen as 0.13 m, which is the highest length of the cantilever that can fit inside the composite plate harvester having length and width of 0.2 m. Moreover, it can be seen that when length value is 0.1260 m and 0.1280 m then the cantilever can also generate some reasonable power that is 0.0471Watt and 0.0748 Watt, respectively.

4.2.2 Impact of thickness of the piezoelectric layer of the cantilever harvester on average power generation

Figure 4-5 demonstrates the impact of thickness of the piezoelectric layer of the composite cantilever harvester attached inside the plate harvester on its average power generation.

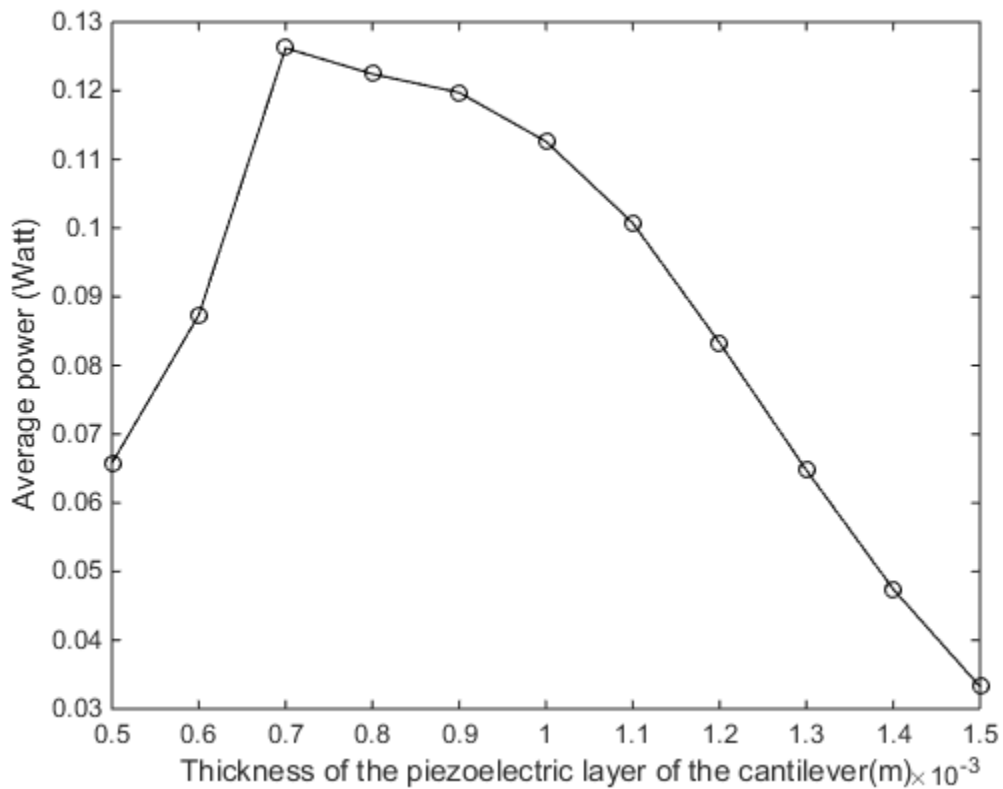


Figure 4-5 Power generation with changing thickness of the piezoelectric layer of the cantilever composite harvester with fixed length of 0.13 m. The thickness of the substrate layer is kept fixed at 0.002 m and the velocity is kept constant at 22.2 m/s.

Table 4-3 Change in average power generation from the cantilever composite harvester with the variation of thickness of the piezoelectric layer.

Thickness of the piezoelectric layer of cantilever harvester (m)	Average power generation (Watt)
0.0005	0.0658
0.0006	0.0873
0.0007	0.1262
0.0008	0.1224
0.0009	0.1197
0.0010	0.1126
0.0011	0.1007
0.0012	0.0833
0.0013	0.0648
0.0014	0.0474
0.0015	0.0332

Figure 4-5 illustrates the change in average power generation from the cantilever composite harvester with the change of thickness of the piezoelectric layer. The detailed values of change in average power generation with changing thickness of the piezoelectric layer are shown in Table 4-3. In that calculation the length of the harvester is kept fixed as 0.13 m, width as $(0.14-1)*2$ m and the thickness of the substrate layer is kept fixed at 0.002 m. It is seen from Table 4-3 that when the thickness of the piezoelectric layer of the cantilever is small (0.0005 m), the average power generation is also small, which is 0.0658 Watt. However, with the increase in thickness of the

piezoelectric layer of the harvester the average power generation also increases up to a thickness of 0.0007 m and then again starts to decrease. The highest value of average power generation is 0.1262 Watt which can be found with the thickness of the piezoelectric layer as 0.0007 m. From Table 4-3, it can also be seen that after the thickness of 0.0007 m the average power generation by the harvester keep decreasing and reaches the lowest value of 0.0332 Watt with the thickness of the piezoelectric layer of 0.0015 m. However, from the above discussion it is clear that the optimum thickness value for the piezoelectric layer of the cantilever can be chosen as 0.0007 m.

4.2.3 Impact of thickness of the substrate steel layer of the cantilever harvester on average power generation

Figure 4-6 demonstrates the impact of thickness of the substrate steel layer of the composite cantilever harvester, attached inside the plate harvester, on average power generation.

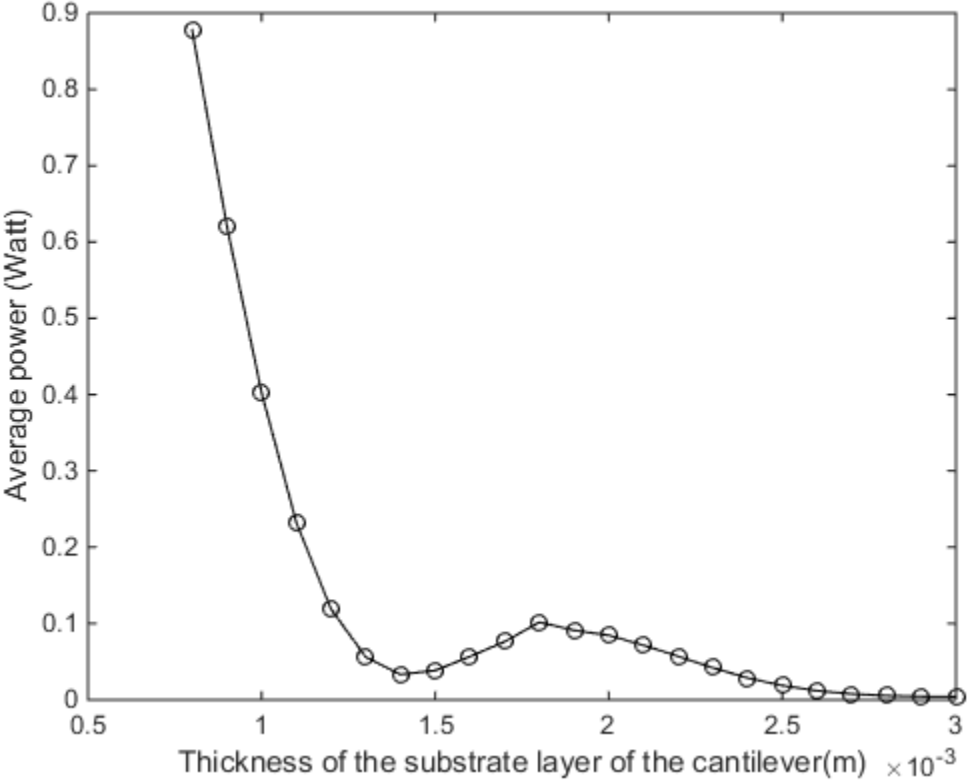


Figure 4-6 Power generation with changing thickness of the substrate layer of the cantilever composite harvester with fixed length of 0.13 m. The thickness of the piezoelectric layer is kept fixed at 0.0007 m and the velocity is kept constant at 22.2 m/s.

Table 4-4 Change in average power generation from the cantilever composite harvester with the variation of thickness of the substrate steel layer.

Thickness of the substrate layer of cantilever harvester (m)	Average power generation (Watt)
0.0008	1.1650
0.0009	1.0117
0.0010	0.8059
0.0011	0.5875
0.0012	0.3862
0.0013	0.2230
0.0014	0.1119
0.0015	0.0524
0.0016	0.0355
0.0017	0.0474
0.0018	0.0713
0.0019	0.0969
0.0020	0.1262
0.0021	0.1261
0.0022	0.0991
0.0023	0.0778
0.0024	0.0593
0.0025	0.0419

0.0026	0.0278
0.0027	0.0177
0.0028	0.0112
0.0029	0.0077
0.0030	0.0060

Figure 4-6 illustrates the change in average power generation from the cantilever composite harvester with the change in thickness of the substrate layer. The detailed values of change in average power generation with changing thickness of the substrate layer is shown in Table 4-4. During the simulation, the length of the harvester is kept fixed as 0.13 m, width as $(0.14-1)*2$ m and the thickness of the piezoelectric layer is kept fixed at 0.0007 m. From figure 4-6, it can be seen that with the increase in thickness of the substrate steel layer average, the power generation decreases. When the thickness of the substrate layer of the cantilever is 0.0008 m then the average power output is 1.1650 Watt, which is the highest value of power generation from the harvester. When the thickness of the substrate steel layer varies from 0.0009 m to 0.0030 m the value of average power generation decreases from 1.0117 Watt and reaches the lowest value of 0.0060 Watt. It can hence be concluded that the optimum value of thickness of the substrate layer can be chosen as 0.0008 m. Moreover, when the thickness of the substrate steel layer is 0.0009 m and also 0.0010 m the cantilever harvester can also generate some reasonable power which are 1.0117 Watt and 0.8059 Watt, respectively.

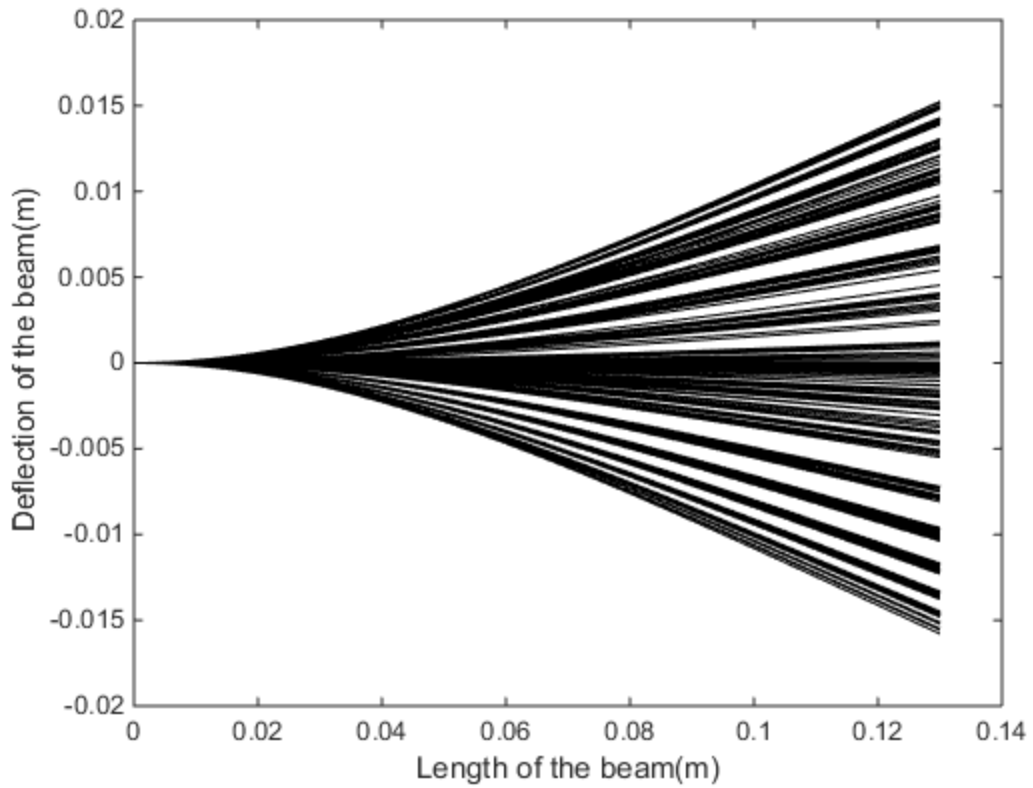


Figure 4-7 Deflection curve of the cantilever composite harvester at different time points.

Figure 4-7 describes the deflection curves of the optimized cantilever composite harvester when it is subjected to base motion.

Table 4-5 Dimension of the piezoelectric cantilever composite harvester after the optimisation

Parameters	Host beam (A514 steel)	PZT layer
$L (m)$	0.13	0.13
$h_{PZT} (m)$	0.0007	0.0007
$h (m)$	0.0008	0.0008

4.3 Conclusions

In this chapter, numerical simulations have been carried out and calculations are done by MATLAB coding to calculate the charge, current and voltage generated by the cantilever composite harvester attached to the composite plate harvester. The deflection of the composite plate provides the base motion to the attached cantilever harvester. Vibration simulations are done to find out the average power generation by the cantilever harvester, when the host composite plate harvester is under dynamic pressure bulb loading due to the passing vehicle. Through numerical simulations with different designs of the cantilever harvester, the average power generation with one optimum sized cantilever harvester having the dimension of 0.13 m * 0.02 m * 0.0015 m is 1.1650 Watt. Using more cantilever harvesters attached to the plate harvester, more electrical power can be generated, and the power that can be generated from the cantilever harvester can be added up with the 23.36 Watt found from the composite plate harvester. In conclusion, it can be stated that by adding four cantilever composite harvesters inside the composite plate harvester, it is possible to increase the average power generation of the piezoelectric plate harvester by 19.949%.

Chapter 5

Conclusions and future works

The primary objective of this thesis is to develop and study different designs of energy harvesters in the road pavement made from a piezoelectric material to collect energy from the passing vehicles. Based on the property of the piezoelectric materials different designs of piezoelectric harvesters are placed inside the pavement to study the energy harvesting efficiency. For the first time, a numerical model based on the Westergaard's stress model is proposed to calculate the three dimensional (3D) stress distribution in the pavement and to find the potential of energy harvesting from the piezoelectric layers placed inside the pavement. The model is also validated by comparing the stress generation results found from MATLAB simulation results with the ANSYS simulation results. The average error percentage found by comparing the stress values from ANSYS and MATLAB simulations among 5 data points at 5 cm depth inside the pavement is only 3.646%, which certainly validates the MATLAB simulation results and describes that the stress distribution results inside the pavement found from MATLAB simulation is accurate. Numerical simulations have been carried out and calculations are done by MATLAB coding to calculate the power generation by the piezoelectric energy harvesters. Based on the proposed numerical model, simulations are conducted to reveal the effects of changing vehicle velocity, changing loads on wheel, location of the piezoelectric harvesters inside the flexible pavement and also dimensions of the harvesters, on the generated power. Moreover, an attempt for proposing an optimum design for different piezoelectric harvesters in piezoelectric layer is conducted to obtain maximum power.

- First, an approach to design a simple piezoelectric patch harvester for flexible pavements is discussed taking the effects of size of piezoelectric harvester unit, depth of piezoelectric

harvester located in the pavement and velocity of vehicle passing the pavement. It is found that one single optimum sized (25 cm * 25c m) piezoelectric patch has a potential to generate 30 mW of when placed under the pavement, with velocity of moving vehicle as 45 km/hr and 40 KN load on each tyre of the moving vehicle.

- After the patch harvester design a piezoelectric composite plate energy harvester in the road pavement is designed and studied to increase the generated power. It is calculated that the optimum dimension of the harvester is 0.2 m * 0.2 m * 0.0026 m. When the optimum sized harvester is under dynamic loading with the passing vehicle velocity of 22.2 m/s, then it can generate up to 23.36 W electrical power in total. This power generation can be used to collect enough energy within 2.5 hours to raise the temperature of the ice with the thickness of 1 cm, covering a 5 m wide road by 20 degree Celsius.
- Moreover, to further increase the generated power, a piezoelectric composite cantilever harvester attached on the plate energy harvester is proposed. The average power generation by one optimum sized cantilever harvester with the dimension of 0.13 m * 0.02 m * 0.0015 m is 1.1650 Watt. In conclusion, it can be stated that by adding four cantilever composite harvesters inside the composite plate harvester it is possible to increase the average power generation by 19.949 %.

In all the designs piezoelectric harvesters are placed below pavement layers rather than directly on surface to ensure that piezoelectric ceramic does not go any fatal failure due to complex forces induced on pavement surface. Life of piezoelectric harvester will be affected adversely with direct contact with the vehicle tires, so placing of the harvester below the surface coating of bitumen/asphalt and to the top of base layer is a reasonable choice. Significant increase in traffic

at present time also shows a potential of larger scope of power generation by piezo-electric harvester below road pavements.

As recommendation for future works, the following tasks can be considered for any possible continuation of the research, which can guide us to the path of alternate energy from vehicles in highways, urban and rural roads.

- Designing of electrical circuit network to collect the generated power with best efficiency for different applications. The actual power output from the energy harvesters can be lower than what we have calculated from our mathematical simulation because of the probable loss during the collection process of power with electrical circuits. Therefore, it is very important to design the electric circuit network very efficiently to minimise that loss. This will need further simulations based on more accurate models considering the coupling effects between the mechanical structures and electrical circuits.
- Experimental testing of the numerical model in practical field. It is one of the very important future works to do the experimental testing of the numerical model to determine the actual power generation capability of different energy harvesters placed inside the pavement with passing vehicle wheels in practical scenario.
- Use of materials with higher Young's modulus and yield strength and study of the effects on generated power. By using material with higher yield strength generated power can be higher. From mathematical simulation, it is proved that with higher deflection higher power can be generated by the harvesters. Therefore, with higher yield strength of the material, the harvesters can be subjected with higher strain with lower risk of breaking the harvester.

- Determination of maximum deformation that the harvester can sustain in practical scenario by considering the possible shear strain.

References

- [1] Martinot, E., & Sawin, J. L. (2012). Renewables 2012 global status report. Renewable Energy Policy Network for the 21st Century.
- [2] Le Quéré, C., Raupach, M. R., Canadell, J. G., Marland, G., Bopp, L., Ciais, P., ... & Friedlingstein, P. (2009). Trends in the sources and sinks of carbon dioxide. *Nature Geoscience*, 2(12), 831-836.
- [3] Jacobson, M. Z., & Delucchi, M. A. (2009). A path to sustainable energy by 2030. *Scientific American*, 301(5), 58-65.
- [4] <http://www.theglobeandmail.com/news/toronto/icy-canadian-winter-has-left-cities-snow-removal-budgets-running-dry/article16926817/>
- [5] Despesse, G., Jager, T., Jean-Jacques, C., Léger, J. M., Vassilev, A., Basrour, S., & Charlot, B. (2005, June). Fabrication and characterization of high damping electrostatic micro devices for vibration energy scavenging. In *Proc. Design, Test, Integration and Packaging of MEMS and MOEMS* (pp. 386-390).
- [6] Glynne-Jones, P., Tudor, M. J., Beeby, S. P., & White, N. M. (2004). An electromagnetic, vibration-powered generator for intelligent sensor systems. *Sensors and Actuators A: Physical*, 110(1), 344-349.
- [7] Saha, C. R., O'Donnell, T., Loder, H., Beeby, S., & Tudor, J. (2006). Optimization of an electromagnetic energy harvesting device. *IEEE Transactions on Magnetics*, 42(10), 3509-3511.
- [8] Jeon, Y. B., Sood, R., Jeong, J. H., & Kim, S. G. (2005). MEMS power generator with transverse mode thin film PZT. *Sensors and Actuators A: Physical*, 122(1), 16-22.

- [9] Ajitsaria, J., Choe, S. Y., Shen, D., & Kim, D. J. (2007). Modeling and analysis of a bimorph piezoelectric cantilever beam for voltage generation. *Smart Materials and Structures*, 16(2), 447.
- [10] Wang, Q., & Wu, N. (2012). Optimal design of a piezoelectric coupled beam for power harvesting. *Smart Materials and Structures*, 21(8), 085013.
- [11] Xie, X. D., Wu, N., Yuen, K. V., & Wang, Q. (2013). Energy harvesting from high-rise buildings by a piezoelectric coupled cantilever with a proof mass. *International Journal of Engineering Science*, 72, 98-106.
- [12] Anton, S. R., & Sodano, H. A. (2007). A review of power harvesting using piezoelectric materials (2003–2006). *Smart materials and Structures*, 16(3), R1.
- [13] Wu, N., Wang, Q., & Xie, X. (2013). Wind energy harvesting with a piezoelectric harvester. *Smart Materials and Structures*, 22(9), 095023.
- [14] Priya, S. (2005). Modeling of electric energy harvesting using piezoelectric windmill. *Applied Physics Letters*, 87(18), 184101.
- [15] Li, S., Yuan, J., & Lipson, H. (2011). Ambient wind energy harvesting using cross-flow fluttering. *Journal of Applied Physics*, 109(2), 026104.
- [16] Martinot, E., & Sawin, J. L. (2012). Renewables 2012 global status report. Renewable Energy Policy Network for the 21st Century.
- [17] <http://www.thecanadianencyclopedia.ca/en/article/ocean-wave-energy/>
- [18] Junfeng, Li, et al. "Renewable Energy Policy Network for the 21st Century."
- [19] "Ocean renewable energy-2015-2050 Australia's ocean energy potential", Commonwealth Scientific and Industrial Research Organisation (CSIRO) (2012).

- [20] Taylor, G. W., Burns, J. R., Kammann, S. A., Powers, W. B., & Welsh, T. R. (2001). The energy harvesting eel: a small subsurface ocean/river power generator. *IEEE journal of oceanic engineering*, 26(4), 539-547.
- [21] Gao, X., Shih, W. H., & Shih, W. Y. (2013). Flow energy harvesting using piezoelectric cantilevers with cylindrical extension. *IEEE Transactions on Industrial Electronics*, 60(3), 1116-1118.
- [22] Xie, X. D., Wang, Q., & Wu, N. (2014). Energy harvesting from transverse ocean waves by a piezoelectric plate. *International Journal of Engineering Science*, 81, 41-48.
- [23] Zurkinden, A. S., Campanile, F., & Martinelli, L. (2007, October). Wave energy converter through piezoelectric polymers. In *Proceedings of the COMSOL Users Conference (Grenoble)*.
- [24] Sodano, H. A., Inman, D. J., & Park, G. (2005). Comparison of piezoelectric energy harvesting devices for recharging batteries. *Journal of Intelligent Material Systems and Structures*, 16(10), 799-807.
- [25] Xie, X. D., Wang, Q., & Wu, N. (2014). A ring piezoelectric energy harvester excited by magnetic forces. *International Journal of Engineering Science*, 77, 71-78.
- [26] Minazara, E., Vasic, D., & Costa, F. (2008, March). Piezoelectric generator harvesting bike vibrations energy to supply portable devices. In *Proceedings of International Conference on Renewable Energies and Power Quality (ICREPQ'08)*, Santander, Spain (pp. 12-14).
- [27] Li, X., & Strezov, V. (2014). Modelling piezoelectric energy harvesting potential in an educational building. *Energy Conversion and Management*, 85, 435-442.

- [28] Van den Ende, D.A., Van de Wiel, H.J., Groen, W.A., and Van der Zwaag, S. (2012). "Direct strain energy harvesting in automobile tires using piezoelectric PZT-polymer-Composites." *Smart Mater. Struct.*, 21, 015011.
- [29] Malotte, C. (2012). *Feasibility of Energy Harvesting Using a Piezoelectric Tire* (Doctoral dissertation, Arizona State University).
- [30] Danesh, W., Muktadir, N., Bhowmick, S., and Alam, S. (2011). "A proposal for large scale electricity generation from high pressure applications using piezoelectric materials." *International journal of science and advance technology*, 1, 14-19.
- [31] Yehia, Sherif A., and Christopher Y. Tuan. "Bridge deck deicing." (1998).
- [32] Chang, C., Ho, M., Song, G., Mo, Y. L., & Li, H. (2009). A feasibility study of self-heating concrete utilizing carbon nanofiber heating elements. *Smart Materials and Structures*, 18(12), 127001.
- [33] Gao, Q., Huang, Y., Li, M., Liu, Y., & Yan, Y. Y. (2010). Experimental study of slab solar collection on the hydronic system of road. *Solar energy*, 84(12), 2096-2102.
- [34] Pan, P., Wu, S., Xiao, Y., & Liu, G. (2015). A review on hydronic asphalt pavement for energy harvesting and snow melting. *Renewable and Sustainable Energy Reviews*, 48, 624-634.
- [35] Innovattech study of harvesting piezoelectricity, viewed 1 June 2014, <http://www.innowattech.co.il/>
- [36] Li, Z. X., Yang, X. M., & Li, Z. (2006). Application of cement-based piezoelectric sensors for monitoring traffic flows. *Journal of transportation engineering*, 132(7), 565-573.

- [37] Xiang, H.J., Wang, J.J., Shi, Z.F., and Zhang, Z.W. (2013). "Theoretical analysis of piezoelectric energy harvesting from traffic induced deformation of pavements." *Smart Mater. Struct.* , 22, 095024.
- [38] Ali, S.F., Friswell, M.I., and Adhikari, S. (2011). "Analysis of energy harvesters for highway bridges." *Journal of Intelligent Material Systems and Structures*, 22, 1929-1938.
- [39] Tianchen, Y., Jian, Y., Ruigang, S., & Xiaowei, L. (2014). Vibration energy harvesting system for railroad safety based on running vehicles. *Smart Materials and Structures*, 23(12), 125046.
- [40] Zhang, Y., Cai, S. C., & Deng, L. (2014). Piezoelectric-based energy harvesting in bridge systems. *Journal of Intelligent Material Systems and Structures*, 25(12), 1414-1428.
- [41] Duarte, F., Casimiro, F., Correia, D., Mendes, R., & Ferreira, A. (2013, March). A new pavement energy harvest system. In *Renewable and Sustainable Energy Conference (IRSEC), 2013 International* (pp. 408-413). IEEE.
- [42] Xiang, H. J., Wang, J. J., Shi, Z. F., & Zhang, Z. W. (2014). Corrigendum: Theoretical analysis of piezoelectric energy harvesting from traffic induced deformation of pavements (2013 *Smart Mater. Struct.* 22 095024). *Smart Materials and Structures*, 23(11), 119502.
- [43] Xiong, H., Wang, L., Wang, D., & Druta, C. (2012). Piezoelectric energy harvesting from traffic induced deformation of pavements. *International Journal of Pavement Research and Technology*, 5(5), 333.

- [44] Zhao, H., Yu, J., & Ling, J. (2010). Finite element analysis of cymbal piezoelectric transducers for harvesting energy from asphalt pavement. *Journal of the Ceramic Society of Japan*, 118(1382), 909-915.
- [45] Tao, Y., Niu, Y., & Ling, J. (2014). Harvesting energy from asphalt pavement by piezoelectric generator. *Journal of Wuhan University of Technology-Mater. Sci. Ed.*, 29(5), 933-937.
- [46] Zhao, H., Ling, J., & Yu, J. (2012). A comparative analysis of piezoelectric transducers for harvesting energy from asphalt pavement. *Journal of the Ceramic Society of Japan*, 120(1404), 317-323.
- [47] <https://www.rocscience.com/documents/pdfs/rocnews/fall2009/Westergaard-Stress-Solution-Method.pdf>.
- [48] Punmia, B. C., & Jain, A. K. (2005). *Soil mechanics and foundations*. Firewall Media.
- [49] Moazami, D., Muniandy, R., Hamid, H., & Yusoff, Z. M. (2011). Effect of tire footprint area in pavement response studies. *International Journal of the Physical Sciences*, 6(21), 5040-5047.